



Norwegian University of  
Science and Technology

# Development of an Analytical Method for the Determination of the Antigen Binding Capacity of Radiolabeled Antibodies

**Lene Andersen**

Chemical Engineering and Biotechnology

Submission date: Januar 2012

Supervisor: Per Bruheim, IBT

Co-supervisor: Olav B. Ryan, Algeta



# Acknowledgement

---

This master thesis was performed at Algeta ASA's offices in Oslo during the period from August 2011 to January 2012. It was the final part of my Master of Science studies in Biotechnology at the Biotechnology Department of the Norwegian University of Science and Technology (NTNU).

The supervisors for the project were Professor Per Bruheim at NTNU and Olav B. Ryan with co-supervisor Kristine Sponheim at Algeta. I would like to thank all of my supervisors and give a special thanks to Kristine and Olav for all help, support and motivation during this work. Thank you for giving me the opportunity to work with such an interesting project, and for everything I have learned along the way. I would also like to show my gratitude to Hanne and Ellen for all wise advices and comments in this last, stressing period.

The employees in Algeta's Research and Development department contributing with cell cultivation and fixation, and the production of Thorium-227 and antibody-chelator conjugates used in this project need to be mentioned as well. Thank you! In addition, all of you have to be thanked for welcome me like you did and making these five months so nice and interesting. I am looking forward to stay with you for three more months!

And at last I want to thank friends at NTNU for making these five years so special, especially my flat mates for three years, Marthe and Kahle, and Randi for so many good memories from our year in Aachen. A big thanks also to my family for supporting and encouraging me throughout my studies, and to Yago for being patient and always cheering me up.

Lene Andersen

Oslo, January 2012



# Abstract

---

The foundation of Algeta's second alpha-pharmaceutical platform is thorium-227, a radionuclide that emits alpha particles with high energy. By linking thorium-227 to tumor binding monoclonal antibodies, Algeta has the potential to develop a new generation of radioactive drugs that can fight cancer with limited damage to surrounding tissue. Determination of the immunoreactive fraction (IRF) of these molecules is an important part of the quality control of such a product. IRF is determined by examination of the tumor-binding molecule's ability to bind to antigens on the surface of living or fixated cells. This is a labor-intensive method in which a large number of cells must be cultivated and fixated prior to the analysis. It is therefore desirable to develop an immunoreactivity assay independent of cells.

The Lindmo method is a widely used method for the determination of IRF. The method used by Algeta today is a simplification of the Lindmo method, and in this report called the one-point assay. This is a timesaving method, but there are uncertainties about the reliability of its results. A part of this project was to examine if the one-point analysis could be used as a timesaving alternative to the Lindmo assay. The conclusion was that a full Lindmo assay should be performed whenever a new system is examined, or whenever high accuracy is required. However, the one-point analysis is a timesaving method that can be used to estimate IRF in a routine quality check.

Microbeads coated with antigen might have a potential to substitute cells in these immunoreactivity assays. The main objective of this project was to develop a quantitative bead-based method adapted to the tumor-binding systems used by Algeta, and to perform a comparison study between the cell- and bead-based methods. The results demonstrated that antigen-coated beads with advantage can be used as a substitute for cells. The bead-based assays were timesaving, demonstrated a high degree of reproducibility and provided more consistent and reliable results than the cell-based measurements. The bead-based assays have the potential to be used for any antibody-antigen systems where the antigen or the epitope of the antigen can be isolated.



# Sammendrag

---

Grunnlaget for Algetas andre alpha-farmasøytiske plattform er thorium-227, en radionuklide som sender ut alfapartikler med høy energi. Ved å knytte thorium-227 til tumorbindende monoklonale antistoffer, har Algeta potensial til å utvikle en ny generasjon av radioaktive medikamenter som kan bekjempe kreft med begrenset skade til omliggende vev. Bestemmelse av immunoreaktiv fraksjon (IRF) av disse molekylene er en viktig del av kvalitetskontrollen av et slikt produkt. IRF blir bestemt ved å undersøke de tumorbindende molekylenes evne til å binde seg til antigener på overflaten av levende eller fikserte celler. Dette er en arbeidskrevende metode hvor et stort antall celler må dyrkes og fikseres før selve analysen. Det er derfor ønskelig å utvikle en ny immunoreaktivitets-analyse som er uavhengig av celler.

Lindmo-metoden er en mye brukt metode for bestemmelse av IRF. Den analysen som brukes av Algeta i dag, og i denne rapporten kalt ett-punkts-metoden, er en forenkling av Lindmo-metoden. Dette er en tidsbesparende metode, men det er usikkerhet rundt påliteligheten av målingene fra denne metoden. En del av dette prosjektet var å undersøke om ett-punkts-analysen kan brukes som et tidsbesparende alternativ til Lindmo-analysen. Konklusjonen er at en full Lindmo-analyse bør utføres når et nytt system skal undersøkes, eller når en høy nøyaktighet er påkrevet. Ett-punkts-analysen er imidlertid en tidsbesparende metode som kan brukes til å estimere IRF i en rutinemessig kvalitetskontroll.

Mikrokuler belagt med antigen er en potensiell erstatning for celler i disse immunoreaktivitets-analysene. Hovedmålet med dette prosjektet var å utvikle en kvantitativ, kule-basert metode tilpasset de tumorbindende systemene som brukes av Algeta, og å utføre et sammenligningsstudie mellom den celle- og kulebaserte metoden. Resultatene viste at antigenbelagte kuler med fordel kan brukes som en erstatning for celler. Den kule-baserte analysen var tidsbesparende, viste en høy grad av reproduserbarhet og ga mer konsistente og pålitelige resultater enn de cellebaserte målingene. Den kulebaserte analysen har potensial til å brukes for ethvert antistoff-antigen system der antigen eller epitop på antigenet kan isoleres.





# Table of Contents

---

<b>1</b>	<b>INTRODUCTION .....</b>	<b>1</b>
1.1	Background.....	1
1.2	Antigen binding capacity .....	3
1.3	The aims of this project.....	4
<b>2</b>	<b>THEORY .....</b>	<b>5</b>
2.1	Radioactivity .....	5
2.1.1	Thorium.....	7
2.1.2	Measurement of radioactivity - gamma counting.....	8
2.2	Antibody-antigen binding in tumor cells.....	10
2.2.1	Antibodies.....	10
2.2.2	HER-2 - a tumor associated antigen .....	11
2.3	Radioimmunotherapy .....	13
2.3.1	Radioimmunoconjugates .....	13
2.3.2	Targeted Thorium Conjugates.....	15
2.4	Binding assays – a theoretical analysis .....	18
2.4.1	Lindmo analysis.....	18
2.4.2	Scatchard analysis .....	20
2.4.3	Assumptions of the binding models .....	21
2.5	Microbead technology .....	22
2.5.1	Biotinylation of antigen.....	23
<b>3</b>	<b>MATERIALS AND METHODS.....</b>	<b>27</b>
3.1	Materials and equipment.....	27
3.2	Radiolabeling of antibody-chelator conjugate.....	31
3.3	Biotinylation of antigen.....	33
3.3.1	Determination of the degree of biotinylation.....	34
3.4	Preparation of cells.....	35

3.4.1	Preparation of Ag(01) expressing cells .....	35
3.4.2	Preparation of Ag(03) expressing cells .....	35
<b>3.5</b>	<b>Preparation of beads .....</b>	<b>36</b>
<b>3.6</b>	<b>Binding assays.....</b>	<b>37</b>
3.6.1	Procedure.....	37
<b>3.7</b>	<b>Analysis of binding data.....</b>	<b>41</b>
3.7.1	One-point-analysis.....	41
3.7.2	Lindmo analysis.....	42
3.7.3	Scatchard analysis .....	43
<b>4</b>	<b>RESULTS .....</b>	<b>45</b>
<b>4.1</b>	<b>Preparation of RICs and biotinylated antigens .....</b>	<b>45</b>
4.1.1	Yield and specific activity after radiolabeling.....	46
4.1.2	Degree of biotinylation.....	46
<b>4.2</b>	<b>Scatchard analysis .....</b>	<b>47</b>
<b>4.3</b>	<b>Initial development of the immunoreactivity assays .....</b>	<b>49</b>
4.3.1	Initial development of the cell-based immunoreactivity assays .....	49
4.3.2	Initial development of the bead-based immunoreactivity assays .....	51
<b>4.4</b>	<b>Cell-based immunoreactivity measurements for <sup>227</sup>Th-AC0103 .....</b>	<b>52</b>
<b>4.5</b>	<b>Bead-based immunoreactivity measurements for <sup>227</sup>Th-AC0103.....</b>	<b>55</b>
4.5.1	Immunoreactivity measurements with high nonspecific binding.....	55
4.5.2	Immunoreactivity measurements with reduced nonspecific binding .....	56
<b>4.6</b>	<b>Immunoreactivity measurements for <sup>227</sup>Th-AC0303.....</b>	<b>59</b>
4.6.1	Cell-based immunoreactivity measurements for <sup>227</sup> Th-AC0303 .....	59
4.6.2	Bead-based immunoreactivity measurements for <sup>227</sup> Th-AC0303.....	61
<b>5</b>	<b>DISCUSSION.....</b>	<b>65</b>
<b>5.1</b>	<b>Yield, specific activity and degree of biotinylation.....</b>	<b>65</b>
5.1.1	Yields and specific activity after radiolabeling .....	65
5.1.2	Degree of biotinylation.....	66
<b>5.2</b>	<b>Scatchard analysis .....</b>	<b>68</b>
<b>5.3</b>	<b>Initial development of the immunoreactivity assays .....</b>	<b>70</b>

5.3.1	Initial development of the cell-based immunoreactivity assays .....	70
5.3.2	Initial development of the bead-based immunoreactivity assays .....	72
5.3.3	Linear regression in the Lindmo plots .....	73
<b>5.4</b>	<b>Overview of the immunoreactivity measurements .....</b>	<b>74</b>
<b>5.5</b>	<b>Cell-based immunoreactivity measurements for <sup>227</sup>Th-AC0103 .....</b>	<b>76</b>
<b>5.6</b>	<b>Bead-based immunoreactivity measurements for <sup>227</sup>Th-AC0103.....</b>	<b>Error!</b>
	Bookmark not defined.	
5.6.1	The significance of nonspecific binding.....	78
5.6.2	Bead-based measurements with reduced nonspecific binding .....	79
<b>5.7</b>	<b>Immunoreactivity measurements for <sup>227</sup>Th-AC0303.....</b>	<b>80</b>
5.7.1	Cell-based immunoreactivity measurements for <sup>227</sup> Th-AC0303 .....	80
5.7.2	Bead-based immunoreactivity measurements for <sup>227</sup> Th-AC0303.....	80
<b>5.8</b>	<b>Comparison of cells and beads .....</b>	<b>82</b>
<b>5.9</b>	<b>Comparison of one-point- and Lindmo analyses .....</b>	<b>84</b>
<b>5.10</b>	<b>Further work.....</b>	<b>86</b>
<b>6</b>	<b>CONCLUSION .....</b>	<b>89</b>
	<b>LIST OF REFERENCES.....</b>	<b>91</b>

# List of Appendices

---

**Appendix A** NAP-5 Purification

**Appendix B** Yield and Specific Activity

**Appendix C** Biotinylation

**Appendix D** Scatchard Analysis

**Appendix E** Initial development of the immunoreactivity assays

**Appendix F** Cell-based Immunoreactivity Assays for  $^{227}\text{Th}$ -AC0103

**Appendix G** Bead-based Immunoreactivity Assays for  $^{227}\text{Th}$ -AC0103

**Appendix H** Cell-based Immunoreactivity Assay for  $^{227}\text{Th}$ -AC0303

**Appendix I** Bead-based Immunoreactivity Assays for  $^{227}\text{Th}$ -AC0303

# List of Symbols and Abbreviations

---

$\alpha$	Alpha	
$\beta$	Beta	
$\gamma$	Gamma	
$\varepsilon$	Extinction coefficient	[M <sup>-1</sup> ·cm <sup>-1</sup> ]
$\lambda$	Wavelength	[nm]
A	Activity	[cpm or MBq]
A <sub>492</sub>	Absorption measured at 492 nm	
Ab	Antibody	
Ab01	Trastuzumab (Herceptin <sup>®</sup> )	
Ab03	Monoclonal antibody from external partner	
ABC	Antigen binding capacity	
AC0103	Ab01-chelator conjugate	
AC0303	Ab03-chelator conjugate	
Ag	Antigen	
AgAb	Antigen-antibody complex	
Ag(01)	Antigen targeted by Ab01	
Ag(03)	Antigen targeted by Ab03	
b	Light path length	[cm]
BL	Blocked sample	
BSA	Albumin from bovine serum	
Bq	Becquerel	
B/T	Fraction specifically bound RIC	
(B/T)*	Total fraction bound RIC (specifically and nonspecifically)	
B/T <sub>BL</sub>	Fraction nonspecifically bound RIC	
C	Purification column	
C <sub>x</sub>	Concentration of x	[M = mol·L <sup>-1</sup> ]
CDR	Complementary determining regions	

cpm	Counts per minute	
D	Daughter nuclide	
Da	Dalton	
DMSO	Dimethyl sulfoxide	
DOTA	1,4,7,10-tetraazacyclododecane-1,4,7,10-tetraacetic acid	
DTPA	Diethylenetriamine-pentaacetic acid	
ELISA	Enzyme-linked immunosorbent assay	
Fab	Fragment antigen binding	
Fc	Fragment crystallizable	
B/F	Ratio between bound and free RIC	
HABA	4'-hydroxyazobenzene-2-carboxylic acid	
HER-2	Human epidermal growth factor receptor 2	
HMW	High molecular weight	
HPGe	High-Purity Germanium detector	
Ig	Immunoglobulin	
<i>in vitro</i>	Studies conducted using components of an organism that have been isolated from their usual biological context	
<i>in vivo</i>	Studies conducted with living organisms in their normal, intact state	
IRF	Immunoreactive fraction at infinite antigen excess	
IRF*	Immunoreactive fraction at limited antigen excess	
$K_a$	Association constant	$[M^{-1}]$
LMW	Low molecular weight	
MeV	Mega electron volt	
MF-H <sub>2</sub> O	Metal-free water	
MoAbs	Monoclonal antibodies	
$M_w$	Molecular weight	$[Da = g \cdot mol^{-1}]$
MWCO	Molecular weight cut off	$[Da = g \cdot mol^{-1}]$
n	Number of moles	$[mol]$
N	Number of atoms or units	

$N_A$	The Avogadro constant	$[\text{mol}^{-1}]$
NaI	Sodium iodide	
NaOAc	Sodium acetate	
NRPA	Norwegian Radiation Protection Authority	
P	Parent nuclide	
PBS	Phosphate buffered saline	
$R^2$	Coefficient of determination	
rcf	Relative centrifugal force	
RIC	Radioimmunoconjugate	
rpm	Revolutions per minute	
SKOV-3	Human HER-2 expressing ovarian cancer cells	
S.D.	Standard deviation	
s.f.	Sterile filtrated	
Sulfo-NHS	Sulfo- N-hydroxysuccinimide	
$t_{1/2}$	Half life	[s, min, days, years]
TTC	Targeted Thorium Conjugate	
UBL	Unblocked sample	
V	Void	
$V_x$	Volume of x	$[\mu\text{L}, \text{mL}]$
X	Aminohexanoic acid spacer	
Y	Atom mass number	
Z	Atomic number	
[Ag]	Free antigen concentration	$[\text{M} = \text{mol}\cdot\text{L}^{-1}]$
$[\text{Ag}]_{\text{tot}}$	Total antigen concentration	$[\text{M} = \text{mol}\cdot\text{L}^{-1}]$
[B]	Bound RIC concentration	$[\text{M} = \text{mol}\cdot\text{L}^{-1}]$
[F]	Free RIC concentration	$[\text{M} = \text{mol}\cdot\text{L}^{-1}]$
[T]	Total RIC concentration	$[\text{M} = \text{mol}\cdot\text{L}^{-1}]$
$^{223}\text{RaCl}_2$	Radium-223 chloride (Alpharadin <sup>®</sup> )	
$^{227}\text{Th}$	Thorium-227	





# 1 Introduction

---

This chapter gives a brief introduction to the background of the radiolabeled antibodies used in this project, followed by a description of the antigen binding capacity (ABC) of these molecules. Finally, the aims for the development of a new method to determine ABC are presented.

---

## 1.1 Background

---

Cancer is a major health problem worldwide. It is estimated that there are more than 12 million new cases of cancer diagnosed yearly around the globe, and more than 7 million people die each year from this disease.<sup>[1]</sup> Chemotherapy has up to this time been one of the leading treatments of cancer. However, the cytotoxic agents used in chemotherapy are not tumor specific, and are therefore affecting normal, healthy cells as well as the tumor cells.<sup>[2]</sup> During the last decades, new knowledge of pathways and characteristics of different tumor entities has been obtained and used to generate more tumor specific therapies.<sup>[3]</sup> One such approach is the use of antibodies as tools for the selective targeting of drugs to tumors, providing a more effective and direct way to kill tumor cells.

Already at the turn of the 19th century, Paul Ehrlich proposed antibodies as “magic bullets” that could specifically trace and kill microbes and tumor cells,<sup>[4]</sup> but it was not until 1975, when Köhler and Milstein described the generation of monoclonal antibodies (MoAbs), that antibody-based therapy got its major breakthrough.<sup>[5]</sup> MoAbs can alone induce the body's immune mechanisms to kill cells expressing the target of the antibody.<sup>[6]</sup> Moreover, MoAbs used as a tool for the selective targeting of drugs to tumors provides an effective and direct way to kill tumor cells. The motivation for this approach is that by delivering cancer drugs to tumor cells, it may be possible to both enhance therapeutic efficiency and spare normal tissues from chemotherapeutic damage.<sup>[7]</sup> Cytotoxic drugs, cytokines, toxins and radionuclides are examples of therapeutic agents that have been conjugated to MoAbs, developed for the treatment of cancer.<sup>[3]</sup> An illustration of such immunoconjugates is given in Figure 1.1.

The pharmaceutical company Algeta ASA (Oslo, Norway) is one of the first companies in the world that has successfully developed a product for targeted radiotherapy emitting alpha( $\alpha$ )-particles. The product Alpharadin<sup>®</sup> is the  $\alpha$ -emitting radionuclide radium-223 ( $^{223}\text{RaCl}_2$ ).  $\text{Ra}^{2+}$ , which mimics the behavior of  $\text{Ca}^{2+}$  in the body and thus selectively seeks to bone, is developed for the treatment of skeletal metastasis in advanced cancer. The product has recently finished phase III clinical development for the treatment of skeletal metastasis in hormone-refractory metastatic prostate cancer, indicating significantly improvement in overall survival.<sup>[8]</sup> For the treatment of skeletal metastasis from breast cancer, the development is in clinical phase II.<sup>[9]</sup> The first launch of Alpharadin<sup>®</sup> is predicted to be within 2013.<sup>[10]</sup>

One of the most promising, new strategies for treating malignancies is the use of radioimmunoconjugates (RICs) for targeted radiotherapy.<sup>[11]</sup> This is the basis of Algeta's second  $\alpha$ -pharmaceutical platform is RICs with the  $\alpha$ -emitting radionuclide thorium-227 ( $^{227}\text{Th}$ ). The combination of  $^{227}\text{Th}$  with tumor binding molecules such as monoclonal antibodies constitute the potential for improved effectiveness of the treatment for a broad variety of cancer types.<sup>[12]</sup> These RICs are called Targeted Thorium Conjugates (TTCs) and are currently under preclinical research. They are described in more detail in Section 2.3.2 - "Targeted Thorium Conjugates". In this project, two TTCs will be used in the development of an analytical method for the determination of ABC for radiolabeled antibodies.

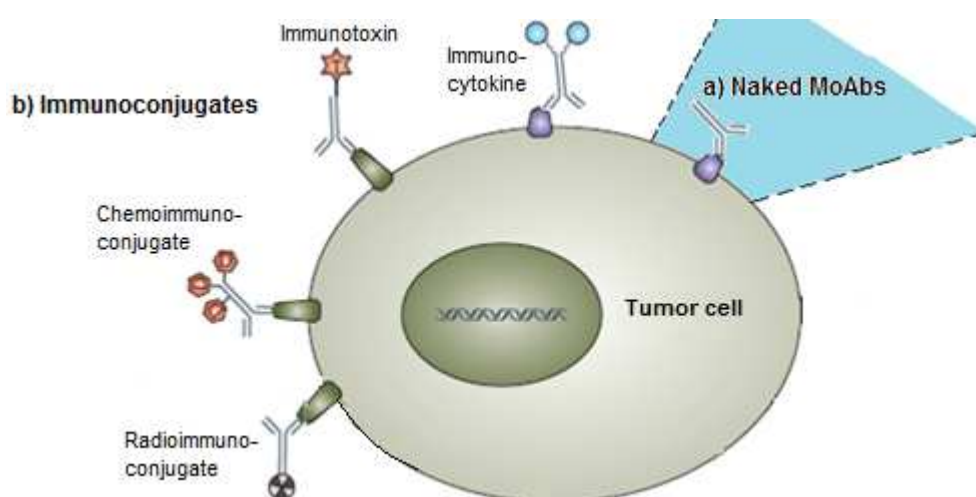


**Figure 1.1:** **a)** By targeting of naked monoclonal antibodies (MoAbs) to the tumor, destruction of the tumor cells may occur by induction of the body's immune mechanisms. **b)** A more direct way to kill the targeted cells is by conjugation of cytokines, cytotoxic drugs (D), toxins (T) or radionuclides to the MoAbs.<sup>[3]</sup>

---

## 1.2 Antigen binding capacity

---

The ABC of radiolabeled MoAbs depends on two qualities. One is the immunoreactive fraction (IRF), which provides information about the fraction of radiolabeled MoAbs that are able to bind their target epitopes or receptors at infinite antigen excess.<sup>[13]</sup> The other quality is the association constant  $K_a$ , which says something about the affinity of the binding.<sup>[14]</sup> The IRF of the MoAbs might decrease during chelator conjugation or radiolabeling due to modification of the binding sites on the antibodies. Preservation of IRF for radiolabeled MoAbs is critical for successful radioimmunotherapy, as a decrease in IRF would result in decreased tumor uptake and increased nonspecific localization, and thus generate unnecessary radiation exposure for non-target tissue.<sup>[15]</sup> Therefore, IRF of RICs intended for cancer therapy is a very important quality control parameter to assure an optimal *in vivo* behavior, and is one of the most commonly measured parameters for these products.<sup>[16]</sup> Thus, the method of determining the IRF should be simple, reproducible, practical and applicable.

A method used to determine the IRF is called an immunoreactivity assay, which is a type of binding assay. The conventional immunoreactivity assay was developed by Lindmo *et. al.* in 1984.<sup>[17]</sup> This method measures binding at various antigen concentrations and extrapolates the results in a way that IRF can be determined at conditions representing infinite antigen excess. The immunoreactivity assay used by Algeta today is a simplification of this method, in which the immunoreactive fraction at limited antigen excess, IRF\*, is determined. This method measures immunoreactivity at one given antigen concentration, and will in this report be named the one-point analysis.

To examine the  $K_a$  values, a binding assay developed by Scatchard in 1949 can be used.<sup>[18]</sup> This Scatchard analysis can also be used to determine the antigen expression on different cell lines.

---

### 1.3 The aims of this project

---

The Lindmo assay and one-point analysis examine the tumor-binding molecule's ability to bind to antigens on the surface of living or fixated tumor cells. However, this is a labor-intensive method in which a large number of cells must be cultivated and fixated prior to the analysis. The main objective of this project is therefore to develop a new, cell independent immunoreactivity assay based on the use of microbeads as a substitute for cells. Prior to the analysis, these microbeads will be coated with antigens specific for the radiolabeled antibody being analyzed.

In addition, the results given by the one-point-analysis are sometimes varying and inconsistent, and there are uncertainties regarding the reliability of these results. A secondary aim is therefore to compare the original Lindmo method with the one-point assay. The present, cell based assay will also be compared with the new, microbead based analysis to discuss the trustworthiness of the measurements.

A Scatchard analysis will be performed to substantiate the results from the immunoreactivity assays. The  $K_a$  values for the two different TTCs and the antigen expression on the two tumor cell lines will be examined by this method.

To summarize, a comparison study between the different methods will be performed, and a quantitative microbead-based method adapted to the tumor-binding systems used by Algeta will be developed. A schematic drawing of the binding systems used in the present and new method is given in Figure 1.2.

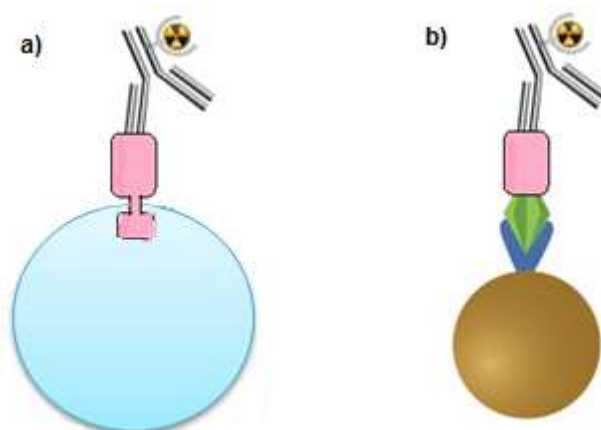


**Figure 1.2:** A schematic illustration of the antigen-antibody systems used to determine the antigen binding capacity (ABC) in this project; **a)** The present method using antigen-expressing cells. **b)** The new method using microbeads coated with antigen.

## 2 Theory

---

This chapter gives a theoretical introduction to radioactivity and to antibody-antigen binding in cancer cells, which together make up the foundation of radioimmunotherapy. Moreover, radioimmunotherapy and RICs are presented, with emphasis on TTCs. Finally, principles for the binding assays used to measure the ABC of MoAbs are described together with microbead technology, which will be the basis of the new method for the determination of IRF of the RICs.

---

### 2.1 Radioactivity

---

In the periodic table of elements, each element is characterized by a fixed number of protons, denoted by the atomic number  $Z$ . In addition to protons, the element's nucleus contains a variable number of neutrons, and the total number of protons plus neutrons in the atomic nucleus is known as the mass number  $Y$ . Atoms of an element with different numbers of neutrons are known as isotopes of that element.<sup>[19]</sup> Many nuclides are energetically unstable or radioactive, and loses energy by radioactive decay. Radioactive decay is a spontaneous nuclear transformation that results in emission of ionizing radiation. In this process, an unstable "parent" nuclide  $P$  is transformed into a more stable "daughter" nuclide  $D$ . In proton rich nuclides, an  $\alpha$ -particle ( ${}^4_2\text{He}$ ) can be emitted, and the daughter nucleus contains two protons and two neutrons less than the parent. In neutron rich nuclides, a neutron in the nucleus can transform to a proton by emitting a beta particle ( $\beta^-$ ).<sup>[20]</sup> Gamma ( $\gamma$ ) emission is electromagnetic radiation and is normally a by-product of  $\alpha$ - and  $\beta$ -decay.<sup>[19]</sup>  $\gamma$ -emission does not give a change in the number of neutrons or protons in the nucleus.  $\alpha$ - and  $\beta$ -decay are illustrated in Equation 2.1 and 2.2, respectively.



The different types of ionizing radiation vary in their abilities to penetrate matter.  $\alpha$ -particles may be completely stopped by a sheet of paper,  $\beta$ -particles by aluminum shielding, while  $\gamma$ -radiation is attenuated by massive barriers such as a thick layer of lead.<sup>[20]</sup> This is illustrated in Figure 2.1.

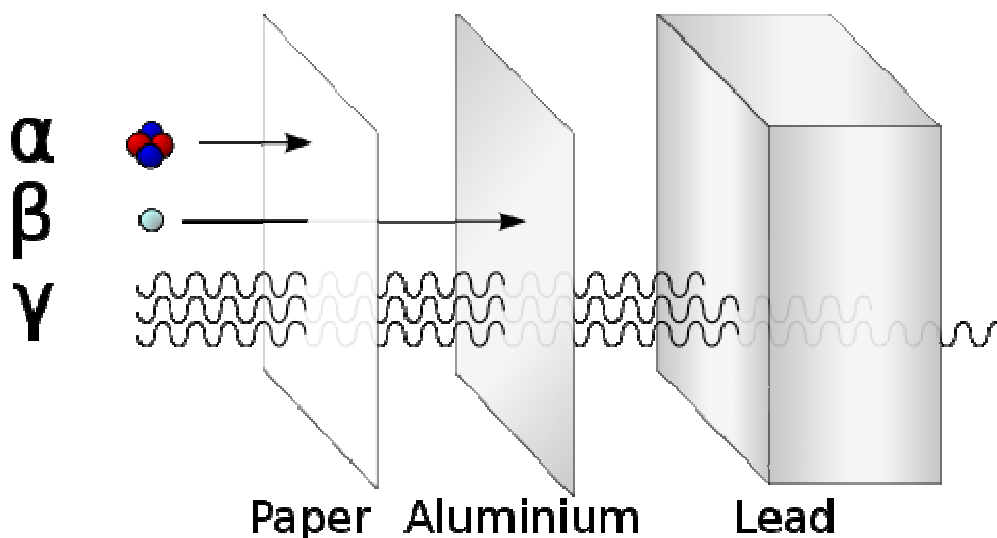


**Figure 2.1:** The different penetration abilities of  $\alpha$ -,  $\beta$ - and  $\gamma$ -radiation.  $\alpha$ -particles are stopped by a sheet of paper,  $\beta$ -particles by aluminum shielding, while  $\gamma$ -radiation is attenuated by a thick layer of lead.<sup>[21]</sup>

$\alpha$ -particles generally carry more energy than  $\beta$ -particles and  $\gamma$ -radiation. In their interaction with matter,  $\alpha$ -particles give up this energy and become neutral helium atoms. Because of their short range, external  $\alpha$ -radiation does not normally cause hazard to humans; the  $\alpha$ -particles are absorbed in the outer layers of skin before they can cause any damage. However, internal  $\alpha$ -radiation is very toxic because of the large amount of energy released in a short distance within living tissue.<sup>[19]</sup> By targeting the  $\alpha$ -emitters to the site of a tumor in the body, this property can be used for the killing of cancer cells. In this project, the  $\alpha$ -emitter  $^{227}\text{Th}$  will be linked to MoAbs that target antigens on cancer cells. The RIC's ability to bind to these antigens is a crucial property in this treatment of cancer, as a considerable non-specific radiation-dose can cause damage to healthy tissue. This antigen-binding property is the main focus of this project, and will be discussed in more detail later. First, some properties of  $^{227}\text{Th}$  and the principles of gamma counting, the method used to measure radioactivity in this project, will be presented.

## 2.1.1 Thorium

The element thorium, with the atomic number  $Z=90$ , was discovered in 1828 by the Swedish chemist Jons Jakob Berzelius.<sup>[22]</sup> He named it after Thor, the Norse god of thunder. There are 29 known isotopes of thorium, ranging in mass number from 209<sup>[23]</sup> to 238.<sup>[24]</sup> In nature, thorium exists in a single isotopic form,  $^{232}\text{Th}$ , which is found in small amounts in rock and soil and decays very slowly, with a half-life about three times the age of the Earth.<sup>[25]</sup> As already mentioned, the isotope  $^{227}\text{Th}$  will be used in this project.

$^{227}\text{Th}$  has a half-life ( $t_{1/2}$ ) of 18.72 days. It can be produced in clinically relevant amounts from  $^{227}\text{Ac}$ , which is generated by thermal neutron irradiation of  $^{226}\text{Ra}$ .  $^{227}\text{Th}$  and its daughters emit 5  $\alpha$ -particles and 2  $\beta$ -particles, which radiate a total  $\alpha$ -energy of 32.5 MeV.<sup>[26]</sup> This is illustrated in Figure 2.2.

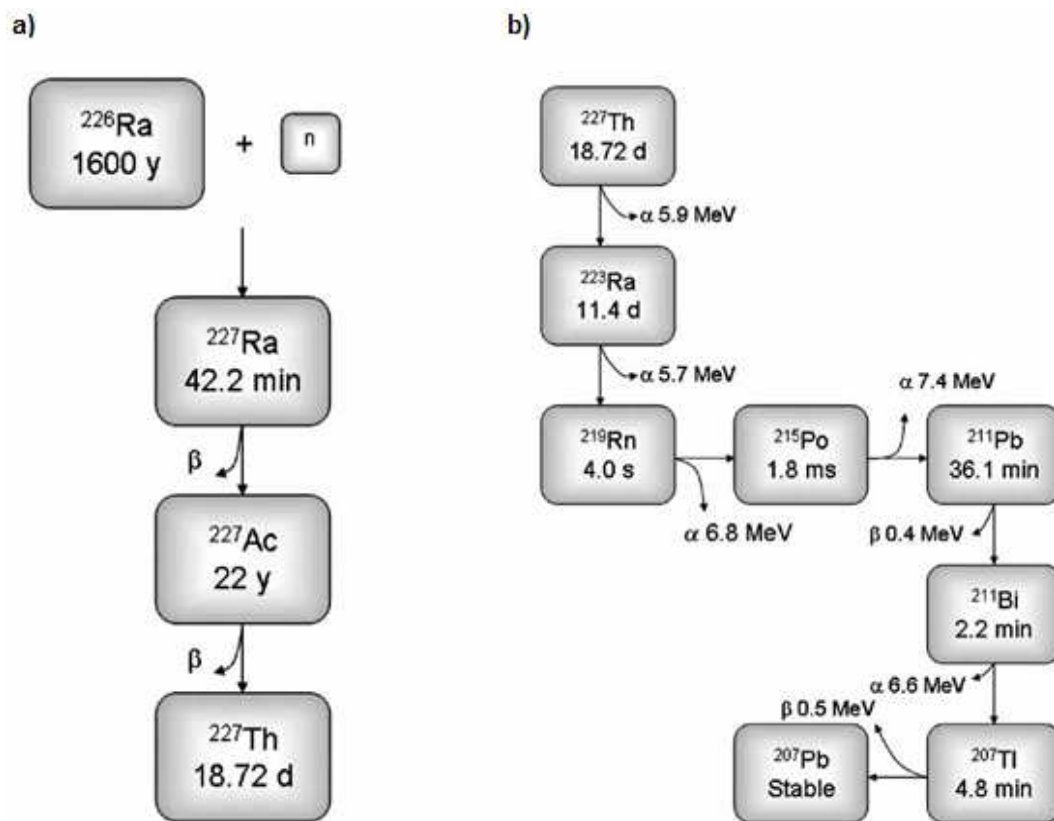


**Figure 2.2:** a)  $^{227}\text{Th}$  is produced from  $^{227}\text{Ac}$ , which is produced from thermal neutron irradiation of  $^{226}\text{Ra}$ . b)  $^{227}\text{Th}$  and daughters emit 5  $\alpha$ -particles and 2  $\beta$ -particles, with a total  $\alpha$ -energy of 32.5 MeV. The half-lives of the different nuclides are indicated under their names.<sup>[26]</sup>

### 2.1.2 Measurement of radioactivity - gamma counting

---

Activity (A) is defined as the number of nuclear decays occurring per unit time, and is proportional to the quantity of radioactive material in a sample.<sup>[27]</sup> The International System (SI) unit for activity is Becquerel (Bq), and one Bq is equal to one disintegration per second.<sup>[28]</sup> Counts per minute (cpm) is another measure of radioactivity, and gives the number of atoms that is *detected* to have decayed in one minute.<sup>[29]</sup> In this project, two gamma spectrometers were used to measure activity, one being a High Purity Germanium (HPGe) detector and the other being a sodium iodide (NaI) scintillation counter. The activity measured with the HPGe detector is given in MBq, and this detector has the ability to distinguish between different nuclides. The activity measured with the NaI scintillation counter is given in cpm. This counter measures  $\gamma$ -radiation in general, and is thus unable to distinguish between the different nuclides.

Most radioactive nuclides, included  $^{227}\text{Th}$ , produce  $\gamma$ -radiation of specific energies and intensities, providing a fingerprint for each nuclide. When these emissions are detected and analyzed with a  $\gamma$ -spectroscopy system, a  $\gamma$ -energy spectrum can be produced. The  $\gamma$ -spectrum is characteristic of the  $\gamma$ -emitting nuclides contained in the sample, and a detailed analysis of this spectrum is used to determine the identity and quantity of  $\gamma$ -emitters present in the sample. The equipment used in  $\gamma$ -spectroscopy includes an energy sensitive radiation detector, a multichannel analyzer, associated amplifiers and data readout devices.<sup>[30]</sup>

The examined radionuclides emit  $\gamma$ -radiation at known energies. These interact with the crystal (NaI or Ge) in the detector, which in turn emits signals corresponding to the energies of the incoming radiation. The signals from the detector crystal are routed through the preamplifier and amplifier, to the multichannel analyzer system. Here, the signals are displayed as a spectrum in which emission counts are plotted against energy. Software packages can then convert the peak-count information to activity using calibration procedures.<sup>[31]</sup> Figure 2.3 shows a general schematic drawing of a gamma spectrometer. More details on NaI scintillation counters and HPGe detectors can be found in the "The gamma counting handbook"<sup>[32]</sup> and "The GEM series coaxial HPGe detector guide"<sup>[33]</sup>, respectively.



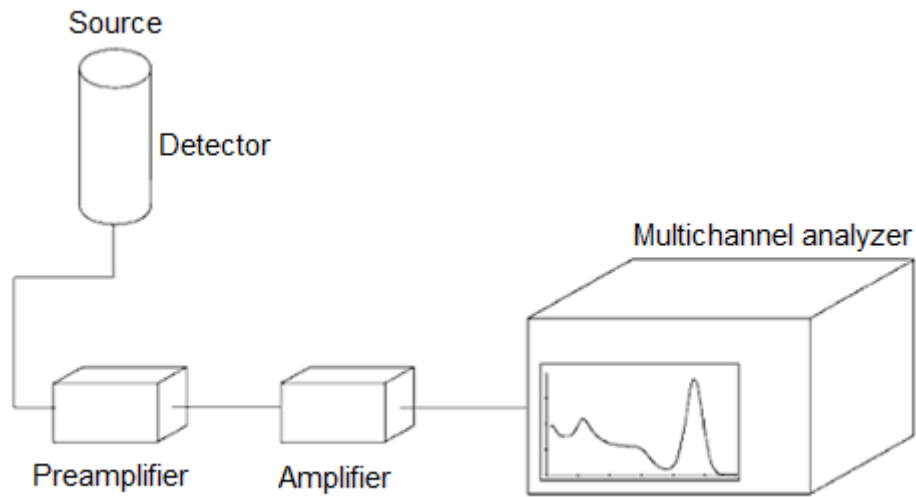


**Figure 2.3:** The principles of a gamma spectrometer. The preamplifier takes the charge produced from the detector (by the gamma radiation from the sample) and integrates and amplifies this to produce a pulse with amplitude proportional to the total charge. The amplifier takes the pulse signal from the preamplifier and considerably magnifies it. The pulses that emerge from the amplifier are then registered in one of the channels of the multi-channel analyzer, providing a spectrum of counts versus energy.<sup>[30]</sup>

---

## 2.2 Antibody-antigen binding in tumor cells

---

Cell division is a complex process that normally is tightly regulated. Healthy cells control their own growth and will destroy themselves if they are damaged.<sup>[34]</sup> When changes in the genes of a cell prevent these control mechanisms from functioning properly, cancer might arise. In cancer, cells divide and grow uncontrollably, forming malignant tumors that invade nearby parts of the body. The cancer may also spread to more distant parts of the body through the lymphatic system or bloodstream.<sup>[34]</sup>

---

### 2.2.1 Antibodies

---

Antibodies, also called immunoglobulins (Ig), are an integrated part of our immune system.<sup>[14]</sup> They are synthesized by B-lymphocytes or plasma cells in response to the presence of unknown substances, called antigens. The antibodies can then bind to these antigens, which can be on for example tumor cells or pathogens, and tag them to induce the body's immune mechanisms.<sup>[14]</sup>

Antibodies are built up of a common basic structure, as illustrated in Figure 2.4. This structure constitutes two identical, so-called 'heavy' polypeptide chains, paired with two identical, so-called 'light' chains.<sup>[35]</sup> The heavy chains are coupled together with sulfide bonds in the hinge region, and the light chains are in a similar way coupled to the heavy chains. The two identical arms are called Fab (Fragment antigen binding), and are responsible for the binding to antigens. Within the variable regions on each Fab unit there are three areas of hypervariable sequence, known as complementary determining regions (CDRs). The six CDRs on each arm of the antibody together form the antigen-binding site. The lowest part of the antibody is called Fc (fragment crystallizable). This region is not a part of the recognition of antigen but it has other important properties, such as binding to Fc-receptors on many important cell-types.<sup>[35]</sup> Antibodies can be divided into five classes or isotypes; IgA, IgD, IgE, IgG and IgM, according to variations in the heavy chain. IgG is the isotype that is most common in human serum.<sup>[14]</sup> The two antibodies used in this project are both IgG antibodies. One of these is trastuzumab, which will be presented in the next section.

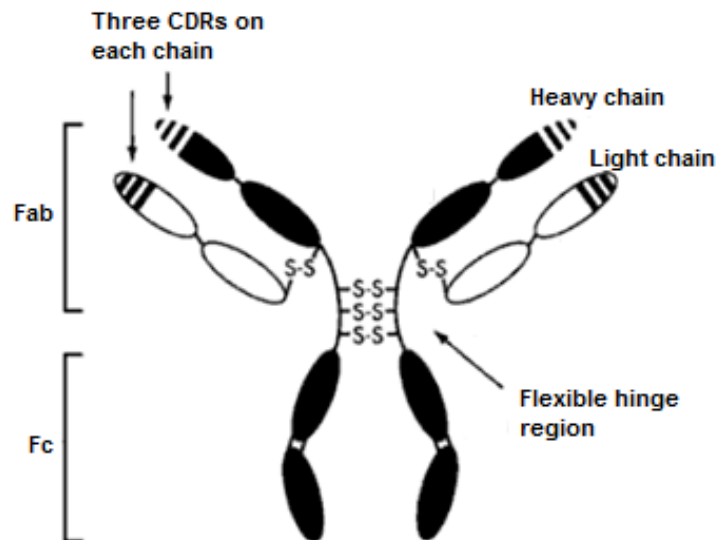


**Figure 2.4:** Basic antibody structure illustrating a pair of identical heavy chains linked to a pair of identical light chains through sulfide bonds. Sulfide bonds also bind the two heavy chains together in the flexible hinge region. The variable domains of each chain have three hypervariable loops (CDRs), which constitute the antigen binding domain on each of the two Fab fragments.<sup>[36]</sup>

### 2.2.2 HER-2 - a tumor associated antigen

---

An antigen is any substance that stimulates the immune system to produce a set of specific antibodies and combines with the antibody through a specific binding site.<sup>[27]</sup> An antigen is normally considerably bigger than its binding site. Therefore, an antibody often only binds to a small part of an antigen, called an epitope.<sup>[35]</sup> The antigen-antibody binding induces an immune response, which aims to destroy the antigen expressing substance.

Some tumor cells express characteristic tumor-cell derived proteins, which after intracellular processing and presentation at the surface of the cells differ in structure or amount from proteins on healthy cells. Thus, these proteins function as tumor antigens.<sup>[35]</sup> There are three different types of tumor antigens. One type is proteins that due to mutations have a changed amino acid sequence compared to normal proteins. These tumor-specific antigens are only found on tumor cells. The two other groups are tumor-associated antigens. These are also found on normal cells but they are overrepresented on tumor cells. Some tumor cells express antigens which are normally only found on cells in the fetal life or very early in the differentiation process. When these antigens appear in adult individuals, the immune system might interpret them as foreign.<sup>[35]</sup> These antigens constitute one of the groups tumor-associated antigens.

The last type of tumor associated antigens are normal expressed proteins in the body, but where cancer cells display an overexpression of these proteins.<sup>[35]</sup> The classical example of this last group is Human epidermal growth factor receptor 2 (HER-2). HER-2 is a cell membrane surface-bound receptor tyrosine kinase, which is normally involved in the signal transduction pathways leading to cell growth and differentiation. This marker is overexpressed in 20-30% of human breast cancers, and overexpression of HER-2 is correlated with poor prognosis and poor treatment response in patients with breast and ovarian cancers.<sup>[37]</sup> HER-2 expression in normal tissues is generally low.<sup>[38]</sup> Trastuzumab (Herceptin<sup>®</sup>) is a humanized IgG1, anti-HER-2 MoAb developed by Genentech/Roche,<sup>[39]</sup> and is now widely known to target HER-2. Trastuzumab works by attaching to HER-2 receptors and blocking signals that make the cancer more aggressive, and also by signaling to the body's immune system to destroy the cancer cells.<sup>[40]</sup> This is illustrated in Figure 2.5. Treatment of metastatic breast cancer with trastuzumab in combination with chemotherapy has demonstrated an improvement in survival compared with chemotherapy alone.<sup>[39]</sup> The binding of cytotoxic drugs, such as radionuclides to trastuzumab, might greatly enhance this effect.

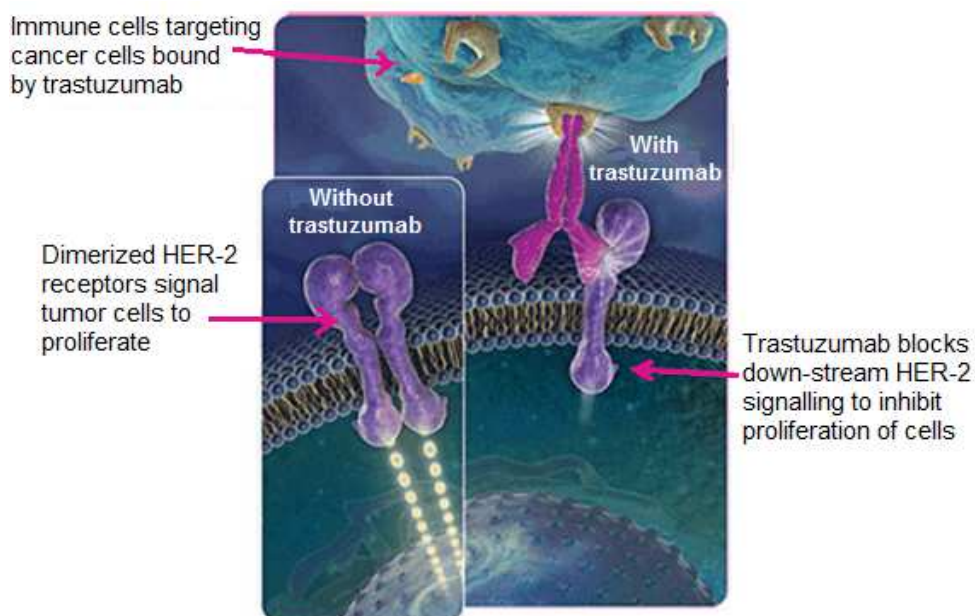


**Figure 2.5:** The proposed mechanism of action for trastuzumab (Herceptin<sup>®</sup>) binding to HER-2 on tumor cells.<sup>[41]</sup>

---

## 2.3 Radioimmunotherapy

---

The exploration of monoclonal antibodies as vehicles for delivery of therapeutic radionuclides has been ongoing for more than 50 years<sup>[42]</sup>. In 1948, Pressman and Keighley reported the first *in vivo* use of a radiolabeled antibody for imaging.<sup>[43]</sup> Ten years later, the first report of radiolabeled tumor-specific antibodies used for radioimmunodiagnosis was published<sup>[44]</sup>, and in 1960, radiolabeled antibodies were for the first time used to selectively deliver a therapeutic dose of radiation to tumor tissue.<sup>[42]</sup> Today, radioimmunotherapy is finally coming up as a new therapeutic approach, involving multiple disciplines, including immunology, radiochemistry, oncology, and nuclear medicine.<sup>[45]</sup>

### 2.3.1 Radioimmunoconjugates

---

Radioimmunotherapy depends mainly on the availability of MoAbs of high affinity and specificity, a suitable radionuclide with desired physical properties, and an appropriate linker moiety, a chelator, to produce a stable RIC that remains intact under the challenge of human catabolism.<sup>[46]</sup> The definition of a chelator is a molecule that forms bonds with two or more separate binding sites within the same ligand to a single central atom.<sup>[27]</sup> The central atom in this case is the radionuclide that through the chelator can be coupled to the antibody.

An illustration of the structure of a RIC is given in Figure 2.6. In this illustration, the widely used 1,4,7,10-tetraazacyclododecane-1,4,7,10-tetraacetic acid (DOTA) chelator, here conjugated via a benzyl isothiocyanate group (DOTA-NCS,  $M_w = 688$  Da), is used as an example of a linker unit. The chelator is covalently bound to the antibody through an amine reaction with lysine, and a TTC is formed when this chelator binds  $^{227}\text{Th}$ . The chelator used in this project binds  $^{227}\text{Th}$  in a similar way as DOTA, but has a higher molecular weight ( $M_w = 997$  Da). This chelator is still under development and has not yet been published by Algeta. Therefore, the name and structure of the chelator cannot be given in this report.

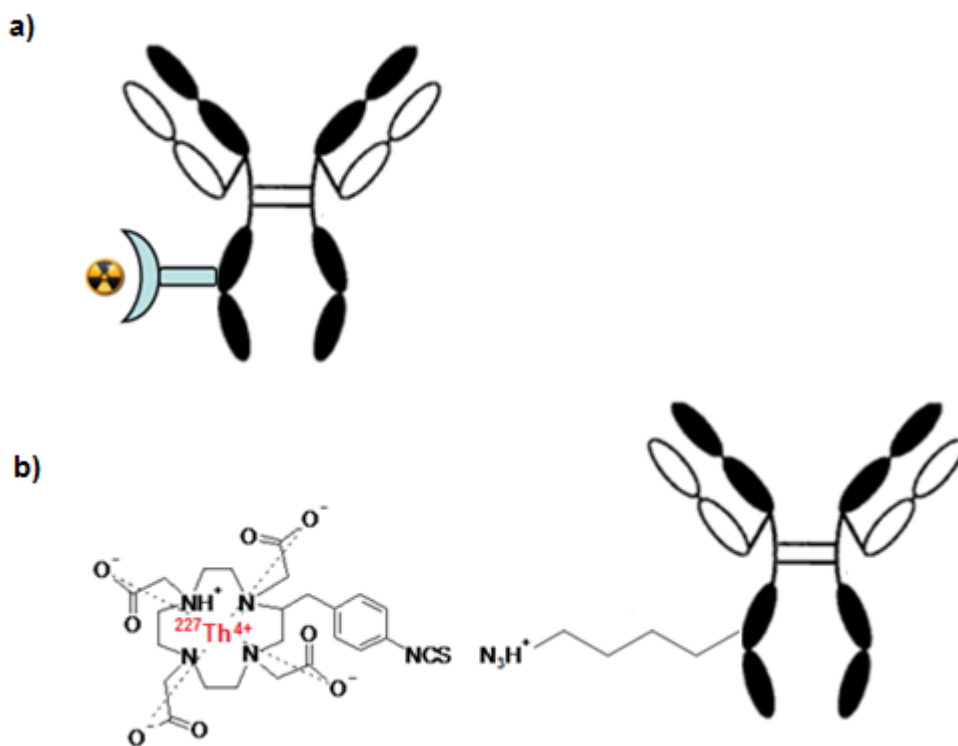


**Figure 2.6:** a) A schematic illustration of a RIC, consisting of a monoclonal antibody (MoAb), a linker moiety and a radionuclide. b) The 1,4,7,10-tetraazacyclododecane-1,4,7,10-tetraacetic acid (DOTA-NCS) chelator is an example of a linker moiety used to bind the radionuclide, here illustrated with thorium-227, to the MoAb. The chelator can be conjugated to the MoAb through an amine reaction with lysine.

The first two RICs to be approved by regulatory authorities for treating cancer were <sup>90</sup>Y-ibritumomabtiuxetan (Zevalin) in 2002 and <sup>131</sup>I-tositumomab (Bexxar) in 2003. These therapies make use of MoAbs targeting the CD20 antigen conjugated to  $\beta$ -emitting <sup>90</sup>Y or <sup>131</sup>I, to treat patients with non-Hodgkin's lymphoma.<sup>[47]</sup> However, for micrometastases and spread cancers,  $\beta$ -particles, which consist of high-energy electrons and travel 2–12 mm in tissues (200–1200 cell diameters), might have too large ranges to give efficient absorbed radiation doses in the cancer cells without high normal-tissue toxicity. Therefore, for smaller tumors, micrometastases and isolated cells, radioimmunotherapy based on  $\alpha$ -particle emitters could have benefits over  $\beta$ -emitters.<sup>[48]</sup>

$\alpha$ -emitting radionuclides emit  $\alpha$ -particles with high energy that travel 50–100  $\mu$ m (5–10 cell diameters) in tissues.<sup>[14]</sup>  $\alpha$ -particles produce clustered DNA double-strand breaks and highly reactive hydroxyl radicals when hitting biological tissue. The high energy and short range of  $\alpha$ -particles offer the possibility of more efficient and selective killing of tumor cells with low damage to surrounding normal tissue.<sup>[48]</sup> This new approach of pharmaceuticals is called  $\alpha$ -pharmaceuticals.<sup>[48]</sup>

Although investigators have long recognized the potential advantages of  $\alpha$ -particle emitters, there is still no approved treatment. Only four  $\alpha$ -emitting RICs have been studied clinically: 1)  $^{213}\text{Bi}$ -anti CD30 MoAb for treatment of leukemia<sup>[49]</sup>; 2)  $^{211}\text{At}$ -anti tenacin MoAb for treatment of brain cancer<sup>[50]</sup>; 3)  $^{211}\text{At}$ -anti NaPi2b MoAb for treatment of ovarian cancer<sup>[51]</sup>; and 4)  $^{225}\text{Ac}$ -anti CD33 MoAb for the treatment of acute myeloid leukemia.<sup>[52]</sup> As described introductorily, Algeta has developed an  $\alpha$ -pharmaceutical using the bone-seeking property of radium to target bone metastasis with the  $\alpha$ -emitter radium-223.

### 2.3.2 Targeted Thorium Conjugates

---

A new class of  $\alpha$ -pharmaceuticals from Algeta, Targeted Thorium Conjugates (TTCs), is now under pre-clinical development.<sup>[12]</sup> The schematic structure of a TTC, included illustrations of its mode of action, is given in Figure 2.7.

*In vivo* testing of  $^{227}\text{Th}$  started in 2004, and initial evaluation of  $^{227}\text{Th}$ -immunoconjugates in radioimmunotherapy in 2005 showed that  $^{227}\text{Th}$  can be stably conjugated to antibodies and provides a significant antigen-dependent inhibition of cell growth.<sup>[53]</sup> Although  $^{227}\text{Th}$  can be produced in clinically relevant amounts<sup>[54]</sup> and has been shown to be an efficient and safe nuclide in lymphoma<sup>[55]</sup>, breast cancer and ovarian cancer<sup>[56]</sup> preclinical models, no clinical studies have yet been started. However, the results warrant further studies on treatment of these cancer types using  $^{227}\text{Th}$ -immunoconjugates.<sup>[57]</sup>

$^{227}\text{Th}$  can be stably conjugated to trastuzumab (Herceptin<sup>®</sup>), and the targeted cancer cell-killing effect of  $^{227}\text{Th}$ -trastuzumab was presented for the first time at the 56th annual Society of Nuclear Medicine meeting in June 2009 (Toronto, Canada).<sup>[57]</sup> The presented data demonstrated that this TTC could selectively target and kill breast cancer cells and suggested that further studies should be conducted with this  $\alpha$ -pharmaceutical as a novel treatment for breast cancer.

Other TTCs are under development, using different chelators and antibodies. For example, Algeta has a collaboration agreement with Genzyme for a novel and proprietary tumor-targeting antibody used to deliver conjugated  $^{227}\text{Th}$  to an undisclosed target<sup>[58]</sup>, and with Affibody for two Affibody molecules to target  $^{227}\text{Th}$  to HER-2 and PDGFR $\beta$ .<sup>[59]</sup>

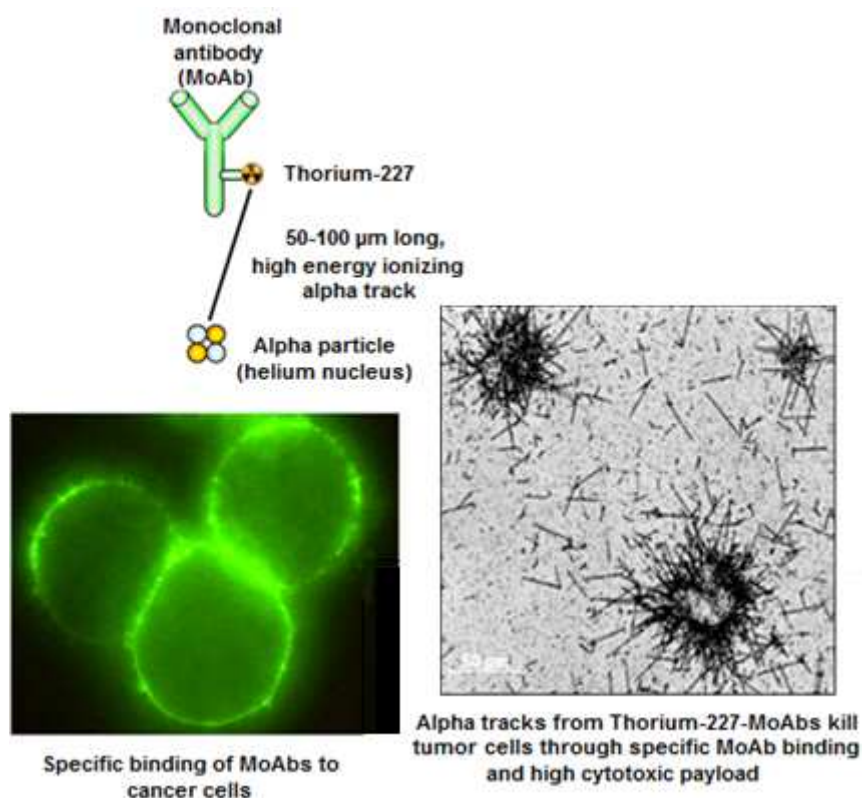


**Figure 2.7:** By conjugation of the  $^{227}\text{Th}$  to a MoAb, the MoAb will specifically bind to the antigen-expressing cancer cell so that  $\alpha$ -particles emitted from  $^{227}\text{Th}$  have the potential to kill the tumor cells.<sup>[12]</sup>

The two TTCs used in this experiment are called  $^{227}\text{Th}$ -AC0103 and  $^{227}\text{Th}$ -AC0303. The first TTC is trastuzumab (Ab01), conjugated to chelator and labeled with  $^{227}\text{Th}$ . The second TTC consists of an antibody (Ab03) from an external partner conjugated to chelator and labeled with  $^{227}\text{Th}$ . Due to confidentiality agreements between Algeta and the external partner, the name and structure of Ab03 and its target cannot be given in this report. The same chelator is conjugated to both TTCs. The name and structure of this chelator cannot be given. A schematic structure of the two TTCs together with an overview of their properties is given in Table 2.1.

Several studies have been performed by Algeta to determine the quality of the different TTCs. It is important to fully characterize the properties of radiolabeled MoAbs intended for targeted radiotherapy. Characterization includes various analytical tests and studies to evaluate homogeneity, purity, stability *in vitro*, and biodistribution, pharmacokinetic, dosimetry and radiation-absorbed doses *in vivo*. In addition, the ABC of the antibodies is an important characteristic examined by both *in vitro* and *in vivo* studies.<sup>[14]</sup>



If a decrease in IRF occurs from the value for the original MoAb, it is usually caused by conjugation of chelators to the binding site of the MoAbs, by the labeling procedure or by radiolysis during storage of the RIC.<sup>[60]</sup> Radiolabeling requires conjugation of a chelator, usually to lysine residues. If the chelator targets critical lysines in the binding regions of an antibody, the immunoreactivity may decrease.<sup>[13]</sup>

**Table 2.1:** An overview of the structures, naming and molecular weights ( $M_w$ ) of the two Targeted Thorium Conjugates (TTCs) used in this project.

$^{227}\text{Th-AC0103}^a$	$^{227}\text{Th-AC0303}^a$
<p style="text-align: center;">Ab01</p>	<p style="text-align: center;">Ab03</p>
Ab01 = Trastuzumab	Ab03 = <i>confidential</i>
Chelator = <i>confidential</i> ; $M_w = 997$ Da	
Average $M_w = 148$ kDa	Average $M_w = 147$ kDa
Targets Ag(01) = HER-2	Targets Ag(03) = <i>confidential</i>

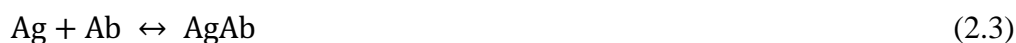
<sup>a</sup>The blue and red color used here to illustrate the two different antibodies, are also used in the results to distinguish between the two different RICs.

---

## 2.4 Binding assays – a theoretical analysis

---

A binding assay gives a measurement of the binding properties of the antibody to an antigen, that may be a receptor either on living cells, dead cells or receptor fragments.<sup>[60]</sup> The reaction between antibody, Ab, and antigen, Ag, forming an immune complex, AbAg, may be described by the law of mass action (Equation 2.3):



The association constant,  $K_a$ , can further be expressed as the ratio between the concentration of the bound antibody-antigen complex, [B], and the product of free antigen and free antibody concentration at equilibrium; [Ab] and [Ag] respectively. This is described by Equation 2.4;<sup>[36]</sup>

$$K_a = \frac{[\text{B}]}{[\text{Ab}] \cdot [\text{Ag}]} \quad (2.4)$$

These equations for antibody-antigen binding make up the foundation of the two binding assays used in this project; the Lindmo- and Scatchard analyses.

### 2.4.1 Lindmo analysis

---

The conventional way of determining IRF is based on the method introduced by Lindmo in 1984, in which the fraction of radiolabeled MoAbs bound to antigen under conditions of infinite antigen excess is determined.<sup>[17]</sup> By this binding assay, a small amount of radiolabeled MoAbs is incubated with increasing concentrations of tumor cells that display the target epitopes/receptors. The IRF is determined by linear extrapolation of the results to obtain the IRF value at infinite antigen-excess. According to Lindmo himself, the infinite excess of antigen ensures that the true value of IRF is obtained as opposed to the apparent IRF determined by a limited excess of antigen.<sup>[17]</sup>

If not all, but only a fraction of the total amount of antibody is immunologically reactive, the law of mass action (Equation 2.3) only applies to the immunoreactive fraction, IRF, of the antibody. If [T] is the total concentration of antibody applied, then  $\text{IRF} \cdot [\text{T}]$  is the

concentration of reactive antibody. Since the bound antibody necessarily must have come out of the reactive fraction, the concentration of remaining free, reactive antibody is  $IRF \cdot [T]$  minus  $[B]$ . By inserting this to Equation 2.4, Equation 2.5 is obtained:

$$K_a = \frac{[B]}{(IRF \cdot [T] - [B]) \cdot [Ag]} \leftrightarrow [B] = K_a \cdot ((IRF \cdot [T]) - [B]) \cdot [Ag] \quad (2.5)$$

Further, Equation 2.5 can be transformed into Equation 2.6:

$$\frac{B}{T} = IRF \frac{[Ag]}{[Ag] + 1/K_a} \quad (2.6)$$

By plotting the relative binding of antigen,  $B/T$ , as a function of increasing antigen concentration,  $B/T$  will approximate the plateau value,  $IRF$ , if  $[Ag] \gg 1/K_a$ . Thus, to give an accurate determination of the  $IRF$  value, it is required that the free antigen concentration is much higher than  $1/K_a$ . This can be used to give an estimate of  $IRF$ , and is the principle behind the one-point-analysis used by Algeta today (see Section 1.2 "Antigen Binding Capacity"). In this method, a high cell concentration is used to ensure antigen excess and a free antigen concentration much higher than  $1/K_a$ . An approximate value of  $IRF$ , in this report denoted  $IRF^*$ , can then be determined as the percentage bound antibody in this single sample.

Often the  $K_a$  is unknown for the system in question, thus making it difficult to choose a proper antigen concentration. It has also been seen that for weakly binding antibodies ( $K_a = 10^7 - 10^8 \text{ M}^{-1}$ ), it may be difficult to achieve the necessary antigen concentration with cells having a realistic surface density of antigen. For example, if  $K_a = 10^8 \text{ M}^{-1}$  and it is assumed that there are 1 million binding sites per cell, a cell concentration of 100 million cells/mL would be required to come within 5% of the true value of  $IRF$ .<sup>[61]</sup> Therefore, an extrapolation to approach the condition of infinite antigen excess could give a more correct measurement. A linear relationship between  $T/B$  and  $1/[Ag]$  can be seen in Equation 2.7, which is the inverse of Equation 2.6:

$$\frac{T}{B} = \frac{1}{IRF} + \frac{1}{IRF \cdot K_a [Ag]} \quad (2.7)$$

A double inverse plot of the graph made by Equation 2.7, T/B as a function of 1/[Ag], will yield a straight line. The origin of the abscissa will represent infinite antigen excess (1/[Ag]=0), and the corresponding value of T/B will be equal to 1/IRF. Thus, by plotting the data according to Equation 2.7 and extrapolating a fitted straight line to its intercept with the y-axis, the fraction of immunoreactive antibody is determined as the inverse of the intercept value.

In the Lindmo assays of this project, the coefficient of determination,  $R^2$ , will be an important parameter to indicate how good the regression model in Equation 2.7 fit the experimental data.  $R^2$  is defined as the proportion of the total variation that is explained by the linear regression of y on x, in this case of B/T on 1/[Ag].<sup>[62]</sup>

## 2.4.2 Scatchard analysis

---

In 1949 Scatchard developed a method of using a linear plot of equilibrium binding values to calculate  $K_a$  and the number of binding sites in the system.<sup>[18]</sup> This method will be used in this project to estimate the number of antigen binding sites per cell or bead and to compare the apparent association constants for the two TTCs to their antigens. The equations describing the binding model used in the Scatchard analysis can be derived from Equation 2.4.

By renaming the concentration of free, unbound antibody to [F] for this purpose, and by introducing that free antigen concentration equals the total concentration of antigen in the system,  $[Ag]_{tot}$ , minus [B], Equation 2.4 can be rewritten to Equation 2.8:

$$K_a = \frac{[B]}{[F] \cdot ([Ag]_{tot} - [B])} \quad (2.8)$$

Equation 2.8 can again be rewritten to Equation 2.9:

$$\frac{B}{F} = K_a \cdot [Ag]_{tot} - K_a \cdot [B] \quad (2.9)$$

A plot of the ratio between bound and free antibody,  $B/F$ , against  $[B]$  will yield a straight line with the slope  $-K_a$ . From Equation 2.9 it can be seen that when  $B/F=0$ , the value of  $[B]$  will be equal to  $[Ag]_{tot}$ . Thus, by extrapolating a fitted straight line of the plot of  $B/F$  against  $[B]$  to its intercept with the x-axis, the corresponding value of  $[B]$  will be equal to the total antigen concentration in the system. From this value, the number of antigens and the corresponding number of receptor sites per cell or bead can be calculated.

### **2.4.3 Assumptions of the binding models**

---

The models described by Equation 2.3 to 2.9 represent many simplifications of the normal situation. These assumptions are made:<sup>[36]</sup>

- Both antigen and antibody are homogenous
- Each antigen represents only one epitope for binding
- The antibody has a single binding site that recognizes only one epitope
- Binding is uniform with no positive or negative allosteric effects (the binding of one antibody binding site will not influence the binding of another site)
- There are no nonspecific binding, such as to the walls of the reaction tube

The last assumption can in some cases represent a big error, and should be taken into account. The fraction of nonspecific binding will therefore be measured and subtracted from measured binding in all binding assays in this project. Although it is impossible for all the other assumptions to be completely met in practice, the Equations 2.6, 2.7 and 2.9 provide useful theoretical models for the binding assays used in this project.

---

## 2.5 Microbead technology

---

As described introductorily, the main objective of this project is to develop a new immunoreactivity assay that is independent of cells. In this section the basis of the new method, microbeads, will be presented. Further, the biotinylation of antigens for the purpose to coat them to the beads will be described.

The microbeads used in this project are Dynabeads<sup>®</sup> from Invitrogen Dynal. These were developed after professor John Ugelstad in 1976 managed to create uniform polystyrene spherical beads of exactly the same size at the Norwegian Institute of Technology (NTH; today the Norwegian University of Science and Technology (NTNU)).<sup>[63]</sup> Professor Ugelstad and his colleagues made these beads superparamagnetic, meaning that they are only magnetic in a magnetic field. Due to this property, the beads can easily be resuspended when the magnetic field is removed. This innovation can be used for many applications, among others cell isolation, immunoassays, protein or nucleic acid isolation, and chromatography.<sup>[64]</sup>

Microbeads might have many advantages compared to cells in analyzing the binding properties of radiolabeled antibodies. The microbeads are uniform and monodispersed, and should thus significantly reduce the variability and increase the reproducibility compared to cells. Microscope pictures of Dynabeads and SKOV-3 ovarian cancer cells used in this project are given in Figure 2.8. When working with living cells, care has to be taken to keep the cells alive. This is not a problem with the beads. In addition, it is easy to obtain uniform conjugation of antigen to the beads because big amounts of particles can be processed at the same time. The beads used in this project are 2.8  $\mu\text{m}$  in diameter, and are thus considerably smaller than the SKOV-3 cells with an average diameter of 14  $\mu\text{m}$ .<sup>[65]</sup>

The beads used in this project are pre-coated with streptavidin, and can thus bind biotinylated antigen to simulate the antigen-expressing tumor cells. Streptavidin, a biotin-binding protein isolated from the culture medium of *Streptomyces avidinii*, is a tetrameric nonglycosylated analog of avidin with a molecular weight of about 60 kDa. Streptavidin is a part of the avidin family of proteins including avidin and the avidin-like molecules; streptavidin, deglycosylated avidin, and NeutraLite avidin.<sup>[66]</sup> Like avidin, each molecule of streptavidin can bind four molecules of biotin, with an association constant that is the strongest known biological interaction between a ligand and a protein ( $K_a = 1.3 \times 10^{15} \text{ M}^{-1}$ ).<sup>[67]</sup>

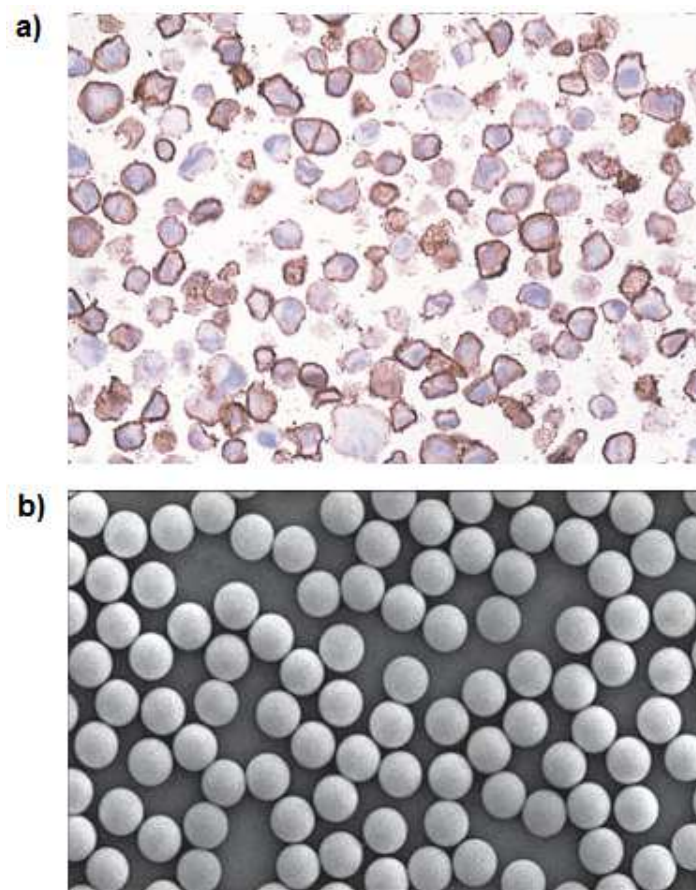


**Figure 2.8:** a) A magnified picture of cells from the ovarian cancer SKOV-3 cell-line.<sup>[68]</sup> b) A magnified picture of Dynabeads (2.8  $\mu\text{m}$  in diameter) used in this project.<sup>[69]</sup> The uniformity of the beads are thought to lead to increased reproducibility compared to the heterogenic cells. The proportions between cell- and bead sizes are not reflected by these pictures.

### 2.5.1 Biotinylation of antigen

---

Biotin is a small, hydrophobic molecule, which is present in all living cells. Its structure is shown in Figure 2.9. The addition of one (X) or two (XX) aminohexanoic acid "spacers" to the carboxyl group of biotin (see Figure 2.10) greatly enhances the efficiency of formation of the complex between the biotinylated protein and streptavidin.<sup>[70]</sup>

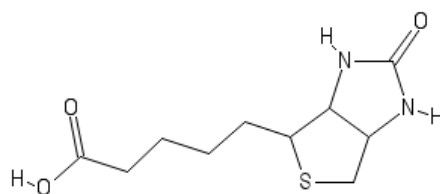


**Figure 2.9:** Structure of biotin.

The simplest and most common biotinylation method is to label the amino groups of lysine residues on the protein with a succinimidyl ester conjugated to biotin.<sup>[67]</sup> The biotin used in this project contains two spacers and the succinimidyl ester sulfo-N-hydroxysuccinimide (sulfo-NHS). The structure of sulfo-NHS-XX-biotin and reaction scheme for biotinylation is illustrated in Figure 2.10.

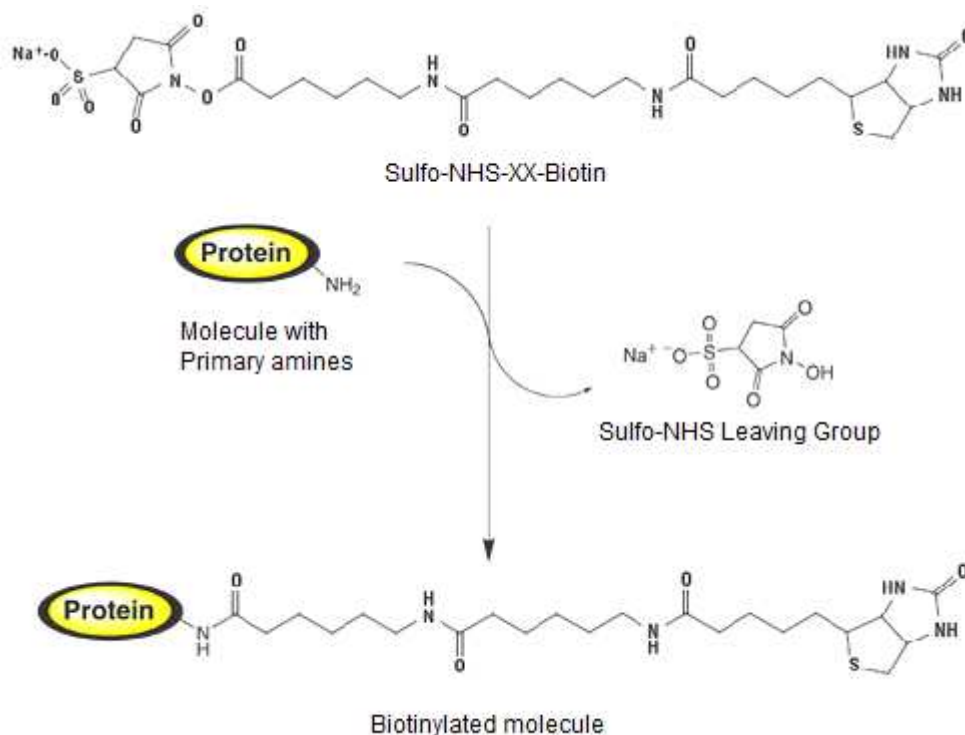


**Figure 2.10:** Structure of sulfo-NHS-XX-biotin and the reaction scheme of protein biotinylation.<sup>[71]</sup>

The 4'-hydroxyazo-benzene-2-carboxylic acid (HABA)-avidin reaction can be used to determine the degree of biotinylation. The dye HABA interacts with avidin yielding a complex with absorption maximum at 500 nm. Biotin, because of its higher affinity to avidin, displaces HABA, causing a decrease in absorbance at 500 nm proportional to the amount of biotin present in the assay.<sup>[72]</sup> This is illustrated in Figure 2.11. The absorption spectra of HABA and avidin-HABA are given in Figure 2.12.



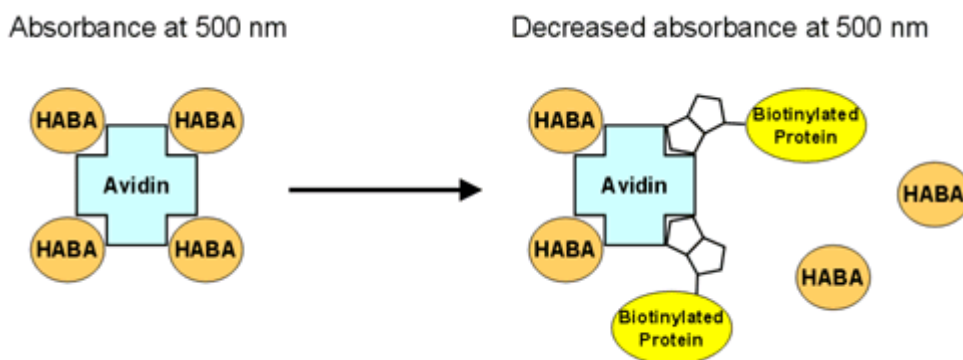


**Figure 2.11:** The principles of the HABA-Avidin reaction in determination of degree of biotinylation. Biotin binds to Avidin with a greater affinity than HABA, and will thus decrease the absorbance resulting from HABA bound to Avidin.<sup>[73]</sup>

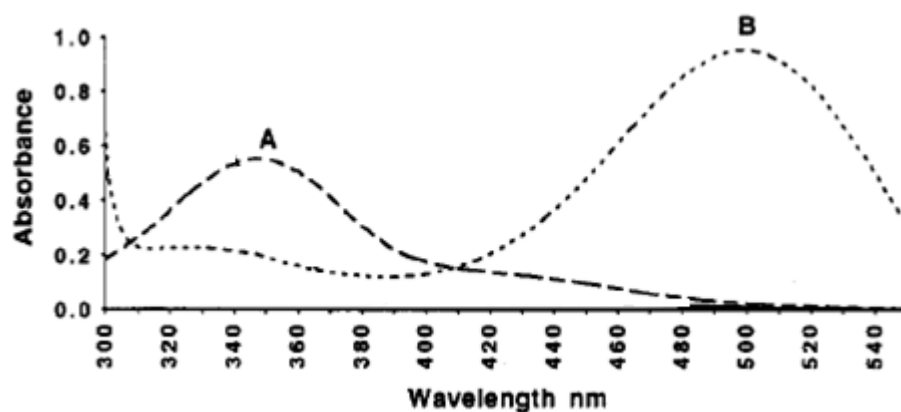


**Figure 2.12:** The absorption spectra of HABA (A) and the avidin-HABA complex (B) with absorption maxima of 348 nm and 500 nm, respectively.<sup>[72]</sup>

Due to limitations of the equipment used for absorbance measurements in this project, the absorption will be measured at 492 nm instead of at 500 nm. As seen in Figure 2.12, the absorption measured at 492 nm should give a good approximation to the absorbance at 500 nm. The equations used to determine the degree of biotinylation are derived in Section 3.3.1 “Determination of the degree of biotinylation”.



# 3 Materials and Methods

---

All experiments performed in this project were directed following the rules and guidelines stated by the Norwegian Radiation Protection Authority (NRPA)<sup>[74]</sup>, as well as Algeta's own safety guidelines. The antibody-chelator conjugates used in the experiments are named after the naming system used by Algeta. Due to a confidential agreement, Chelator03, Antibody03, the antigen targeted by Antibody03 (Ag(03)) and the cells expressing this antigen cannot be given by structure or name in this report.

The first section gives an overview of the materials and equipment used in the experiments. The following sections describe experimental procedures of the different methods used in this project. First, the preparations for the binding assays are described, including radiolabeling with <sup>227</sup>Th to produce RICs, biotinylation of antigen, antigen coating of beads and cell preparation.

Secondly, the three binding assays one-point-, Lindmo- and Scatchard analyses are described. It is chosen to describe the three different assays together, as their experimental procedures are very similar. Where the procedure differs, the description is divided into sections for the different assays. The procedures of the binding assays with cells and beads are the same.

---

## 3.1 Materials and equipment

---

The main materials used to set up the different binding assays, including the RICs, antibodies, their antigen-targets, cells expressing antigens and beads conjugated with these antigens, are given in Table 3.1. All other chemicals and solutions are given in Table 3.2 and the equipment used in the experiments is given in Table 3.3.

**Table 3.1:** An overview over the main materials used to set up the different binding assays.

Abbreviation	Full name	Description/ Properties	Provider/ Catalogue number
<b>Ab01</b>	Trastuzumab (Herceptin®)	10 mg/mL, $M_w = 148$ kDa	Roche (Welwyn Garden City, UK) Cat# 57 34 77
<b>Ab03</b>	<i>confidential</i> MoAb	~10 mg/mL, $M_w = 147$ kDa	External partner of Algeta ASA
<b>AC0103</b>	Ab01-chelator conjugate; <i>confidential</i> chelator	10 mg/mL in 0.9% NaCl, conjugation ratio (A:C) = 1:0.37, frozen vials of 100 $\mu$ L. $M_w \sim 148$ kDa	Algeta ASA (Oslo, Norway)
<b>AC0303</b>	Ab03-chelator conjugate	10 mg/mL, conjugation ratio (A:C) = 1:0.26, frozen vials of 100 $\mu$ L. $M_w \sim 147$ kDa	Algeta ASA (Oslo, Norway)
<b>Ag(01)</b>	Antigen for Ab01: Recombinant human HER-2/Fc Chimera.	The extracellular domain of human HER-2 fused with the Fc region of human IgG1 at the C-terminus. Homodimeric.  0.72 mg/mL in PBS, pH 7.5, $M_w = 192$ kDa for dimer	Sino Biological Inc. (Beijing, Kina) Cat# 10004-H02H
<b>Ag(03)</b>	Human antigen for Ab03: <i>confidential</i>	0.5 mg/mL, monomer, $M_w = 86.5$ kDa	External partner of Algeta ASA
<b>Ag(01) expressing cells</b>	SKOV-3; human HER-2 expressing ovarian cancer cells	Cells cultivated at 37°C with 5% CO <sub>2</sub> atmosphere in cell medium with 10% FBS and 1% penicillin/streptavidin. Fixated with 2 % paraformaldehyd. Frozen in vials of 10 million cells/mL	Algeta ASA (Oslo, Norway)
<b>Ag(03) expressing cells</b>	Human cells expressing Ag(03): <i>Confidential cell line</i>	Cells cultivated at 37°C with 5% CO <sub>2</sub> atmosphere in cell medium with 10% FBS, 1% non-essential amino acid, 1% NaPyr and 1% Geneticin	Freshly provided by Algeta ASA (Oslo, Norway)
<b>Magnetic beads</b>	Dynabeads® M-270 Streptavidin	10 mg (= 6-7 x 10 <sup>8</sup> ) beads/mL in PBS pH 7.4	Invitrogen Dynal AS (Oslo, Norway) (Cat# 653.06)
<b><sup>227</sup>Th</b>	227-Thorium	In 0.5 M HCl, varying activities (MBq)	Freshly provided by Algeta ASA (Oslo, Norway)

**Table 3.2:** Chemicals and solutions used in the experiments.

<b>Abbreviation</b>	<b>Full name</b>	<b>Description/ Properties</b>	<b>Provider/ Catalogue number</b>
<b>BSA</b>	Albumin from bovine serum	Solid powder	Sigma Aldrich Co. (St. Louis, MO, USA) Cat# A3294
<b>Biotin</b>	Biotin-XX; 6-((6-((biotinoyl)amino)hexanoyl)-amino)hexanoic acid, sulfosuccinimidyl ester, sodium salt	$M_w=669.7$ Da	Invitrogen by Life Technologies (Oslo, Norway) Cat# B-6352
<b>DMSO</b>	Dimethyl sulfoxide	Biotech. grade, 99.8%	Sigma Aldrich Chemie GmbH (Steinheim, Germany) Cat# 494429
<b>DTPA</b>	Diethylenetriaminepentaacetic acid	$\leq 99.0\%$	Sigma Aldrich Chemie GmbH (Steinheim, Germany) Cat# F32319
<b>HABA/Avidin</b>	4'-hydroxyazo-benzene-2-carboxylic acid (HABA)/Avidin reagent	Reconstituted with 10 mL MF-H <sub>2</sub> O	Sigma Aldrich Co. (St. Louis, MO, USA) Cat# H-2153
<b>MF-H<sub>2</sub>O</b>	Fluka TraceSELECT <sup>®</sup>	Metal free water	Sigma Aldrich Chemie GmbH (Steinheim, Germany) Cat# 95305
<b>NaOAc</b>	Sodium acetate trihydrate	Anhydrous, Molecular Biology Grade	Merck KGaA (Darmstadt, Germany) Cat# 567418
<b>PBS</b>	Phosphate buffered saline solution	Without Ca <sup>2+</sup> /Mg <sup>2+</sup> , sterile filtrated before each use	Biochrome AG (Berlin, Germany) Cat# L1825
<b>Tween20</b>	TWEEN <sup>®</sup> 20 (Polyethylene glycol sorbitan monolaurate)	Viscous liquid	Sigma Aldrich Co. (St. Louis, MO, USA) Cat# P9416

**Table 3.3:** Equipment used in the experiments.

<b>Abbreviation</b>	<b>Full name</b>	<b>Description/ Properties</b>	<b>Provider/ Catalogue or serial number</b>
<b>Amicon 10K</b>	Amicon Ultra-0.5 Centrifugal Filter Unit with Ultracel-10 membrane	0.5 mL, 10 kDa MWCO	Millipore (Cork, Ireland) Cat# UFC801024
<b>Amicon 30K</b>	Amicon Ultra-4 Centrifugal Filter Unit with Ultracel-30 membrane	4 mL, 30 kDa MWCO	Millipore (Cork, Ireland) Cat# UFC803024
<b>Centrifuge</b>	Centrifuge 5810R	For 15 or 50 mL tubes	Eppendorf AG Serial# 04296
<b>Centrifuge</b>	Centrifuge 5424	For 1.5 or 2 mL tubes	Eppendorf AG Serial# 000 4681
<b>HPGe detector</b>	GEM(15) High-Purity Germanium detector	Used with the software GammaVision-32, version 6.01	ORTEC Serial# 41-TP11566B
<b>Magnetic rack</b>	DynaMag™-2 magnet particle concentrator	Magnetic separation in small sample volumes (1.5 or 2 mL tubes)	Invitrogen Dynal AS (Oslo, Norway) Cat# 123.21D
<b>Microplate reader</b>	EnVision™ 2103 Multilabel Reader	Equipped with a 492 nm optical filter	Perkin Elmer Serial# 1030322
<b>NaI- Scintillation counter</b>	Wizard 1480 Automatic Gamma Counter	Used with the software MultiCalc version 2.7	Perkin Elmer Serial# WL60PGH2J
<b>NAP-5 column</b>	NAP™ -5 column	Separate molecules in solution according to their molecular weight	GE Healthcare (Buckinghamshire, UK) Cat# 17-0853-02
<b>Thermomixer</b>	Eppendorf comfort	For 1.5 or 2 mL tubes	Eppendorf AG Serial# 5355-30322
<b>96-well microtiter plate</b>	ViewPlate® -96 TC	White, 96-well, sterile, with lids	Perkin Elmer (Waltham, MA, USA) Cat# 6005181

---

## 3.2 Radiolabeling of antibody-chelator conjugate

---

The radiolabeling of the antibody-chelator conjugate AC0103 or AC0303 was performed the same day, or the day before the resulting radiolabeled immunoconjugate was used in an experiment. A purification of the radiolabeling product was performed right before use. A flow diagram of the radiolabeling and purification procedure is given in Figure 3.1.

One vial of AC0103 or AC0303 (100  $\mu$ L, 10 mg/mL in 0.9 % NaCl) was thawed and diluted with 100  $\mu$ L sodium acetate (NaOAc) buffer (0.5 M, pH 5.5, sterile filtrated (s.f.)).  $^{227}\text{Th}$  ( $\sim$ 1 MBq; 1-5  $\mu$ L depending on activity) was added to the solution, and the reaction mixture was incubated for 60 minutes at 37°C with shaking (750 rpm, 10 s intervals).

The radiolabeled product was separated from free  $^{227}\text{Th}$  using a NAP-5 column that separates molecules in solution according to their molecular weight. The high molecular weight (HMW) fraction will pass through the column material, while the low molecular weight (LMW) fraction will retain in the column. The column was conditioned with 10 mL of the NaOAc buffer prior to the purification. 10  $\mu$ L diethylenetriamine-pentaacetic acid (DTPA) (saturated solution in MF-H<sub>2</sub>O, s.f.) was added to the product prior to the purification in order to bind any free  $^{227}\text{Th}$ , and was allowed to react 5 minutes at room temperature. The product-DTPA mixture was added to the column together with a volume of NaOAc according to the column description (see Appendix A). The eluted void volume was collected in a tube. A new volume NaOAc buffer was added to the column according to the column description (see Appendix A), and the elute, the purified HMW radiolabeled product, was collected in a new tube. Any LMW free  $^{227}\text{Th}$  was retained in the column.

The activity (A, MBq) of void (V), HMW fraction and LMW fraction was measured by the HPGe-detector ( $^{227}\text{Th}$ -library, 7 cm calibration, 60-120 s), and the yield was calculated by Equation 3.1:

$$\text{Yield} = \frac{A(\text{HMW})}{A(\text{HMW})+A(\text{LMW})+A(\text{V})} \cdot 100\% \quad (3.1)$$

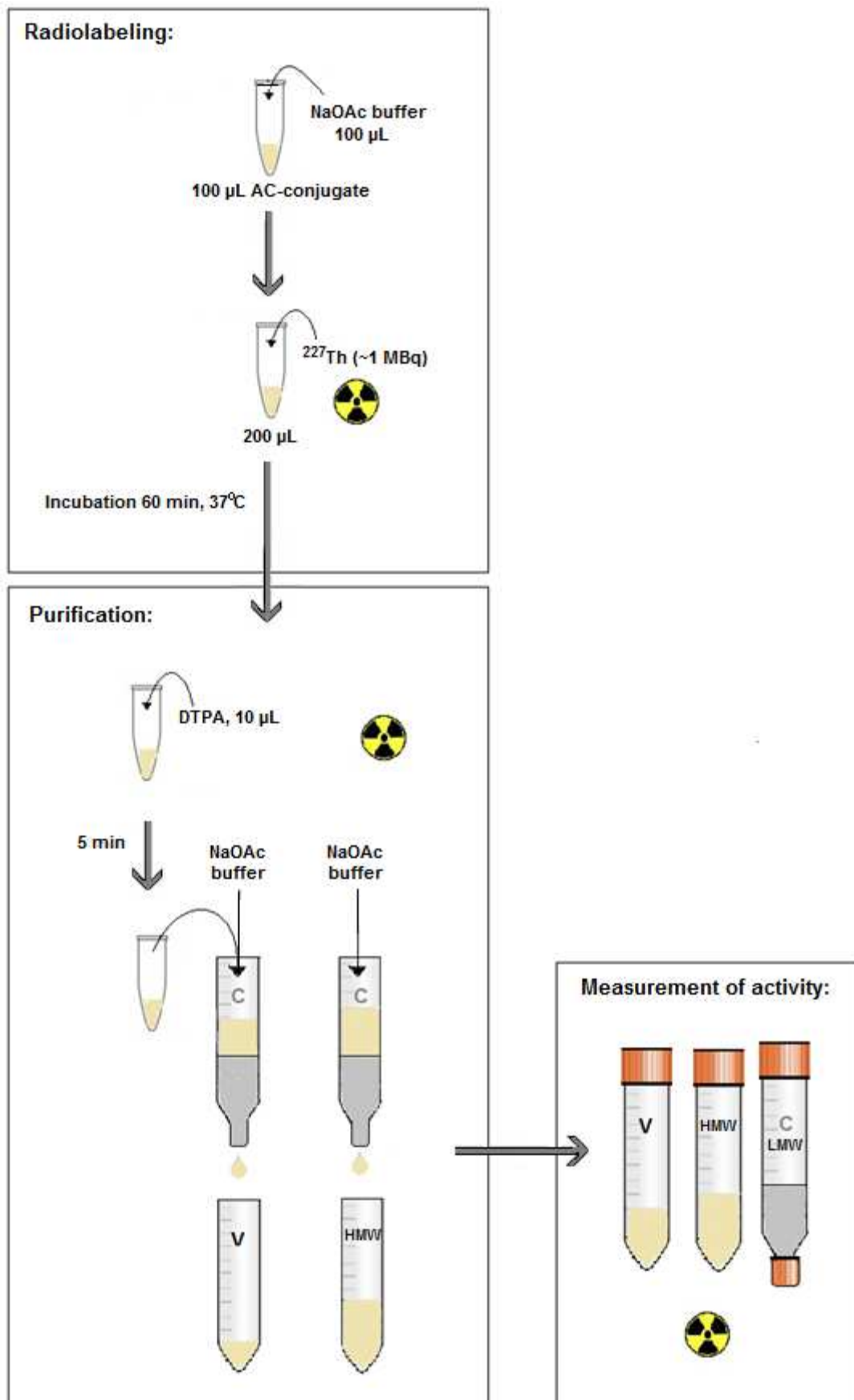


**Figure 3.1:** Flow diagram illustrating the radiolabeling of antibody-chelator conjugate with  $^{227}\text{Th}$  and purification of the radiolabeled product.



### 3.3 Biotinylation of antigen

The antigens Ag(01) and Ag(03) were biotinylated in order to coat these antigens onto the surface of the beads. The beads were pre-coated with streptavidin by the provider, which further binds biotin with high affinity.

A volume of the original antigen solution (0.72 or 0.5 mg/mL) corresponding to 1 mg antigen was up-concentrated by centrifugation (3220 rcf, 10 min) in Amicon 30K filter. The retentate was diluted to 100  $\mu$ L with PBS, resulting in a 10 mg/mL antigen concentration. 25  $\mu$ L biotin solution (10 mg/mL in DMSO) was added to the antigen solution. This corresponds to a 74:1 and 37:1 excess of biotin compared to the Ag(01) dimer and Ag(03) monomer, respectively. The biotinylation mixture with Ag(01) was incubated for 60 minutes and with Ag(03) for 30 min. Ag(03) was incubated for shorter time and with a lower excess of biotin due to instructions in the biotinylation protocol from the provider. Both biotinylation were performed at room temperature with shaking (750 rpm, 10 s intervals).

Non-conjugated biotin was removed from the reaction solution using an Amicon 10K filter. The biotin-antigen solution was centrifuged (14 000 rcf, 10 min), before the retentate was washed in the filter twice with PBS (2 x 500  $\mu$ L, 14 000 rcf, 10 min). The filter was turned upside down onto a new vial and centrifuged (1000 rcf, 2 min) followed by a washing-step with PBS (300  $\mu$ L, 1000 rcf, 2 min). A flow diagram of the procedure for removal of free biotin is given in Figure 3.2. The resulting biotinylated antigen solution was diluted to 2 mg/mL with PBS aliquoted and frozen.

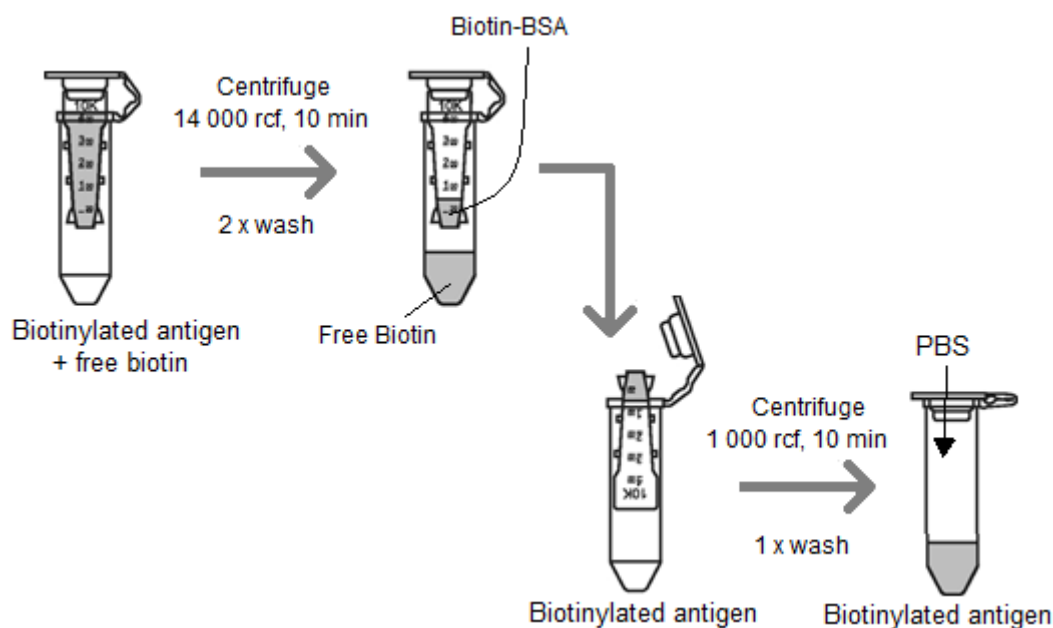


**Figure 3.2:** Removal of free Biotin from biotinylated antigen using an Amicon filter.

### 3.3.1 Determination of the degree of biotinylation

---

To determine the degree of biotinylation, the HABA/Avidin system was used.<sup>[75]</sup> 180  $\mu\text{L}$  of the HABA/Avidin solution was added to a well in a 96-well microtiter plate. The absorbance of the solution was measured by the microplate reader at 492 nm and recorded as  $A_{492}(\text{HABA/Avidin})$ . 20  $\mu\text{L}$  of the biotinylated antigen was added to the well containing HABA/Avidin, and the solution was mixed thoroughly by pipetting up and down several times. The absorbance of the solution was measured at 492 nm and recorded as  $A_{492}(\text{HABA/Avidin/Biotin})$ .

The degree of biotinylation was calculated as mole biotin per mole protein, based on the Beer Lambert Law (Equation 3.2);

$$A_{492} = \epsilon_{492} \cdot b \cdot C \quad (3.2)$$

where  $A_{492}$  is the absorbance of the sample at 492 nm,  $\epsilon_{492}$  is the extinction coefficient at 492 nm,  $b$  is the cell path length, and  $C$  is the concentration of the sample. For a standard 96-well plate and the volumes used in this procedure,  $b = 0.5 \text{ cm}$ .<sup>[75]</sup> For HABA/Avidin samples at 492 nm,  $\epsilon = 34000 \text{ M}^{-1}\text{cm}^{-1}$ .<sup>[75]</sup> First, the difference in absorbance before and after addition of Biotin to the HABA/Avidin solution was calculated by Equation 3.3.

$$\Delta A_{492} = A_{492}(\text{HABA/Avidin}) - A_{492}(\text{HABA/Avidin/Biotin}) \quad (3.3)$$

A correction factor to adjust for the dilution of the mixture by the biotinylated protein sample is not required because the dilution effect is exactly offset by the increased height and light path length of solution in the well.<sup>[75]</sup> The concentration of biotin,  $C_{\text{biotin}}$ , in the reaction mixture can then be calculated by Equation 3.4, which is a modification of Equation 3.2.

$$C_{\text{biotin}} = \Delta A_{492} / (34000 \text{ M}^{-1}\text{cm}^{-1} \cdot 0.5 \text{ cm}) \quad (3.4)$$

The molar ratio between biotin and biotinylated protein can be calculated by Equation 3.5.

$$\text{mole biotin} : \text{mole protein} = (C_{\text{biotin}} \cdot \text{dilution factor}) / C_{\text{protein}} \quad (3.5)$$

The biotinylated protein was diluted a 10-fold in the reaction mixture, giving a dilution factor of 10.  $C_{\text{protein}}$  is the concentration of biotinylated protein in the original sample.

---

## 3.4 Preparation of cells

---

For the cell-based binding assays, a cell solution was prepared freshly right before each experiment. The number of cells and cell concentration of this solution was adjusted to the assay it was going to be used for. The cell concentration had to be high enough to avoid that the sample of highest cell number in the assay exceeded 200  $\mu\text{L}$ . For example, if this sample was going to contain 10 million cells, an appropriate cell concentration would be:  $10 \text{ mill cells}/200 \mu\text{L} = 50\,000 \text{ cells}/\mu\text{L}$ .

For experiments where the binding capacity of  $^{227}\text{Th-AC0103}$  was examined, fixated Ag(01)-expressing cells were used. For experiments with  $^{227}\text{Th-AC0303}$ , living Ag(03)-expressing cells were used.

---

### 3.4.1 Preparation of Ag(01)-expressing cells

---

- The desired amount of fixated SKOV-3 cells were thawed.
- The cells were washed in PBS, centrifuged (300 rcf, 5 min) and the PBS was decanted away from the cell pellet.
- The cell pellet was resuspended in PBS to the desired cell concentration.

---

### 3.4.2 Preparation of Ag(03)-expressing cells

---

- The desired amount of Ag(03)-expressing cells were provided in cell medium and kept at  $4^{\circ}\text{C}$ .
- The cells were centrifuged (300 rcf, 5 min) right before the start of the experiment, and the cell medium was removed from the cell pellet by decantation.
- The cells were washed in PBS, centrifuged (300 rcf, 5 min) and the PBS was decanted away from the cell-pellet.
- The cell pellet was resuspended in PBS with 1% sodium azide to the desired cell concentration. Sodium azide was used to prevent internalization of antigen-receptors during the experiment.

---

## 3.5 Preparation of beads

---

A bead-solution was prepared freshly before each bead-based binding assay. This included antigen coating of the beads and preparation of a bead solution with appropriate number of beads and bead-concentration. For experiments where the binding capacity of  $^{227}\text{Th-AC0103}$  was examined, the beads were coated with Ag(01). For experiments with  $^{227}\text{Th-AC0303}$ , beads were coated with Ag(03). The antigens were in advance biotinylated as described in Section 3.3 "Biotinylation of antigen". The beads were always coated with 10  $\mu\text{g}$  biotinylated antigen per mg beads.

The number of beads and bead concentration of this solution was adjusted to the assay it was going to be used for. The bead concentration had to be high enough to avoid that the sample of highest cell number in the assay exceeded 200  $\mu\text{L}$ . The provider informed that there were 60 to 70 million beads per mg beads in the original batch. The approximation 65 million beads per mg was used to calculate the amount of beads needed from the original vial.

A solution of antigen-coated beads was prepared by the following steps:

- A volume  $V$  corresponding to the desired numbers of beads was taken out from the original vial.
- The beads were washed three times with PBS containing 0.1% Tween20 according to the user manual.<sup>[76]</sup>
- The beads were resuspended in a  $3xV$  volume of PBS with 0.1% Tween20.
- 10  $\mu\text{g}$  biotinylated Ag(01) or Ag(03) was added per mg beads in the solution.
- The bead-biotinylated antigen mixture was incubated for 30 minutes at room temperature with shaking (750 rpm, 10 s intervals).
- The mixture was washed three times as described above to remove unbound antigen.
- The antigen-coated beads were resuspended in PBS containing 0.1% Tween20 and 1% BSA to the desired bead concentration. BSA was used to prevent nonspecific binding of the RICs to the beads.

---

## 3.6 Binding assays

---

Three different types of binding assays were performed in this project; one-point analysis, Lindmo analysis and Scatchard analysis. In all of these assays, both antigen-expressing cells and antigen-coated beads were used to examine the antigen binding capacity of  $^{227}\text{Th-AC0103}$  and  $^{227}\text{Th-AC0303}$ . In all of the experiments, nonspecific binding was measured and corrected for in the analysis of data.

In the Lindmo assay, samples containing different numbers of cells or beads were used to examine binding of RIC at different antigen concentrations. IRF was determined from the results. In the one-point analysis, a predetermined number of cells or beads giving antigen excess were used to measure IRF\*. A constant amount of RIC was added to each sample of these two assays. For the Scatchard experiment, samples of a constant number of cells or beads, and thus constant amount of antigen, were prepared. Increasing concentrations of RIC were added to the different samples, and  $K_a$  and antigen expression on the cells or beads could be determined from the binding data.

---

### 3.6.1 Procedure

---

The procedures for sample preparation and binding measurements were basically the same for all three binding assays. It was also the same for cells and beads. The differences between the methods are the amounts of cells and beads in each sample, the amount of RIC, the solvent and the incubation times and temperatures. These differences are summarized in Table 3.4, and this table will be referred to several times during the description of the procedure. A flow diagram of the procedure is given in Figure 3.3. The procedure can be described by the 11 following steps:

1. A cell- or bead solution was prepared with the requisite cell- or bead concentration as described in Section 3.4 or 3.5, respectively.
2. A number of samples were prepared with the number of cells or beads specified in Table 3.4. One control sample was prepared with the number of cells or beads specified in the same table.
3. All samples were diluted with the solvent given in Table 3.4 to a volume of 200  $\mu\text{L}$ .
4. The control sample was added 10  $\mu\text{L}$  (=100  $\mu\text{g}$ ) of antibody specific for the antigen on the cells or beads in the sample. The rest of the samples were added 10  $\mu\text{L}$  solvent.

5. The control sample was blocked with shaking (750 rpm, 10 s intervals) for the time and at the temperature stated in Table 3.4. The other samples were incubated together with the control sample.
6. RIC was added by the following procedures, depending on the type of assay:

a) ***One-point- and Lindmo-analysis:***

The radioactivity (A) of a small amount of RIC (5-10  $\mu\text{L}$ ) was measured with NaI-scintillation counter (Thorium-program, 1 min), and the sample was diluted in order to obtain  $A \sim 100$  cpm/ $\mu\text{L}$ . 5  $\mu\text{L}$  ( $\sim 500$  cpm) of the dilution was added to each sample, including the blocked sample.

b) ***Scatchard-analysis:***

A 1:4 dilution series of the RIC was made, starting at 3 pmol (starting at 7 pmol for Ag(01)-expressing cells). The result was 4 different dilutions with concentrations from 0.05-3 pmol (0.1-7 pmol). 10  $\mu\text{L}$  of each dilution was added to 5 samples of equal antigen concentration, resulting in a decreasing concentration of RIC in each sample.

7. All samples were incubated with shaking (750 rpm, 10 s intervals) for the time and at the temperature specified in Table 3.4.
8. Solvent was added to each sample up to 1000  $\mu\text{L}$ .
9. Cell-samples were centrifuged (300 rcf, 5 min) and bead-samples were placed on the magnetic rack.
10. 500  $\mu\text{L}$  of the supernatant in each sample was transferred to new vials, labeled S. The original vials, containing cell or bead pellet and half of the supernatant, were labeled P.
11. Radioactivity was measured in all samples using the NaI-scintillation counter (Thorium program, 5 min per sample).

**Table 3.4:** Overview of samples for the different analyses. Parts of the binding assays that differ between cells or beads are also described here.

Experiment/ Part of experiment	Cells		Beads		RIC
	Ag(01)	Ag(03)	Ag(01)	Ag(03)	
<i>One-point analysis</i> 1 sample	1 mill	50 mill	15 mill	15 mill	~500 cpm
<i>Lindmo analysis</i> 6-10 samples	10 000- 5 mill	5 mill- 75 mill	25 000- 25 mill	50 000- 25 mill	~500 cpm
<i>Scatchard analysis</i> 4 samples	500 000 <sup>a</sup>	5 mill	10 mill	10 mill	0.05-3 pmol (0.1-7 pmol <sup>a</sup> )
<i>Control sample</i> 1 sample for every experiment	1 mill  10 µL Ab01	50 mill  10 µL Ab01	15 mill  10 µL Ab03	15 mill  10 µL Ab03	<i>One-point/ Lindmo:</i> ~500 cpm  <i>Scatchard:</i> 0.2 pmol
<i>Solvent</i> Added up to 200 µL	PBS	PBS+ 1% sodium- azide	PBS+ 1% BSA	PBS+ 1% BSA	
<i>Blocking</i> Before addition of RIC	30 min  37°C	30 min  4°C	30 min  37°C	30 min  37°C	
<i>Incubation</i> After addition of RIC	2.5 h  37°C	4.0 h  4°C	2.5 h  37°C	2.5 h  37°C	

<sup>a</sup>The Scatchard experiment with Ag(01) expressing cells were added 0.1-7 pmol <sup>227</sup>Th-AC0103

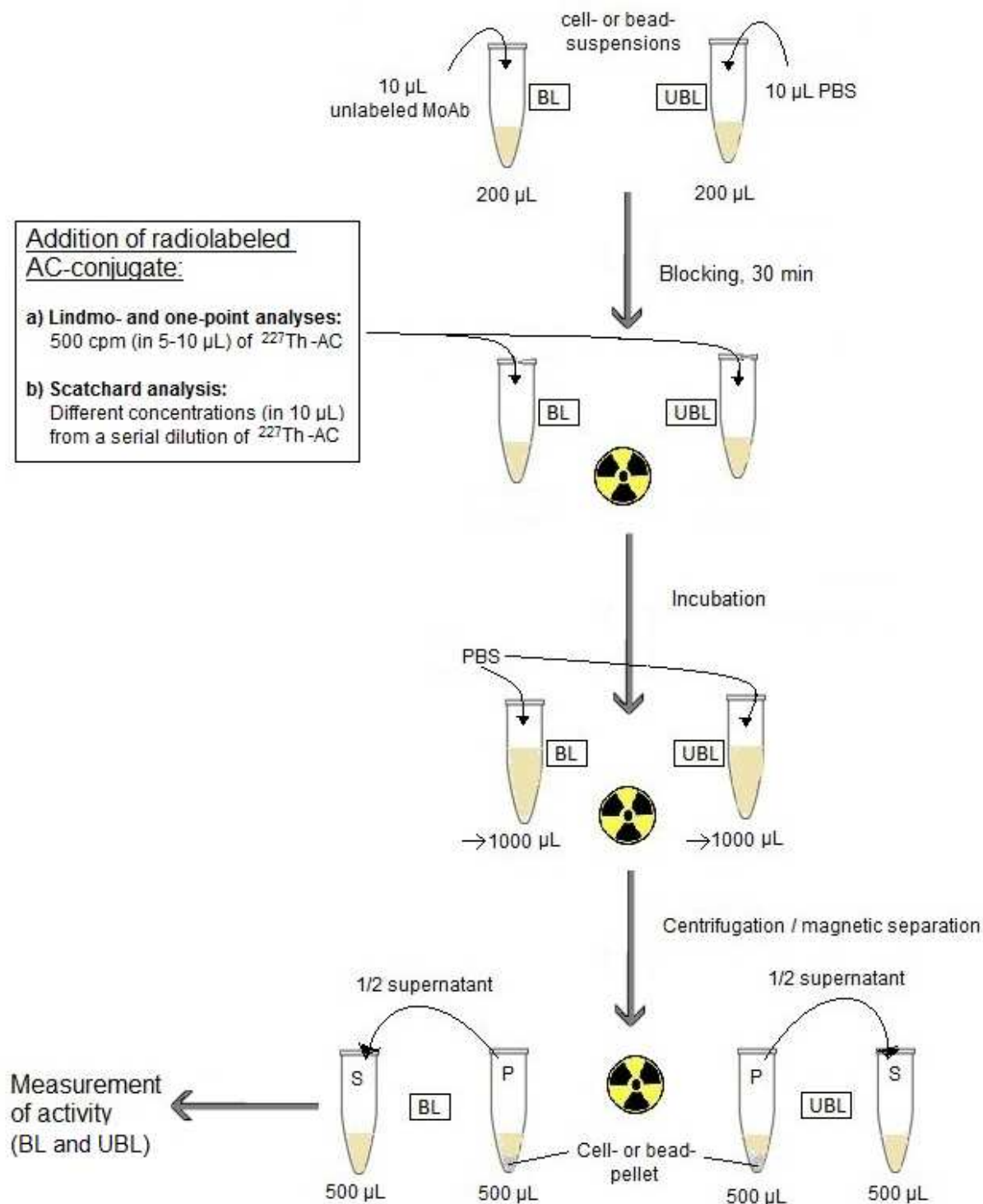


**Figure 3.3:** The general procedure for measuring binding. The amount of radiolabeled antibody added to the samples differs in **a)** the Lindmo- or one-point-analyses and **b)** the Scatchard analysis. BL = Blocked sample, UBL = Unblocked sample,  $^{227}\text{Th}$ -AC = Antibody-chelator conjugate labeled with  $^{227}\text{Th}$ .



---

## 3.7 Analysis of binding data

---

From the binding measurements made as described in the previous section, the data were analyzed in different ways depending on the kind of analyses performed. Common for all analyses was the calculation of fraction bound RIC. This property was calculated for each sample by Equation 3.6;

$$(B/T)^* = [(A_P - A_S)/(A_P + A_S)] \cdot 100\% \quad (3.6)$$

where  $A_P$  is measured activity in the sample with cell or bead pellet and half of the supernatant and  $A_S$  is measured activity in the sample containing half of the supernatant.  $(B/T)^*$  is total bound RIC, including nonspecific binding. To determine the nonspecific binding fraction,  $B/T_{BL}$ , the same calculation was made for the blocked sample, given in Equation 3.7;

$$B/T_{BL} = [(A_{P,BL} - A_{S,BL})/(A_{P,BL} + A_{S,BL})] \cdot 100\% \quad (3.7)$$

Then, specific binding,  $B/T$ , could be determined by subtracting  $B/T_{BL}$  from  $(B/T)^*$  as given in Equation 3.8;

$$B/T = (B/T)^* - B/T_{BL} \quad (3.8)$$

$B/T$  of the samples of an experiment were used in all three assays, but in different ways. In the following sections the data analysis for the one-point-, Lindmo- and Scatchard-assays is described.

### 3.7.1 One-point-analysis

---

In the one-point-analysis, binding was measured at a given, high number of cells or beads, ensuring antigen excess. The apparent immunoreactive fraction,  $IRF^*$ , of this sample equals the fraction of specific bound RIC,  $B/T$ , in this sample.

### 3.7.2 Lindmo analysis

In the Lindmo assay, only one control sample was included, and used to correct for nonspecific binding in all the samples. B/T was calculated for the samples of different cell or bead numbers and plotted against cell or bead number. With the appropriate cell or bead numbers, the resulting binding plot should give a smooth, increasing curve, reaching a plateau. A double inverse plot, a Lindmo plot, was also made. The Lindmo plot should ideally fit a straight, increasing line. An illustration of a binding- and Lindmo plot is given in Figure 3.4.

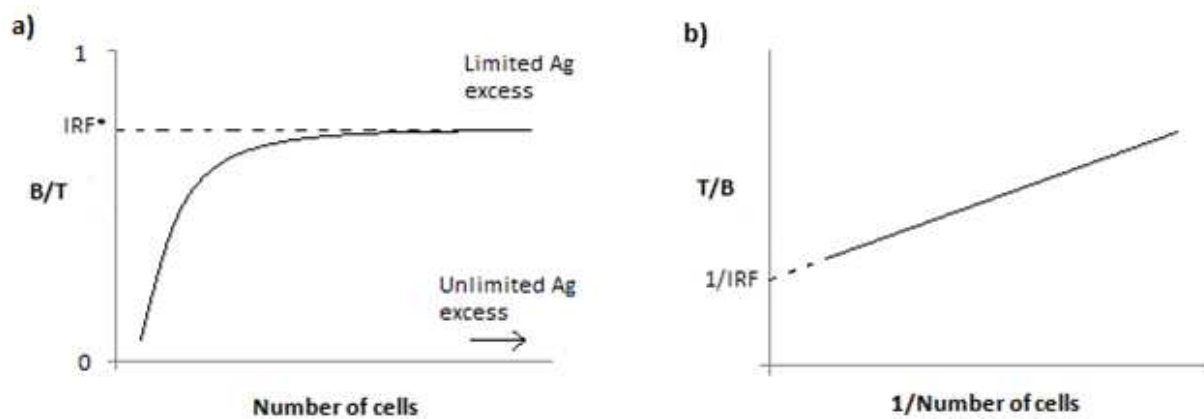


**Figure 3.4:** An illustration of the data analysis in a Lindmo experiment, **a)** a binding plot where IRF\* can be determined from the plateau. **b)** A double inverse plot of the binding plot, a Lindmo plot, where IRF can be determined at unlimited antigen excess.

The following values were determined from the two plots (see Figure 3.4):

- The plateau value of B/T in the binding plot equals IRF\*. Each sample that had reached the plateau could be seen as an one-point analysis. Each sample having the same cell/bead number as the one-point analysis (see Table 3.4), was included as a one-point analysis.
- A fitted straight line was made for the Lindmo plot by inserting a linear trendline Excel. IRF was determined as the inverse of the fitted straight line's intercept with the y-axis.
- The coefficient of determination,  $R^2$ , gives a measurement of the fit of the experimental data to the linear regression model described by Equation 2.7.

### 3.7.3 Scatchard analysis

---

In the Scatchard assay, the ratio of bound over free RIC, B/F, was plotted against [B]. Here, B/F is calculated for each sample with different RIC concentrations, by Equation 3.9;

$$B/F = \frac{B/T}{T/T-B/T} = \frac{B/T}{100\%-B/T} \quad (3.9)$$

The plot should ideally fit a straight line. A fitted straight line of the plot was made in excel. From this, the following properties could be determined;

- $K_a$  was found as the negative of the slope of the line.
- By extrapolation of the line to its intercept with the x-axis, the total number of moles antigen,  $n_{Ag,tot}$ , was determined as the intercept value.
- The number of antigens,  $N_{Ag}$ , per cell or bead unit could then be calculated as number of antigens per unit by Equation 3.10. Here,  $N_A$  is the Avogadro constant ( $6.022 \cdot 10^{23} \text{ mol}^{-1}$ ) and  $N_{unit}$  is the number of units per sample;

$$N_{Ag}/unit = n_{Ag,tot} \cdot N_A / N_{units} \quad (3.10)$$

An illustration of a Scatchard plot with values that can be determined from it is given in Figure 3.5.

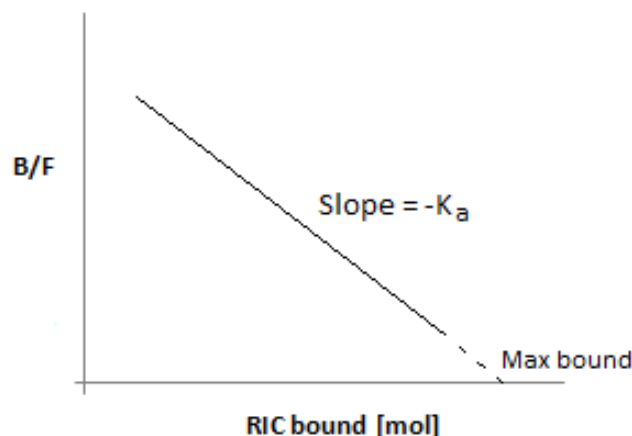


**Figure 3.5:** An illustration of the data analysis in a Scatchard experiment. The ratio of bound over free RIC is plotted against moles of RIC bound.  $K_a$  and the maximum amount of RIC that can bind can be determined from the graph. From maximum bound RIC, the amount of antigen in the system can be calculated.



## 4 Results

---

This chapter gives a summary of the results from this project. First, the results from the preparation of RICs and the biotinylation of antigens are presented. Secondly, the results from the Scatchard analysis are given. By the Scatchard plot, the binding affinities of  $^{227}\text{Th}$ -AC0103 and  $^{227}\text{Th}$ -AC0303 to their target antigens on cells and beads were determined. In addition, the antigen expression on cells and beads was found from this plot. These results form the basis for, and substantiate, the results from the main part of this project; the immunoreactivity measurements.

The results from the different methods measuring immunoreactivity are presented at the end of this chapter. The one-point analysis was used for determination of immunoreactive fraction at limited antigen excess, IRF\*. The Lindmo assay was used to determine immunoreactive fraction at unlimited antigen excess, IRF. First, the results from initial experiments, performed to develop the cell- and bead-based assays are given. Secondly, the results from several experiments with the developed cell- and bead-based assays are given.  $^{227}\text{Th}$ -AC0103 was used to develop and evaluate the methods, while  $^{227}\text{Th}$ -AC0303 was used as a second RIC with different binding properties to evaluate the applicability of the methods.

Only a summary of the most important results is presented in this chapter. All results can be found in Appendices B - I. All raw data used to produce these results, together with calculation examples, are also included in the appendices.

---

### 4.1 Preparation of RICs and biotinylated antigens

---

The RICs were freshly prepared before every experiment, and only used the same day or the day after radiolabeling. The biotinylated antigens were used to coat the beads for the bead-based binding assays. Successful preparation of these materials was thus a presumption for successful results in the binding assays. In the first section, the yields and specific activities of the RICs resulting after radiolabeling and purification are presented. In the second section, the degrees of biotinylation for the biotinylated antigens Ag(01) and Ag(03) are presented.

### 4.1.1 Yield and specific activity after radiolabeling

---

AC0103 was used to develop and assess the binding assays, thus it was labeled with  $^{227}\text{Th}$  for a total of 12 times. AC0303, being a control of the applicability of the methods, was labeled twice. The resulting TTCs were purified immediately after the radiolabeling, and the calculated yield after this first purification represents the fraction of  $^{227}\text{Th}$  bound by the chelator. A second purification was performed if the radiolabeled conjugate was used the day after radiolabeling. The yield from this second purification may give a measurement of how stable the product from the radiolabeling is. The yields and specific activities for all radiolabeled samples, together with raw data from the activity measurements and calculations, are given in Appendix B. A summary of the results is given in Table 4.1. The ranges of the yields in Table 4.1 are within the normal and acceptable range stated by Algeta.

**Table 4.1:** Summary of the results after radiolabeling of antibody-chelator-conjugates (AC) with  $^{227}\text{Th}$ . Average values  $\pm$  S.D. are given. n = number of experiments performed

Measurements	$^{227}\text{Th}$ -AC0103	$^{227}\text{Th}$ -AC0303
Yield after first purification [%]	$95 \pm 2$ (n=12)	$90 \pm 2$ (n=2)
Recovery after second purification [%]	$96 \pm 2$ (n=9)	$92 \pm 5$ (n=2)
Specific activity [Bq/ $\mu\text{g}$ ]	500 - 1000 Bq/ $\mu\text{g}$	
Radiolabeling ratio ( $^{227}\text{Th}$ :AC)	$\sim 1 : 2000^a$	

<sup>a</sup>Calculated from the average specific activity of 750 Bq/ $\mu\text{g}$

### 4.1.2 Degree of biotinylation

---

Each of the antigens Ag(01) and Ag(03) were biotinylated once, and the resulting batches of biotinylated antigen were used throughout the project. The degrees of biotinylation for these antigens were determined as described in Section 3.3.1 "Determination of the degree of biotinylation". The results were as follows:

- **mole biotin : mole Ag(01) = 11.4 : 1**
- **mole biotin : mole Ag(03) = 3.6 : 1**

The raw data from the absorbance measurements, together with calculations, are given in Appendix C. The calculated values are for the Ag(01) dimer and Ag(03) monomer.

## 4.2 Scatchard analysis

A Scatchard binding assay was performed for  $^{227}\text{Th-AC0103}$  with Ag(01)-expressing cells and Ag(01)-coated beads, and for  $^{227}\text{Th-AC0303}$  with Ag(03)-expressing cells and Ag(03)-coated beads. The different cells and beads were expected to have different antigen expressions. It was desirable to add the same series of RIC concentrations to the samples of the different binding systems. Therefore, samples for the four different systems contained different numbers of cells or beads, based on their expected binding capacities (see Table 4.2). The resulting Scatchard plot is given in Figure 4.1.

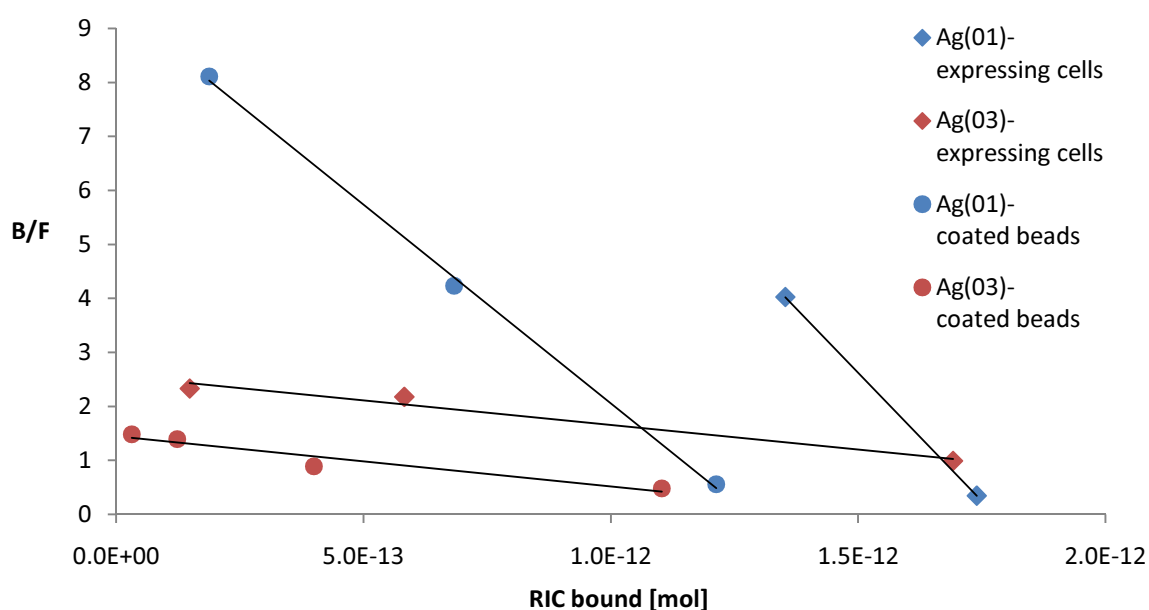


**Figure 4.1:** Scatchard plot for the four different binding systems used in this project. The ratio of bound to free RIC is plotted against moles of RIC bound.

The colors and shapes of the plotted points in Figure 4.1 represent different RICs and antigen expressing units. This is illustrated in the legend of the figure, and will be used throughout the report.

The association constants,  $K_a$ , for the two RICs binding to their target antigens on cells or beads, were determined from the Scatchard plot in Figure 4.1. These  $K_a$  values are measurements of the binding affinity of the RICs to their target. The number of antigens per cell or bead was determined from the same plot. The determined  $K_a$  values and antigen expressions for the different cells and beads are given in Table 4.2.

**Table 4.2:** Numbers of receptors per unit (cell or bead) and  $K_a$  values calculated from the Scatchard plot in Figure 4.1.

Unit	Number of units per sample	Number of antigens per unit	$K_a$ [ $M^{-1}$ ]
Ag(01)-expressing cell	500 000	$2.3 \cdot 10^6$	$9 \cdot 10^{12}$
Ag(03)-expressing cell	5 000 000	$3.4 \cdot 10^5$	$9 \cdot 10^{11}$
Ag(01)-coated bead	10 000 000	$8.1 \cdot 10^4$	$7 \cdot 10^{12}$
Ag(03)-coated bead	10 000 000	$9.7 \cdot 10^4$	$9 \cdot 10^{11}$

When the beads were coated with antigen, 10  $\mu$ g of biotinylated antigen was added per mg of beads. The amount of added antigen bound to the beads was calculated from the numbers of antigens per bead (Table 4.2). This resulted in the following values:

- **8.4  $\mu$ g biotinylated Ag(01) bound per mg beads**
- **9.0  $\mu$ g biotinylated Ag(03) bound per mg beads**

Raw data from activity measurements of all the samples, equations for the fitted straight lines in Figure 4.1 and calculation examples are given in Appendix D.



---

## 4.3 Initial development of the immunoreactivity assays

---

Initial experiments were performed with  $^{227}\text{Th}$ -AC0103 to develop the cell- and bead-based immunoreactivity assays in this project. For the cell-based immunoreactivity assays, Ag(01)-expressing cells were used. The purpose was to find the appropriate number of cells per one-point analysis and the suitable range of cell numbers for the Lindmo analysis.

Ag(01)-coated beads were used for the bead-based immunoreactivity assays. These initial experiments were performed to optimize antigen-coating of the beads and to find adequate bead-numbers for the one-point- and Lindmo assays. Raw data from the activity measurements and binding plots from the initial experiments are given in Appendix E.

---

### 4.3.1 Initial development of the cell-based immunoreactivity assays

---

At the start of this project, the method used by Algeta to measure IRF\* was a cell-based one-point analysis using a high number of cells to ensure antigen excess. For Ag(01)-expressing cells, this amount have been 10 million cells per sample.<sup>a</sup> As a starting point and to determine where this point lies on the curve of a binding plot, a Lindmo analysis was performed with samples containing 1 million to 50 million cells. The resulting plot is given in Figure 4.2a. This binding plot illustrated that the sample containing 10 million cells lies far onto the plateau of the curve. Even the lowest cell number of 1 million cells is on this plateau, and a characteristic binding plot was thus not obtained. Therefore, a new experiment with cell numbers from 100 000 to 1 million cells was performed. The result is given in Figure 4.2b. As illustrated, there appears to be a break in the curve at 100 000 cells. To confirm this, a third experiment with cell numbers in the range 10 000 to 1 million was performed. The result is given in Figure 4.2c and shows a clear decrease in binding fraction from 100 000 to 10 000 cells.

From the results in Figure 4.2, it was determined that 1 million cells per sample would be sufficient to ensure antigen excess. This amount was thus used for further one-point analyses for  $^{227}\text{Th}$ -AC0103 with Ag(01)-expressing cells. For the Lindmo analyses, it was determined that cell numbers in the range 10 000 to 5 million cells should be used to make the characteristic binding plot and the related Lindmo plot.

<sup>a</sup> The cell numbers per sample are only approximate values, and the exact number of cells were not examined. However, the approximate number of cells provides a good way to compare different samples and experiments.

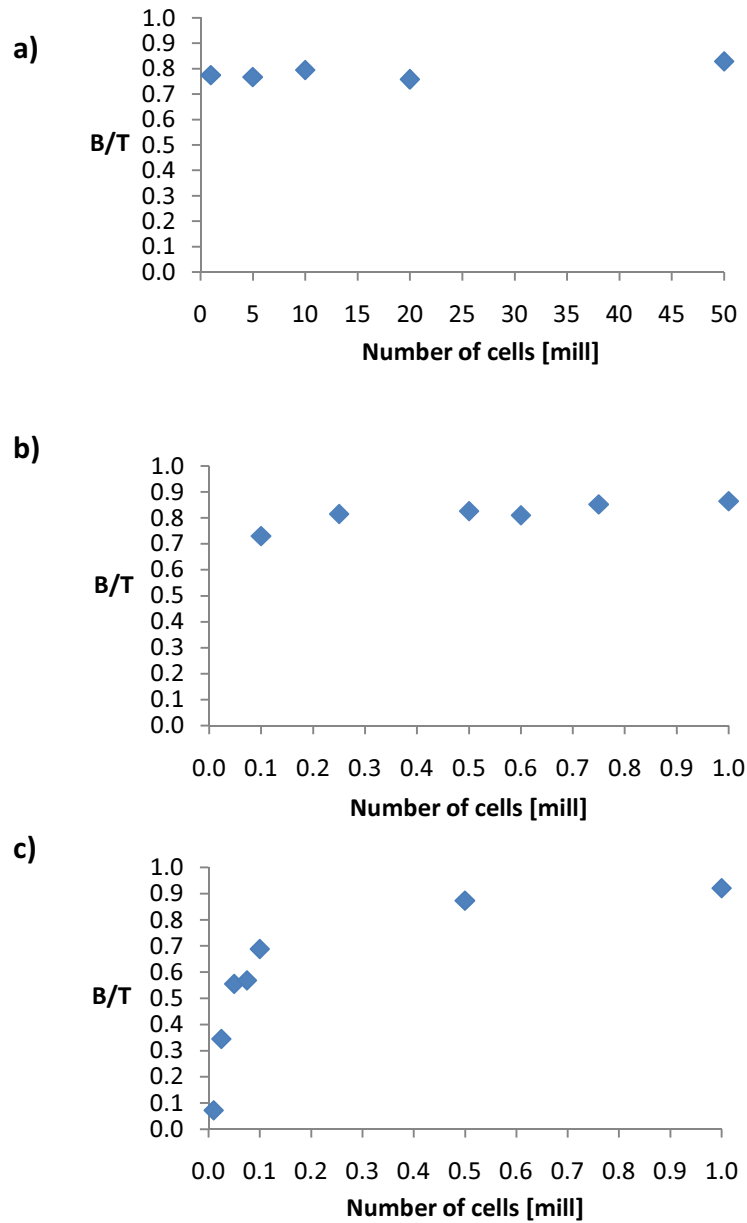


**Figure 4.2:** The binding plots for  $^{227}\text{Th-AC0103}$  resulting from the initial experiments, with cell numbers ranging from **a)** 1 to 50 million, **b)** 100 000 to 1 million and **c)** 10 000 to 1 million cells.

### **4.3.2 Initial development of the bead-based immunoreactivity assays**

---

The number of beads was used as a measure for the amount of antigen in these binding assays, in the same way the number of cells was used in the cell-based measurements. The numbers of beads are only approximate values, based on information of bead density from the provider, but they constitute a good way to compare different samples and experiments. The bead and cell numbers also provide a convenient way to compare the cell- and bead-based experiments.

Initially, the binding capacity of the beads for biotinylated antigen was examined. This was done by Lindmo analyses of  $^{227}\text{Th}$ -AC0103 with differently coated beads and a wide specter of bead numbers. Coatings of 10  $\mu\text{g}$  and 40  $\mu\text{g}$  biotinylated Ag(01) per mg of beads were tested. These quantities were chosen based on recommendations from the provider of the beads. It was concluded that 10  $\mu\text{g}$  biotinylated antigen per mg beads should be used for the further experiments.

Additional experiments were performed in order to determine the numbers of beads to be used for the bead-based immunoreactivity assays. The conclusion from this testing was that bead numbers in the range from 25 000 to 25 million should be used in the Lindmo-analysis and 15 million beads should be used in the one-point analysis. More details about these experiments and results are given in Appendix E.

## 4.4 Cell-based immunoreactivity measurements for $^{227}\text{Th-AC0103}$

The results from the cell-based immunoreactivity assays for  $^{227}\text{Th-AC0103}$  are presented in this section as average data. This includes the results from the one-point and Lindmo assays. All values for IRF\*, IRF and nonspecific binding, illustrated with calculation examples, can be found in Appendix F along with raw data. The same applies to the binding- and Lindmo plots not included in this section.

A summary of the results from the immunoreactivity measurements of  $^{227}\text{Th-AC0103}$  with Ag(01)-expressing cells is given in Table 4.3. The table gives average values for IRF\*, IRF,  $R^2$  and nonspecific binding with standard deviations.

**Table 4.3:** Average IRF\*-, IRF-,  $R^2$ - and nonspecific binding values from the cell-based one-point- and Lindmo analyses of  $^{227}\text{Th-AC0103}$  with Ag(01)-expressing cells. The number of experiments (n) and standard deviation (S.D.) are indicated.

Measurement	$^{227}\text{Th-AC0103}$ Ag(01)-expressing cells
IRF* $\pm$ S.D. [%]	81 $\pm$ 5 (n=12)
IRF $\pm$ S.D. [%]	83 $\pm$ 8 (n=6)
$R^2 \pm$ S.D.	0.83 $\pm$ 0.21 (n=6)
Nonspecific binding $\pm$ S.D. [%]	4 $\pm$ 3 (n=12)

Several cell-based Lindmo analyses were performed with  $^{227}\text{Th-AC0103}$ , including varying cell numbers in the range from 10 000 to 5 million cells. Representative examples of binding- and Lindmo-plots resulting from these experiments are shown in Figure 4.3.

From the binding plot in Figure 4.3, a plateau value of 75-80% binding can be observed. An IRF value of 83% was calculated from the Lindmo plot. IRF\* was determined to be 78% from the 1 million sample in the plot. A comparison of the different binding plots (see Appendix F) reveals relatively big variations in the appearance of the binding curves.

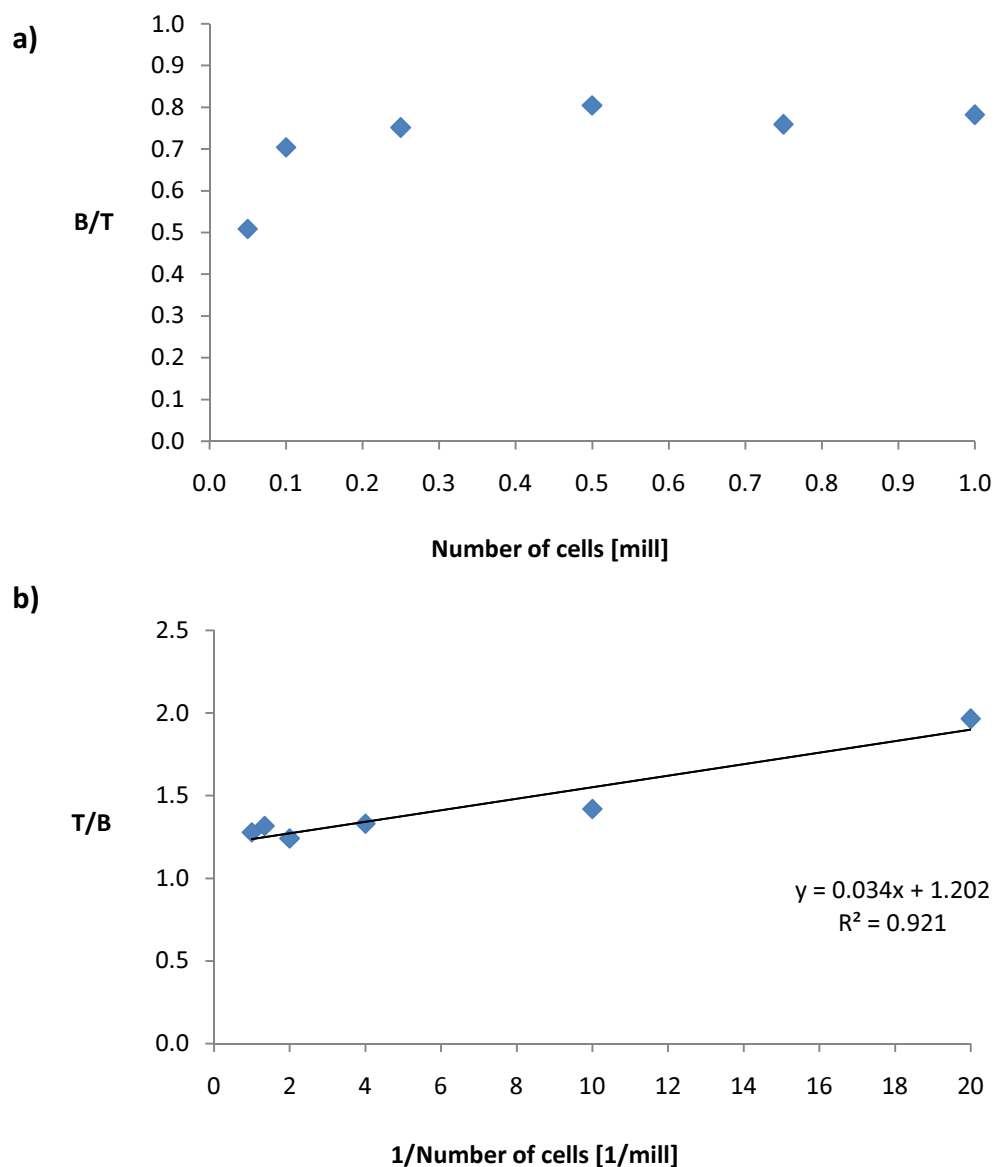


**Figure 4.3:** A representative example of the results from the Lindmo analyses of  $^{227}\text{Th-AC0103}$  with Ag(01)-expressing cells; **a)** binding plot and **b)** Lindmo plot. An IRF of 83% was calculated from the Lindmo plot.

An average binding plot is given in Figure 4.4. This plot includes points from all of the Lindmo experiments with Ag(01)-expressing cells, including the initial experiments. The average values for all measurements of the different cell numbers are given. The standard deviation is indicated for every cell number and represents the variability of the measurements. The numbers of measurements ( $n$ ) varied for the different cell numbers, as indicated in the figure. The plot reveals relatively big variations in some points.

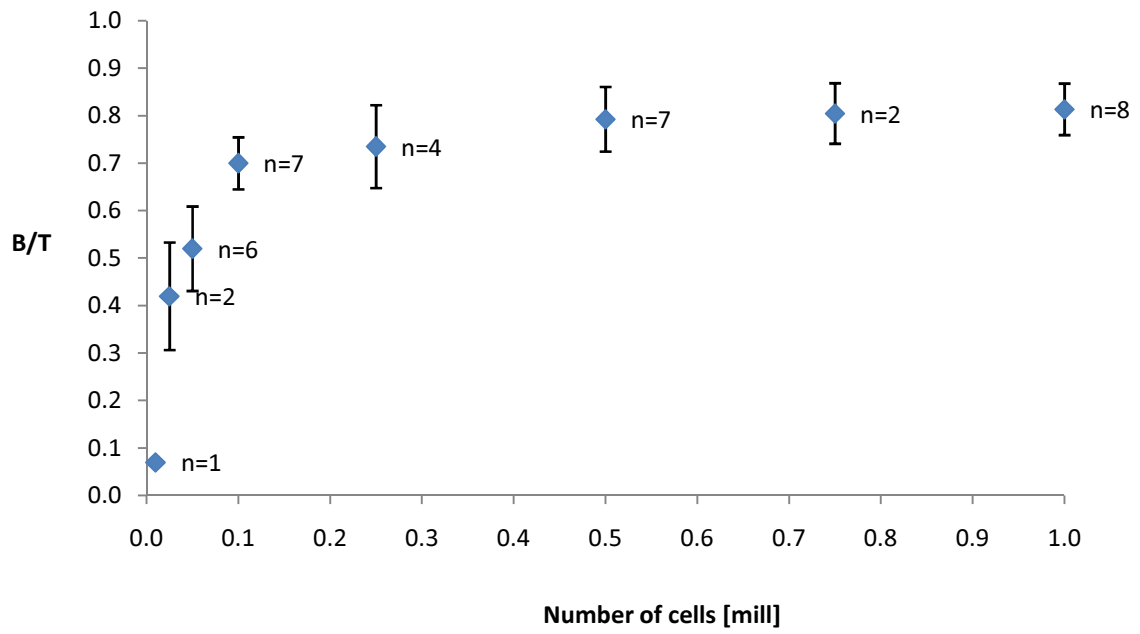


**Figure 4.4:** A binding plot demonstrating the average binding fractions from all of the Lindmo analyses for AC0103 with Ag(01)-expressing cells. Standard deviations and number of measurements (n) are indicated in each point.

---

## 4.5 Bead-based immunoreactivity measurements for $^{227}\text{Th-AC0103}$

---

In the bead-based immunoreactivity assays for  $^{227}\text{Th-AC0103}$ , Ag(01)-coated beads were used in the same way as cells to examine the immunoreactivity of this RIC. The purpose of this part of the project - and the main objective of the project - was to examine if beads can be used as a substitute for cells in these measurements.

The results from this part of the project are divided in two parts. After the optimal conditions were found for the bead-based experiments and experiments of both one-point- and Lindmo analyses had been performed for  $^{227}\text{Th-AC0103}$ , it was noticed that the nonspecific binding always was quite high. To reduce this nonspecific binding, bovine serum albumin (BSA) was added to the bead solution. BSA does not have binding affinity for the target antigens and is a commonly used blocking agent because it binds to membranes and other solid surfaces. The first part of this chapter gives average immunoreactivity values from the initial experiments without BSA. The second part gives the average results from the experiments in which BSA is used to reduce the nonspecific binding. The reason for this partition is to examine the effect the nonspecific binding has on the results. All raw data, calculations, binding- and Lindmo-plots for the bead-based experiments with  $^{227}\text{Th-AC0103}$  are given in Appendix G.

---

### 4.5.1 Immunoreactivity measurements with high nonspecific binding

---

Several experiments with beads were initially performed without BSA added to the bead-solution. A summary of the results from these experiments is given in Table 4.4. The table gives average values for IRF\*, IRF,  $R^2$  and nonspecific binding. The result shows nonspecific binding three times as high for beads compared to cells (see Table 4.3).

**Table 4.4:** Summary of the results from the initial one-point- and Lindmo analyses of  $^{227}\text{Th-AC0103}$ . The samples of these experiments were not added BSA to reduce nonspecific binding. The number of experiments (n) and standard deviation (S.D.) are indicated.

Measurement	$^{227}\text{Th-AC0103}$ Ag(01)-coated beads
IRF* $\pm$ S.D. [%]	78 $\pm$ 7 (n=11)
IRF $\pm$ S.D. [%]	83 $\pm$ 7 (n=6)
$R^2 \pm$ S.D.	0.94 $\pm$ 0.02 (n=6)
Nonspecific binding $\pm$ S.D. [%]	12 $\pm$ 3 (n=11)

## 4.5.2 Immunoreactivity measurements with reduced nonspecific binding

One-point analyses with no BSA, 1% BSA and 5% BSA were performed in order to investigate the amount of BSA needed to reduce nonspecific binding. The results demonstrated a clear decrease in nonspecific binding. From being 8-15% in the samples without BSA, the nonspecific binding decreased to 0-5% in the samples containing BSA. There was no clear difference between 1% and 5% BSA. Therefore, it was decided that 1% BSA should be added to the beads in the further experiments.

A summary of the results from the main immunoreactivity measurements of  $^{227}\text{Th}$ -AC0103 with Ag(01)-coated beads is given in Table 4.5. The beads in these experiments were added BSA. The table gives average values IRF\*, IRF,  $R^2$  and nonspecific binding with standard deviations.

**Table 4.5:** Average IRF\*-, IRF-,  $R^2$ - and nonspecific binding values from the cell-based one-point- and Lindmo analyses for  $^{227}\text{Th}$ -AC0103 with Ag(01)-coated beads. BSA is used to avoid nonspecific binding in these experiments. The number of experiments (n) and standard deviations (S.D.) are indicated.

Measurement	$^{227}\text{Th}$ -AC0103 Ag(01)-coated beads
IRF* $\pm$ S.D.	85 $\pm$ 4 (n=13)
IRF $\pm$ S.D.	93 $\pm$ 5 (n=5)
$R^2 \pm$ S.D.	0.94 $\pm$ 0.08 (n=5)
Nonspecific binding $\pm$ S.D.	2 $\pm$ 2 (n=13)

Several Lindmo analyses were performed for  $^{227}\text{Th}$ -AC0103 with Ag(01)-coated beads. The samples contained 25 000 to 25 million beads, and they were added BSA to reduce nonspecific binding. Representative binding- and Lindmo-plots resulting from these experiments are shown in Figure 4.5. From the binding plot, a plateau value of 87-90% binding can be observed. Calculated IRF from the Lindmo plot is 98%, and IRF\* from the 15 million sample is 90%.

A comparison of the different binding plots (see Appendix G) reveals small variations in the appearance of the binding curve. Most of the binding plots give smooth curves gradually reaching a plateau with few deviating values. Small variations in the measured values can be observed.



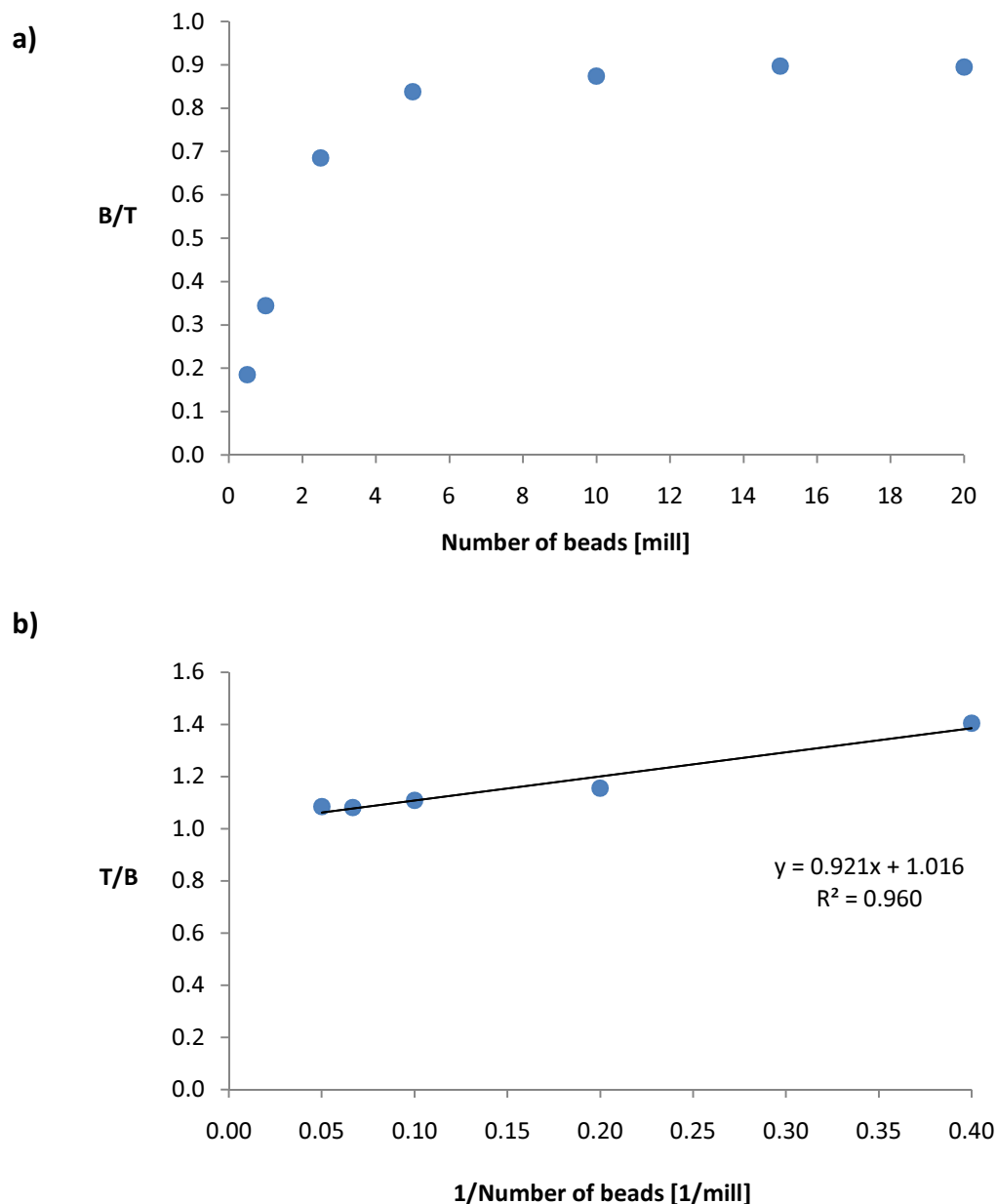


**Figure 4.5:** A representative example of the results from the Lindmo analyses of  $^{227}\text{Th-AC0103}$  with Ag(01)-coated beads; **a)** binding plot and **b)** Lindmo plot. An IRF of 98% was calculated from the Lindmo plot.

A binding plot illustrating the average binding values for each bead number is shown in Figure 4.6. This plot includes points from all of the Lindmo experiments with Ag(01)-coated beads in this project, performed with addition of BSA. The standard deviation in binding is given for each bead number. The number of measurements in each point was constant for most of the bead numbers. The average binding plot shows relatively small variations in all points.

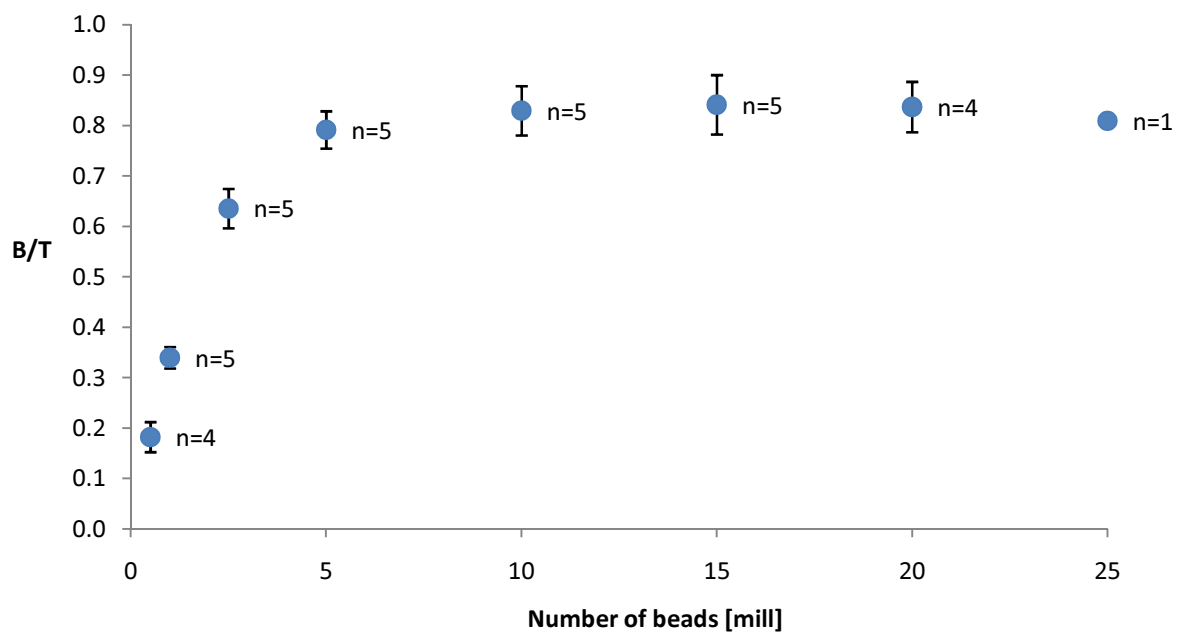


**Figure 4.6:** A binding plot demonstrating the average binding fractions from all of the Lindmo analyses for AC0103 with Ag(01)-coated beads. Standard deviations and number of measurements are indicated in each point.

---

## 4.6 Immunoreactivity measurements for $^{227}\text{Th-AC0303}$

---

$^{227}\text{Th-AC0303}$  is a RIC with different properties than  $^{227}\text{Th-AC0103}$ . Little is known about the binding capacity of this RIC, but it is thought to have a lower binding capacity than  $^{227}\text{Th-AC0103}$ . The purpose of this part of the project was to investigate the applicability of the developed immunoreactivity assays for another RIC. First, the cell-based immunoreactivity measurements are presented, and then the bead-based experiments.

All raw data, calculated values, binding- and Lindmo-plots for the cell-based experiments with  $^{227}\text{Th-AC0303}$  are given in Appendix H. The same data from the bead-based experiments are given in Appendix I.

---

### 4.6.1 Cell-based immunoreactivity measurements for $^{227}\text{Th-AC0303}$

---

Only one Lindmo-analysis was performed for  $^{227}\text{Th-AC0303}$  with Ag(03)-expressing cells. These cells have relatively low antigen expression compared to the Ag(01) expressing cells (see Table 4.2). They were therefore needed in a higher quantity, involving much time-consuming work of cell-cultivation. The high workload involved with cells is also the main reason why a bead-based assay is desired.

The cell numbers in the experiment varied from 5 million to 75 million cells. The 50 million cell sample was used to give a measure for IRF\*. The resulting values from the experiment are given in Table 4.6. The resulting binding- and Lindmo plots are shown in Figure 4.7. From the binding plot, a plateau value of 65-71% binding can be observed. An IRF of 73% was calculated from the Lindmo plot.

**Table 4.6:** The results from the Lindmo analysis of  $^{227}\text{Th-AC0303}$  binding to Ag(03)-expressing cells. Only one experiments was performed.

Measurement	$^{227}\text{Th-AC0303}$ Ag(03)-expressing cells
IRF* [%]	71
IRF [%]	73
$R^2$	0.84
Nonspecific binding [%]	5

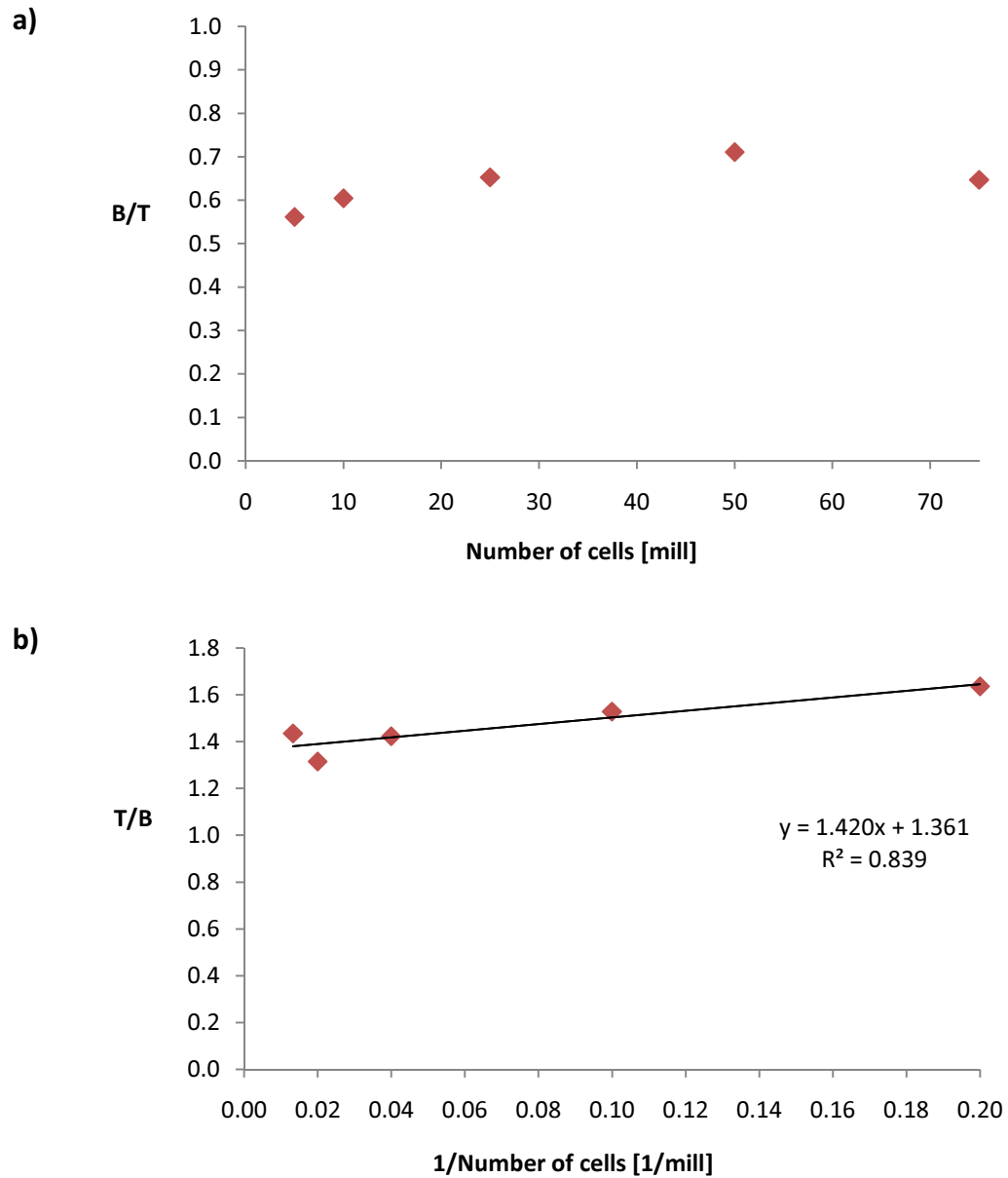


**Figure 4.7:** The result from the Lindmo analysis of  $^{227}\text{Th}$ -AC0303 binding to Ag(03)-expressing cells, displaying; **a)** the binding plot and **b)** the Lindmo plot. An IRF of 73% was calculated from the Lindmo plot.

## 4.6.2 Bead-based immunoreactivity measurements for $^{227}\text{Th-AC0303}$

A summary of the results from the immunoreactivity measurements of  $^{227}\text{Th-AC0303}$  with Ag(03)-coated beads is given in Table 4.7. The table gives average values for IRF\*, IRF,  $R^2$  and nonspecific binding with standard deviations.

**Table 4.7:** Average IRF\*, IRF-,  $R^2$ - and nonspecific binding values from the bead-based one-point- and Lindmo analyses for  $^{227}\text{Th-AC0303}$  with Ag(03)-coated beads. BSA is used to avoid nonspecific binding in these experiments. The number of experiments (n) and standard deviation (S.D.) are indicated.

Measurement	$^{227}\text{Th-AC0303}$ Ag(03)-coated beads
IRF* $\pm$ S.D. [%]	59 $\pm$ 6 (n=3)
IRF $\pm$ S.D. [%]	63 $\pm$ 8 (n=3)
$R^2 \pm$ S.D.	0.97 $\pm$ 0.04 (n=3)
Nonspecific binding $\pm$ S.D. [%]	7 $\pm$ 1 (n=3)

Three Lindmo analyses were performed for  $^{227}\text{Th-AC0303}$  with Ag(03)-coated beads. The samples contained 25 000 to 25 million beads, and they were added BSA to avoid nonspecific binding. Representative binding- and Lindmo-plots resulting from these experiments are shown in Figure 4.8. From the binding plot, a plateau value of 52-56% binding can be observed. Calculated IRF from the Lindmo plot is 61% and IRF\* from the 15 million sample is 56%.

A comparison of the different binding plots (see Appendix I) reveals small variations in the appearance of the binding curve. Most of the binding plots give smooth curves gradually reaching a plateau with few deviating values. However, relatively big variations in the plateau values of the curves can be observed.

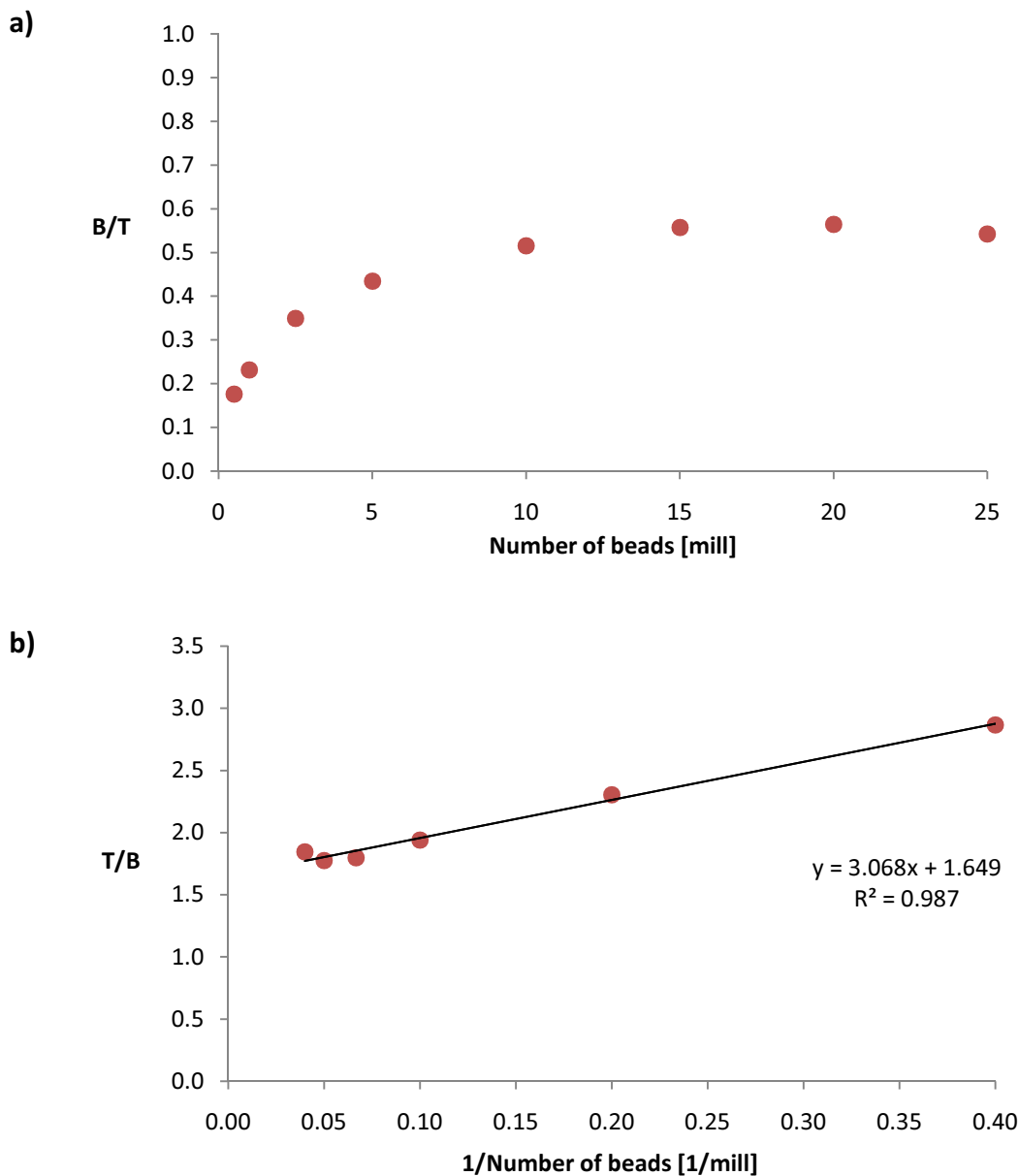


**Figure 4.8:** A representative example of the results from the Lindmo analyses of  $^{227}\text{Th-AC0303}$  with Ag(03)-coated beads; **a)** binding plot and **b)** Lindmo plot. An IRF of 61% was calculated from the Lindmo plot.

A binding plot illustrating the average binding values for each bead number is given in Figure 4.9. This plot includes points from all of the Lindmo experiments with Ag(03)-coated beads in this project. The standard deviation in binding for each bead number is given. The number of measurements in each point was constant for most of the points. This average binding plot shows relatively high variations in some points, especially for the plateau values.

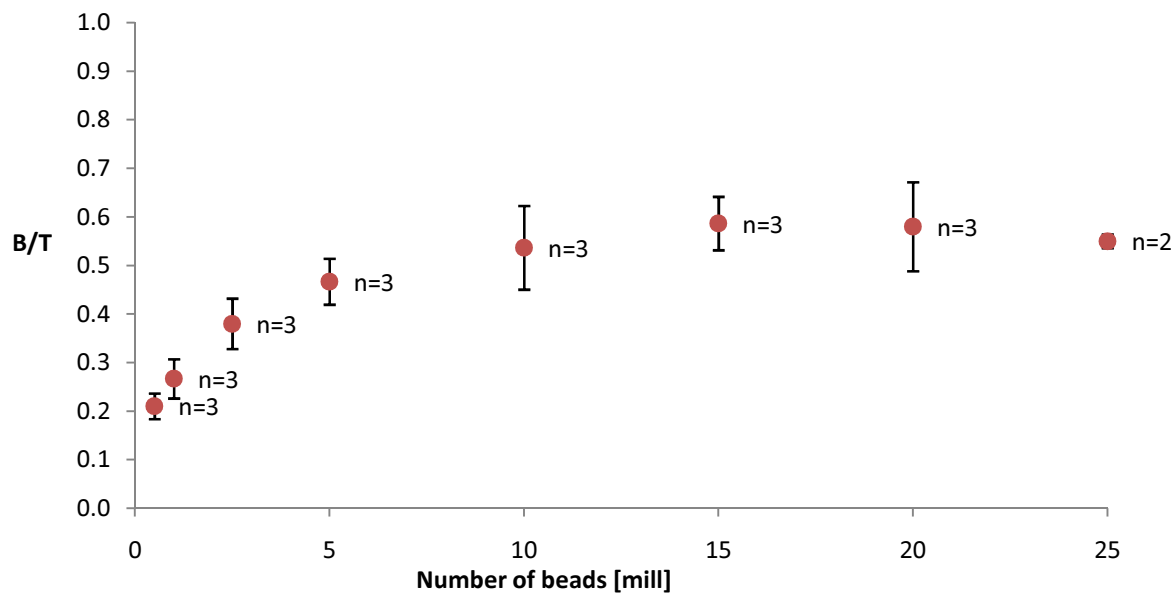


**Figure 4.9:** A binding plot demonstrating the average binding fractions from all of the Lindmo analyses for AC0303 with Ag(03)-coated beads. Standard deviations and number of measurements are indicated in each point.





# 5 Discussion

---

This part of the report gives a discussion of the results presented in the previous chapter, and an evaluation of the objectives of this project. The main purpose of this work was to examine if beads may be used as a substitute for cells in the immunoreactivity assays. A secondary aim was to investigate if the one-point assay might be used as a simplification of the Lindmo analysis.

Introductorily in this chapter, the results from the preparations for the binding assays will be discussed, including measured properties of the RICs and biotinylated antigens. Further, an evaluation of the results from the Scatchard analysis, providing a characterization of the different binding systems, will be given. The discussion of the different immunoreactivity assays and measurements constitute the main part of this chapter. First, the initial experiments with  $^{227}\text{Th}$ -AC0103 performed in order to develop the cell- and bead-based methods will be discussed. The immunoreactivity measurements resulting from these assays will then be evaluated, starting with the results for the well-known  $^{227}\text{Th}$ -AC0103. The cell-based measurements are first presented, followed by the bead-based. The same measurements performed with  $^{227}\text{Th}$ -AC0303 will be discussed to show the applicability of the bead-based method. Further, the different methods will be compared in elucidation of the results, and an evaluation of the objectives of the project will be given. Finally, a discussion of potential experimental improvements and further work is presented.

---

## 5.1 Yield, specific activity and degree of biotinylation

---

The next two sections give a discussion of the measured properties of the materials used in the immunoreactivity assays. First, the yield and specific activity of the RICs are discussed, and then the degrees of biotinylation of the antigens are evaluated.

### 5.1.1 Yields and specific activity after radiolabeling

---

The yields after radiolabeling AC0103 and AC0303 with  $^{227}\text{Th}$  were all in the range from 88% to 98%, which are all considered as acceptable values. The same can be said for the recoveries the next day, which had the same range. It might look like AC0103 with an average yield of  $95 \pm 2\%$  binds  $^{227}\text{Th}$  slightly better than does AC0303, which gives an average yield of  $90 \pm 2\%$ . A reason for this might be that the chelator is less available for

binding of  $^{227}\text{Th}$  when conjugated to Ab01 than to Ab03. Experimental variations might also have an impact on differences in yield and recovery. For example, if a small amount of the RIC solution is retained in the purification column, this might lower the measured yield. However, the differences in yield and recovery for the RICs used in this project are so small (within a 10% range) that this should not have any significance for the results in the further experiments.

The range of specific activity for the RICs was 500-1000 Bq/ $\mu\text{g}$ , corresponding to approximately one  $^{227}\text{Th}$  per 2000 AC-conjugates. A potential  $\alpha$ -emitting RIC used in patients can be predicted to have a specific activity close to this value. This is because limited amounts of radioactivity can be injected per dose, for an  $\alpha$ -emitter usually in MBq amount.<sup>[49-52]</sup> If the RIC for example had a 1:1 labeling ratio, 50 MBq would correspond to a very small amount of antibodies (in the case of Ab01/Ab03 25  $\mu\text{g}$ ). However, it has been found that a considerably higher amount of antibody is needed to ensure that the dose ends up at the site of the tumor. Thus, a relatively low specific activity and labeling ratio is needed. Pandit-Taskar *et. al.* have reported an optimal dose of 50-100 mg antibody for radioimmunotherapy with  $^{90}\text{Y}$ -labeled J591.<sup>[77]</sup> Compared to the RICs used in this project, 50 mg antibody and 50 MBq per dose would correspond to a 1:2000 labeling ratio.

It has also been observed that a high specific activity might lead to radiolysis and/or modification of the binding site of the antibody. This could again lead to a decrease in IRF. Lindmo *et. al.* experienced that their radiolabeling systems showed individual but consistent patterns of decrease in immunoreactivity with increasing radiolabeling.<sup>[17]</sup> This is another reason for using RICs with low specific activity.

### **5.1.2 Degree of biotinylation**

---

The lower degree of biotinylation for Ag(03) (3.6:1) than for Ag(01) (11.4:1) might be due to the shorter incubation time and the lower excess of biotin for Ag(03). The reason for these experimental differences was recommendations from the provider of the Ag(03) antigen. They assumed that a too high degree of biotinylation could lead to modifications of the epitope on the antigen. This modification of the epitope could again lead to an apparently lower IRF of the RIC binding to this antigen. If so, a lower IRF would be detected for the RICs binding to beads, compared with those binding to cells. As shown in the results and discussed later, a lower IRF for the RICs binding to beads is not observed. Hence, the biotinylation degrees obtained in this project are not assumed to affect the binding site on the antigens.

The degrees of biotinylation were calculated for the Ag(01) *dimer* and the Ag(03) *monomer*. The molecular weight of the Ag(01) dimer is more than the double of the Ag(03) monomer, and the Ag(01) dimer is thus expected to have more binding sites than Ag(03). If the degree of biotinylation is calculated for the Ag(01) monomer, this is 5.7:1. Thus, the actual difference in biotinylation between the two antigens is not so large.

---

## 5.2 Scatchard analysis

---

The results from the Scatchard analysis provide a characterization of the binding systems used in the immunoreactivity measurements of this project. The Scatchard plot for the different RICs gives a measure of the RIC's binding affinity for its target antigen. In addition, these plots were used to estimate the antigen expression on the cells and beads.

$K_a$  values of  $9 \cdot 10^{12} \text{ M}^{-1}$  and  $7 \cdot 10^{12} \text{ M}^{-1}$  were measured for  $^{227}\text{Th-AC0103}$  binding to Ag(01) on cells and beads, respectively. Tang *et. al.*<sup>[78]</sup> and Chan *et. al.*<sup>[79]</sup> reported  $K_a$  values for trastuzumab binding to HER-2 on SKOV-3 cells of  $2.5 \cdot 10^{11} \text{ M}^{-1}$  and  $2.0 \cdot 10^{10} \text{ M}^{-1}$ , respectively. These affinity constants are both considerably lower than the once measured in this project. Few experimental data were included in the Scatchard plots ( $n=2-4$ ), and therefore, the measured values have a high uncertainty and might not be correct. However, the measurements gave approximately the same result for the same RIC binding to cells and beads. Therefore it is assumed that the results may be used to compare the two RICs, and cells and beads, relatively to each other.

The slightly lower affinity of Ag(01) for beads than for cells might be due to the measuring uncertainties. At the same time, it might look like there is a slight difference in this RIC's affinity for cells and beads also in the binding plots from the Lindmo analyses. The binding plots with cells have a more rapidly increasing binding curve than the plots with beads, which might indicate different reaction kinetics for the binding reaction to beads and to cells. During the experiments, it was observed that the beads easily form pellets in the bottom of the vials. Also during incubation with mixing, a slight tendency for this precipitation was observed. The beads, which contain iron, are considerably heavier than cells, and might thus require stronger mixing to remain evenly suspended. If the beads precipitate in the bottom of the vial, fewer antigens will be available for binding than if the beads are evenly suspended. This might be a reason for slower reaction kinetics for the binding reaction to beads than to cells. The results also indicated that  $^{227}\text{Th-AC0103}$  has a ten times higher affinity for Ag(01) than  $^{227}\text{Th-AC0303}$  has for Ag(03). Due to the results from the immunoreactivity assays for the two RICs, the higher affinity of  $^{227}\text{Th-AC0103}$  was as expected.

The analysis of the number of antigens per cell indicated that the Ag(01)-expressing cells have  $2.3 \cdot 10^6$  antigens per cell. The HER-2 expression on SKOV-3 cells has been investigated several times before. Tang *et. al.*<sup>[78]</sup> and Chan *et. al.*<sup>[79]</sup> reported antigen expressions of  $1.3 \cdot 10^6$  and of  $1.2 \cdot 10^6$  HER-2 receptors per SKOV-3 cell, respectively. The Scatchard-plot in this project, with only two experimental points for the SKOV-2 cells, cannot

be considered as a reliable measurement. However, it seem like this method can be used to give a good estimate for the antigen expression, preferably with more experimental data in future experiments. The Ag(03)-expressing cells were found to have  $3.5 \cdot 10^5$  antigens per cell. From the binding assays, this seems to be a probable amount. A tenfold excess of Ag(03)-expressing- relative to the Ag(01)-expressing cells were necessary to obtain a characteristic binding plot.

For the beads,  $8.1 \cdot 10^4$  Ag(01) and  $9.7 \cdot 10^4$  Ag(03) were measured per bead. The same amounts of beads are used for the two different RICs. This verifies that the differently coated beads have approximately the same antigen expression.

The amounts of antigen per bead was calculated to be 8.4  $\mu\text{g}$  Ag(01) and 9.0  $\mu\text{g}$  Ag(03) per mg beads. 10  $\mu\text{g}$  of each antigen were added per mg beads. This means that 80-90% of the added antigen was bound to the beads. The fact that less Ag(01) is bound than Ag(03) might have been expected due to the size of the antigens. Ag(01) is a dimer with more than twice the size of Ag(03). The reason that not all Ag(01) has bound might thus be steric hindrance. When the amount of bound antigen is calculated, it is assumed that one antibody binds to one monomer. However, this might represent an error as one antibody might bind to two monomers, or one dimer in the case of Ag(01). Most probably the binding is heterogenic.

---

## 5.3 Initial development of the immunoreactivity assays

---

The initial experiments with  $^{227}\text{Th}$ -AC0103 were directed to develop the one-point- and Lindmo methods with cells and beads. Algeta had performed the cell-based assays many times before. The procedure was therefore already developed, but there was uncertainty about the validity of the measurements. Therefore, initial experiments had to be done to assess the method before it was tested with beads. The bead-based assays had never been performed in Algeta's laboratories before, and much testing had to be done to find the right conditions for the experiments. After the antigens were biotinylated and coated to the beads, the initial experiments were performed to see if the beads could be used in the same way as cells in these assays.

### 5.3.1 Initial development of the cell-based immunoreactivity assays

---

By the beginning of this project, the immunoreactivity assay used by Algeta for  $^{227}\text{Th}$ -AC0103 was a one-point analysis using 10 million fixated SKOV-3 cells per sample. This quantity of cells had been determined based on earlier Lindmo assays with SKOV-3 cells performed by Algeta. The initial experiments in this project showed that 1 million cells were more than sufficient to obtain the same result for IRF\* in a one-point analysis. The reason for this deviation from the older result might have been the fact that different batches of SKOV-3 cells were used. Different cell-batches might have different antigen expressions, and the cells might thus be required in different quantities to obtain antigen excess. Therefore, it is a good idea to always make a full binding plot when a new batch is taken into use. The cell amount used in a one-point analysis should then be adjusted to the result of the binding plot.

The IRF\* measurements made by Algeta with 10 million cells were in the same range as the values obtained with 1 million cells. This is as expected as both cell quantities give antigen excess. However, the nonspecific binding was often higher with 10 million than with 1 million cells. In addition, the IRF\* measurements varied more when using 10 million cells. As will be discussed in Section 5.6.1 "The significance of nonspecific binding", there might be a correlation between a high nonspecific binding and a high variability in the measurements. The high nonspecific binding might be due to the great number of cells, and thus more surface where the antibodies can bind nonspecifically. As will be discussed later, it might be a good idea to use BSA to reduce nonspecific binding in these binding assays. In addition to the decrease in the variability of the measurements, a lower amount of cells also reduce the workload with cultivation and fixation of cells.

The shape of the binding plot is essential for the determination of IRF by a Lindmo assay. For a correct IRF measurement to be done, binding fractions both from the increasing part and the plateau of the curve have to be included in the binding plot. When then a double inverse plot, the Lindmo plot, is made, IRF can be determined by extrapolation to conditions corresponding to infinite antigen excess. The third binding plot from the initial experiments gave a curve with this characteristic shape. This experiment had cell numbers in the range 10 000 to 1 million cells. The Lindmo plot gave an IRF value of impossible 500% when all cell numbers were included. The 10 000 cell point had a much higher T/B value than the other points, leading to an upward curvature of the plot and a very steep fitted straight line. By omitting this value from the plot, a more likely IRF value of 97% was determined. This indicates that too low cell numbers, and thus low antigen concentrations, do not fit the binding model described by the Lindmo equation (Equation 2.7). This will be discussed in more detail in Section 5.3.3 "Linear regression in the Lindmo plots". In the later Lindmo assays with cells, using cell numbers from 25 000 to 5 million, this problem was not encountered again.

For Ag(03)-expressing cells, a few initial experiments had previously been done by Algeta. The fixation of these cells seemed to destroy the antigen. Living cells were therefore used for these immunoreactivity assays, which turned out to be problematic for several reasons. One reason was the antigen expression on these cells, which is considerably lower than on SKOV-3 cells. Therefore, a large amount of cells had to be used. This was especially time consuming as this large amount of cells had to be cultivated and kept alive until the day of the experiment. In addition, no reliable IRF measurement could be obtained by these assays due to cell death. With dead cells in the samples, the antigens might be on fragments of burst cells in the supernatant and not in the cell pellet. Therefore, to avoid cell death, it was decided to incubate the cells at 4°C for 4 hours (previously, incubations were done at 4°C over night or at 37°C for 2 hours). Another reason for the unsuccessful IRF measurements might have been that antigens on the cells internalized during the experiment. To avoid internalization, 1% sodium azide was added to the cell solution. The challenging and time-consuming nature of these experiments increased the motivation for making a cell independent assay.

### **5.3.2 Initial development of the bead-based immunoreactivity assays**

---

No analyses were performed in order to examine if the bead coating had been successful. The first experiment was therefore also a test to investigate if the antigens had successfully been bound to the coated beads. The first binding plot indicated an increase in binding with number of beads, and could thus confirm that the beads had antigens on them. These beads were coated with 40  $\mu\text{g}$  Ag(01) per mg beads.

The next step was to test the binding capacity of the beads for biotinylated antigen. The purpose of this was not to find the exact binding capacity, but to ensure that most of the antigen used to coat the beads actually bound onto the beads and did not go to waste. This is because the antigens were either quite expensive or in shortage. Two different coatings were made, one with 40  $\mu\text{g}$  and one with 10  $\mu\text{g}$  biotinylated Ag(01) per mg beads (40 and 10  $\mu\text{g}/\text{mg}$ ). Two Lindmo assays were then performed, one for each of the differently coated beads. The samples with 10  $\mu\text{g}/\text{mg}$  had four times more beads than the samples with 40  $\mu\text{g}/\text{mg}$ . If one mg beads could bind 40  $\mu\text{g}$  Ag(01), the results from the two assays should thus be the same. The resulting binding plots showed clearly that the samples with 10  $\mu\text{g}/\text{mg}$  contained more antigen than the samples with 40  $\mu\text{g}/\text{mg}$  (see Appendix E). This indicates that one mg of beads binds less than 40  $\mu\text{g}$  Ag(01), and it was therefore decided that 10  $\mu\text{g}$  biotinylated antigen per mg beads should be used in the further experiments.

Since the principle of the one-point- and Lindmo assays is to determine immunoreactivity with antigen excess, the exact amount of antigen and thus the exact binding capacity of the beads is not of importance. However, the Scatchard analysis later indicated that 80-90% of the added antigen had bound to the beads. This means that the antigen binding capacity have to be at least 8  $\mu\text{g}$  biotinylated antigen per mg beads for the antigens used in this experiment.

Finally, experiments were performed to determine the bead numbers to be used for the further immunoreactivity assays. It was concluded that 15 million beads were adequate for the one-point analysis and bead numbers in the range 25 000 to 25 million were suitable for the Lindmo assay.



### 5.3.3 Linear regression in the Lindmo plots

---

Many of the bead-based Lindmo assays resulted in unlikely high IRF-values, in many cases fractions exceeding 100%. When studying the Lindmo plots of these experiments, an upward curvature could be observed caused by experimental data from the lowest bead numbers. The reason for this deviation from the higher bead numbers is that these points do not fit into the binding model described by Equation 2.7. The equation is quoted here to make the discussion clearer. [Ag] is free antigen concentration.

$$\frac{T}{B} = \frac{1}{IRF} + \frac{1}{IRF \cdot K_a [Ag]} \quad (2.7)$$

In the Lindmo plot, T/B is plotted against 1/number of beads. The bead number is here proportional to the total and not the free antigen concentration. By antigen excess, the concentration of free and total antigen will be nearly equal, and the approximation is assumed to be valid. However, under low antigen concentrations, the use of total instead of free antigen concentration is not longer a good approximation. Also Lindmo encountered this problem.<sup>[17]</sup> His solution was to omit the points of lowest cell concentration from the Lindmo plots if they deviated from the theoretical line. Since this deviation is observed for most of the bead-based experiments in this project, samples containing 1 million beads or less were omitted from all Lindmo-plots with beads. The samples were still included in the displayed binding-plots, as they contribute to give the curve its characteristic shape.

## 5.4 Overview of the immunoreactivity measurements

In the next sections, the results from the immunoreactivity measurements are discussed. To make this discussion clearer, the immunoreactivity results presented in the previous chapter are assembled and given in Table 5.1 and Figure 5.1. Table 5.1 gives average IRF\*, IRF,  $R^2$  and nonspecific binding values, while Figure 5.1 gives average binding plots for the different binding systems. Firstly, the cell-based measurements for  $^{227}\text{Th-AC0103}$ , and secondly, the bead-based measurements for the same RIC are presented. These measurements with beads are divided into two parts. One part constitutes the experiments performed without BSA, and the second part the experiments with BSA. The comparison of these results will be used to discuss the relevance of nonspecific binding in Section 5.6.1 “The significance of nonspecific binding”. Further, the bead-based measurements will be discussed and compared to the measurements with cells. The main objective is to examine if the same results can be obtained with beads as with cells. At last, the immunoreactivity measurements of  $^{227}\text{Th-AC0303}$  with both cells and beads are discussed. As  $^{227}\text{Th-AC0303}$  is believed to have different binding characteristics than  $^{227}\text{Th-AC0103}$ , these results might provide a picture of the applicability of the bead-based method for different antibody-antigen systems.

**Table 5.1:** Summary of all immunoreactivity measurements made in this project. The values are average from the specified binding systems. Standard deviations (S.D.) and number of experiments (n) are given each different measurement and binding system.

Measurement	$^{227}\text{Th-AC0103} - \text{Ag(01)}$			$^{227}\text{Th-AC0303} - \text{Ag(03)}$	
	Cells	Beads (-BSA)	Beads (+BSA)	Cells	Beads (+BSA)
IRF* $\pm$ S.D. [%]	81 $\pm$ 5 (n=12)	78 $\pm$ 7 (n=11)	85 $\pm$ 4 (n=13)	71 (n=1)	59 $\pm$ 6 (n=3)
IRF $\pm$ S.D. [%]	83 $\pm$ 8 (n=6)	83 $\pm$ 7 (n=6)	93 $\pm$ 5 (n=5)	73 (n=1)	63 $\pm$ 8 (n=3)
$R^2 \pm$ S.D.	0.83 $\pm$ 0.21 (n=6)	0.94 $\pm$ 0.02 (n=6)	0.94 $\pm$ 0.08 (n=5)	0.84 (n=1)	0.97 $\pm$ 0.04 (n=3)
Nonspecific binding $\pm$ S.D. [%]	4 $\pm$ 3 (n=12)	12 $\pm$ 3 (n=11)	2 $\pm$ 2 (n=13)	5 (n=1)	7 $\pm$ 1 (n=3)

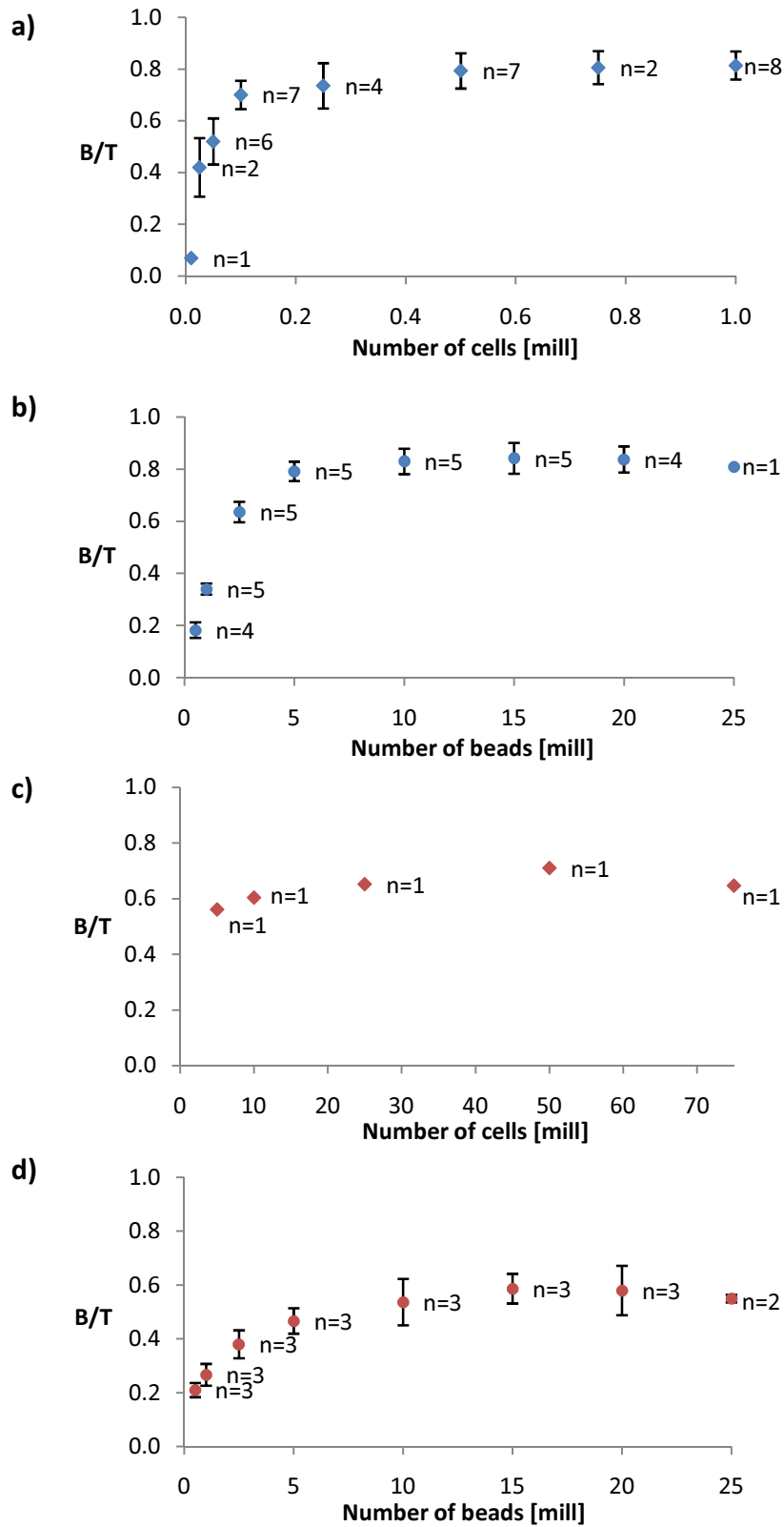


**Figure 5.1:** A summary of all binding plots from the Lindmo analyses. Average binding  $\pm$  S.D. is plotted for all experiments with **a)**  $^{227}\text{Th-AC0103}$  binding to Ag(01)-expressing cells, **b)**  $^{227}\text{Th-AC0103}$  binding to Ag(01)-coated beads, **c)**  $^{227}\text{Th-AC0303}$  binding to Ag(03)-expressing cells, and **d)**  $^{227}\text{Th-AC0303}$  binding to Ag(03)-coated beads.

---

## 5.5 Cell-based immunoreactivity measurements for $^{227}\text{Th-AC0103}$

---

Generally, the binding plots from the cell-based Lindmo assays with  $^{227}\text{Th-AC0103}$  gave rapidly increasing curves that reached a plateau. The plateau values were in the range 70-90%, varying from plot to plot. As seen in Figure 5.1a, there are relatively big variations between the different binding plots, especially seen in connection with the high number of measurements for some of the cell numbers. The cell numbers varied quite much between the experiments. This variation might be a reason for the inconsistency. However, if this was a consistent binding system, the curves between the points should still be the same.

As seen from Table 5.1, the cell-based immunoreactivity measurements for  $^{227}\text{Th-AC0103}$  gave average IRF\* and IRF values of 81% and 83%, respectively. An IRF\* lower than the IRF can be seen for most of the measurements in this project. This was expected, owing to the fact that IRF\* is immunoreactivity at limited antigen excess, while IRF is estimated immunoreactivity at infinite antigen excess.

If IRF\* is measured to be higher than IRF, an error in at least one of the two measurements has to be assumed. An IRF\* higher than IRF is observed for two of the cell-based Lindmo assays with  $^{227}\text{Th-AC0103}$ . For simplicity, these assays will here be mentioned as Exp. 1 and Exp. 2 (see Appendix F, Experiment 5a and 6a, respectively). IRF\* and IRF was measured to be 77% and 74% for Exp. 1, respectively, and 82% and 77% for Exp. 2, respectively. The fit of the regression model to the experimental data used to measure IRF in these experiments,  $R^2$ , was 0.87 for Exp. 1 and 0.40 for Exp. 2. These low values of  $R^2$ , especially for Exp. 2., indicate a high uncertainty of the estimated IRF in these experiments. These are examples showing how important it is that  $R^2$  is taken into consideration as a measurement of the reliability of IRF-estimations. The relationship between IRF\* and IRF will be discussed in more detail in Section 5.9 “Comparison of one-point- and Lindmo assay”.

The average  $R^2$  ( $\pm$  S.D.) for the regression model from all the Lindmo assays is  $0.82 \pm 0.21$ . This indicates a generally bad fit for the experimental data to the model described by Equation 2.7. The  $R^2$  from Exp. 2 (0.40) especially decrease this average. By omitting this value, the new average is  $0.91 \pm 0.05$ . However, there are no obvious explanations for the variances between the binding plots, Lindmo plots and fits of linear regression observed in these experiments. The average  $R^2$  gives a illustration of these general trends. Deviations and variations are observed both within and between the different experiments.

The fact that there are quite large variations in IFR ( $83 \pm 8\%$ ) and  $R^2$  ( $0.83 \pm 0.21$ ), indicates that the cell-based Lindmo assay has a relatively low degree of reproducibility, and that unsuccessful experiments might easily occur. A large variation also in the IRF\* measurements from the one-point assay was previously observed by Algeta. In the measurements from this project, this variation seemed to have been decreased ( $81 \pm 5\%$ ). This might be due to the decrease in the number of cells in the one-point assay samples from 10 million to 1 million. Holland *et. al.*<sup>[80]</sup> and Lub-de *et. al.*<sup>[81]</sup> both reported an average IRF of 87% for trastuzumab binding to HER-2 on SKOV-3 cells. This is slightly higher than the average from the cell-based measurements in this project, and might indicate that the cell-based measurements provide underestimates of the immunoreactivity.

---

## 5.6 Bead-based immunoreactivity measurements for $^{227}\text{Th-AC0103}$

---

After the first bead-based immunoreactivity assays for  $^{227}\text{Th-AC0103}$  were performed, the most conspicuous was the consistent shapes of the binding curves and the good fit of the linear regression for the Lindmo plots. It was therefore thought that these results would lead to much more consistent and reliable immunoreactivity measurements. However, the measurements indicated even greater variability in IRF\* than with cells, while the IRF values were similar to those from the cell-based assays (see Table 5.1). High values of nonspecific binding, in average three times as high as for cells, were also noticed. According to the provider of the beads, nonspecific binding to the beads is normal and might be due to hydrophobicity, charge or other types of interactions between the molecules and the beads.<sup>[82]</sup>

To reduce this nonspecific binding, BSA was added to the bead solution. The result of this, and the significance of nonspecific binding, is discussed in the next section. Further, the bead-based immunoreactivity measurements with reduced nonspecific binding is described and compared to the cell-based measurements.

### 5.6.1 The significance of nonspecific binding

---

To reduce the nonspecific binding observed in the first bead-based measurements, BSA was added to the bead solution. Experiments with no BSA, 1% BSA and 5% BSA demonstrated a clear decrease in nonspecific binding, from 8-15% in the samples without BSA, to 0-5% in the samples containing BSA. There was no clear difference between 1% and 5% BSA. Therefore, 1% BSA was added to the beads in all further experiments with beads. As seen in Table 5.1, the average nonspecific binding of these further experiments for  $^{227}\text{Th-AC0103}$  was  $2 \pm 2\%$ . Another interesting observation from these experiments is the significantly increased immunoreactivity; average IRF\* increased from 78% to 85%, and average IRF increased from 83% to 93%. The standard deviation for these measurements was also 2-3% lower.

These results indicate that a high nonspecific binding can result in a seemingly lower immunoreactivity, and more variable results. This is probably due to some of the RICs binding nonspecifically in a blocked sample, but specifically in the unblocked sample. The subtraction of the nonspecific binding fraction from the immunoreactive fraction might thus result in a too low apparent immunoreactivity. However, it is impossible to say for sure if this is the case, and a low nonspecific fraction is thus a prerequisite for a reliable measurement.

Lindmo *et. al.* have also reported that the opposite situation might occur.<sup>[17]</sup> He observed an increase in nonspecific binding with decreased IRF. He concluded that the reduction in IRF might have been due to impaired specificity of the antibodies caused by radiolabeling. This modification might again have lead to an altered specificity of the antibody, and thus a possible increase in nonspecific binding.

### **5.6.2 Bead-based measurements with reduced nonspecific binding**

As already mentioned, the immunoreactivity increased significantly when the nonspecific binding to the beads decreased. The measured immunoreactivities were also significantly higher than those obtained from the same measurements with cells. Average IRF\* increased from 81% to 85%, and average IRF increased from 83% to 93%. The standard deviation for the measurements decreased with 1-3%. The fit of the regression model also increased to  $0.94 \pm 0.08$ , indicating a lower uncertainty for these IRF measurements. This lower uncertainty is also reflected in the appearance of the binding curves. All curves are smooth with few deviating values.

As shown in Figure 5.1b, the average binding curve for the bead-based experiments with <sup>227</sup>Th-AC0103 has relatively small standard deviations compared to the plot from the cell-based experiments in Figure 5.1a. It has to be noticed that the bead-based measurements had more parallels within the same experiments than the cell-based measurements. This is a factor that might lead to decreased deviations. However, by comparing the different binding plots (see Appendix F and G), it is quite clear that the bead-based measurements give smaller deviations both within and between the different experiments.

---

## 5.7 Immunoreactivity measurements for $^{227}\text{Th-AC0303}$

---

The binding of  $^{227}\text{Th-AC0303}$  to its target antigen Ag(03) is a previously little investigated binding system. However, from a few previous experiments performed by Algeta, this RIC is thought to have different binding properties than  $^{227}\text{Th-AC0103}$  and a lower immunoreactivity. The immunoreactivity of this RIC has been difficult to determine using cells, thus a bead-based immunoreactivity method was desirable. A cell-based assay was first performed to have something to compare the bead-based measurements to.

---

### 5.7.1 Cell-based immunoreactivity measurements for $^{227}\text{Th-AC0303}$

---

The binding plot from the single cell-based immunoreactivity assay performed for  $^{227}\text{Th-AC0303}$  with Ag(03)-expressing cells is given in Figure 5.1c. This plot displays a slight increase before a plateau of 65-70% is formed. It might look like the plot is close to reaching the plateau already at the lowest cell number. It could therefore have been advantageous to include samples with even lower cell numbers.

IRF\* is measured to be 71% from one of the plateau-samples in the binding plot. A Lindmo plot was also made, and an IRF of 73% was calculated. This might be a correct value, as it is slightly higher than IRF\*. But with a  $R^2$  of 0.84, this cannot be said with certainty. The nonspecific binding was 5% and thus in the same range as the assays with SKOV-3 cells.

One conclusion is that  $^{227}\text{Th-AC0303}$ , as expected, has a lower immunoreactivity than  $^{227}\text{Th-AC0103}$ . Because of the great workload of cultivating cells for this assay, it can also be concluded that a different immunoreactivity method, not dependent on cells, is needed.

---

### 5.7.2 Bead-based immunoreactivity measurements for $^{227}\text{Th-AC0303}$

---

The bead-based immunoreactivity assay for  $^{227}\text{Th-AC0303}$  was tested with the same conditions as for  $^{227}\text{Th-AC0103}$ . The beads were coated with 10  $\mu\text{g}$  Ag(03) per mg beads, and the same numbers of beads as in the previous assays for  $^{227}\text{Th-AC0103}$  were used. This gave good results on first try, showing that this system is easy to set up for different antibody-antigen systems.

The average binding plot given in Figure 5.1d has a similar shape as the binding plot with Ag(03)-expressing cells, indicating that the assay with beads gives reliable measurements. The resulting immunoreactivity values are on the other hand deviating from



the measurement with cells. The average IRF\* and IRF ( $\pm$  S.D.) from the bead based assays were  $59 \pm 6\%$  and  $63 \pm 8\%$ , respectively. The Lindmo plots from the bead-based assays gave the highest  $R^2$  values in this project, of  $0.97 \pm 0.04$ . From this it might be concluded that the bead-based measurements are more reliable than the single cell-based measurement with an  $R^2$  of 0.84.

The relatively high standard deviations of the immunoreactivity values, also seen in the plateau of the average binding plot, might be due to the low number of measurements. In addition, it might be expected that the binding of RICs with mediate immunoreactivity (60-70%) deviate more from experiment to experiment than RICs with high immunoreactivity (80-90%). It has to be noticed that two of the measurements with beads for  $^{227}\text{Th-AC0303}$  were parallels of the same experiment. The third measurement was from a new experiment, and can be observed to deviate from the two others. This individual experiment gave an IRF\* of 65% and an IRF of 72%, and thus values closer to the cell-based measurement.

The nonspecific binding for the three bead based assays were  $7 \pm 1\%$ . This is considerably higher than for the bead-based assays with  $^{227}\text{Th-AC0103}$  ( $2 \pm 2\%$ ). The reason for this deviation is unsure. As mentioned earlier, Lindmo suggested that high nonspecific binding could be a consequence of impaired specificity of the antibody.<sup>[17]</sup> If this was the case here, the lower IRF might also have been a consequence of this impairing. To test if the immunoreactivity decreased after conjugation or after radiolabeling, additional analysis would have to be performed. This will be discussed more in Section 5.10 "Future work".

Figure 5.1 shows that the binding curves for  $^{227}\text{Th-AC0103}$  are steeper than for  $^{227}\text{Th-AC0303}$ . This indicates that  $^{227}\text{Th-AC0103}$  binds Ag(01) with higher affinity than  $^{227}\text{Th-AC0303}$  binds Ag(03). The same was also confirmed by the Scatchard analysis, which resulted in a lower  $K_a$  value for  $^{227}\text{Th-AC0303}$  than  $^{227}\text{Th-AC0103}$ . The lower affinity for  $^{227}\text{Th-AC0303}$  to Ag(03) might also partly explain why the immunoreactivity for this RIC is lower. Since the binding kinetics for  $^{227}\text{Th-AC0303}$  probably are slower than for  $^{227}\text{Th-AC0103}$ , this RIC might need longer incubation times for the binding-reaction to reach equilibrium.

These results give a good indication of the applicability of the beads in measuring immunoreactivity. It is likely that a variety of different antibody-antigen systems can be used with the beads, the only requisition being that the antigen or the epitope of the antigen can be isolated.

---

## 5.8 Comparison of cells and beads

---

The results discussed in the previous sections show that beads can be used as a substitute for cells in immunoreactivity assays. The difference in the preparation of the assays is the coating of beads with biotinylated antigen instead of cultivation, and often also fixation, of cells. The biotinylation of antigen and coating of beads together takes a few hours. The cultivation of cells has to be done over several days, especially if high cell numbers are needed. Access to cells and a cell-laboratory is also required. In addition, the handling of beads during the assays is simpler than for the cells. For living cells, the assays have to be performed with extra carefulness to keep the cells alive. This concern do not apply to the beads. Also, the washing and separation procedures are easier with beads. By using the magnetic rack, the supernatant is removed from the beads in less than one minute, while the cells have to be centrifuged for several minutes.

In addition to being a less time-consuming method, the bead-based immunoreactivity assays provide measurements with lower uncertainty than the cell-based assays. The results from this work show that beads give less varying results with fewer deviations. The main reason for this is probably the homogeneity of the beads. All the beads have the same shape and can be coated evenly with antigen, while cells are heterogenic both in shape and the expression of antigen. Living cells can be especially problematic, as internalization of the antigens may happen. The only reason to use cells might be economic, as the antigens and beads might be more expensive than cells. However, compared to the workload and the increased risk of unsuccessful experiments with cells, the beads should still be more profitable.

One might argue that the target for the RICs *in vivo* is tumor cells, and that the *in vitro* assay therefore should use cells to imitate this *in vivo* situation. However, the conditions in this *in vitro* assay are far from the conditions *in vivo* and cannot be compared with a potential situation in a patient. First of all, in this assay the antigens are exposed to the RICs only for the short incubation time of some hours. In the body, the RICs will stay in the blood stream for days, and might have many chances to bind to the antigens on the tumor cells. In addition, the binding capacity of RICs might be altered by the catabolism *in vivo*. The immunoreactivity assays in this project are used to investigate whether the RICs have the potential to bind *in vivo* and might be used as a quality check of the product. Additional research has to be done in order to investigate the behavior of the RICs *in vivo*. The assays are also used to ensure that the conjugation of the chelator and the radiolabeling have not

destroyed the binding sites of the antibody and potentially lowered the immunoreactivity. For these purposes, the measurements should be as simple and reliable as possible. Therefore, beads provide a better option than cells in these immunoreactivity assays.

In addition, the bead-based assays have the potential to compare different RICs at similar conditions. If using cells, the RICs might have to be tested under very different conditions. Some RICs, like  $^{227}\text{Th-AC0103}$ , can be tested with fixated cells, while others, like  $^{227}\text{Th-AC0303}$ , have to be analyzed with living cells. Some cells have a high expression of antigen, like SKOV-3, while other cells, like the Ag(03)-expressing cells, have a low expression of antigen. Beads can be coated with equal amounts of antigen and the same numbers of beads can be used to test the different RICs, thus providing similar conditions.

---

## 5.9 Comparison of one-point- and Lindmo analyses

---

The Lindmo assay will always provide a more correct measure of the immunoreactivity, as it measures the immunoreactive fraction at conditions corresponding to infinite antigen excess. Furthermore, it estimates immunoreactivity with several measured data points, in contrast to the one-point assay that measures the data in one single point. More experimental data and a regression model will always provide more reliable results than a single measurement. In addition, the binding plot obtained in the Lindmo assay provides a way to see if the binding reaction occurs as normal. The increasing part of the curve also provides information about the kinetics of the binding reaction.

There are certain conditions that have to be met when IRF is determined from the Lindmo plot. First, the binding plot has to be examined to see if the experimental data are suitable to measure IRF. This binding plot should consist of at least two data points in the increasing part of the curve, and at least two data points on the plateau.<sup>[15]</sup> The data set should together comprise six to eight experimental data points to provide a reliable measurement of IRF. Further, the  $R^2$  has to be high for the IRF to be estimated correctly. If the data points from the samples with low cell or bead numbers are deviating from the data measured from samples with higher cell or bead numbers, only data from the higher cell or bead numbers should be used to determine IRF.<sup>[17]</sup> If a bead-based Lindmo assay is performed using the same conditions as in this project, experimental data from samples with bead-numbers lower than 1 million should not be included in the Lindmo plot.

As seen from the results in this project, the one-point analysis provides a good estimate of IRF. The measured IRF\* never deviated more than 10% from the measured IRF value. A presumption for the one-point method is that it is performed with an appropriate cell or bead number, determined from a binding plot of a Lindmo assay. This cell or bead number should provide antigen excess, but the number should also not be too high. To ensure this, a Lindmo-plot should always be performed when a new cell line or bead-batch is taken into use. When a new binding system is investigated, a full Lindmo assay should always be performed to determine where the plateau is. Also, the Lindmo assay should be used when high accuracy is required, for example prior to animal experiments or clinical trials. If a one-point analysis is performed, at least two parallel measurements should be done. The one-point method is a good and time saving solution for a routine quality control, but one should keep in mind that IRF\* is an underestimation of the immunoreactivity, and the conclusion that can be drawn

from this value is that  $IRF \geq IRF^*$ . The one-point assay is actually a commonly used method, also used in articles publishing immunoreactivity values.<sup>[83-85]</sup>

The Lindmo method is a widely used method, and the article has been cited more than 680 times.<sup>[86]</sup> But this method has also received some criticism. For example, Mattes points out the fact that the Lindmo extrapolation is not based on exact mathematical relationships, but on approximations which are, in some circumstances, of uncertain validity.<sup>[87]</sup> He points out that this might result in overestimates, and that the experimental measurement in one point might give a more correct value than the extrapolated. This have been followed up by Konishi *et. al.*<sup>[15]</sup> and Glatting *et. al.*<sup>[88]</sup> However, as these articles also point out, published IRF values obtained from the Lindmo assay are typically in the absence of any experimental data, so the reader cannot judge their validity. Konishi *et. al.* suggests that the estimated IRF value only is valid if it is within 10% of  $IRF^*$ .<sup>[15]</sup> This is true for all IRF measurements in this project. However, if the samples of low bead-numbers ( $\leq 1$  million beads) were included in the measurements, the Lindmo plots would in fact produce great overestimates of IRF, in many of the experiments over 100%. Therefore, the extrapolation has to be used with caution. It is important to interpret the results from a Lindmo-plot taking the equations, and simplification of these, that make up the background for this method into consideration. If the estimated IRF is more than 10% higher than  $IRF^*$ ,  $IRF^*$  might give better measure of the immunoreactivity.<sup>[87]</sup>

---

## 5.10 Further work

---

This project has shown that both the cell- and bead-based one-point- and Lindmo assays can be used to measure the immunoreactivity of different antibody-antigen systems. However, some further work might be done to improve the method and make the measurements more accurate. In addition, complementary assays to the immunoreactivity assays have been planned.

All experimental samples in the immunoreactivity assays were added an amount of RIC corresponding to 500 cpm. This had several reasons. First of all, too low activity is not desirable, as this can affect the certainty of the measurement. However, too high activity would result in a higher amount of antibodies, both radiolabeled and unlabeled. This high amount of antibodies need a higher amount of antigens to ensure antigen excess, which again would require a higher amount of cells. Algeta has previously tested different activities, and 500 cpm was found to be appropriate. However, the challenge seen with high cell numbers will not be a problem with beads, as a higher number of beads would not result in an increased workload. Different activities could therefore be tested to find the ideal amount of RIC added to each sample.

Another idea is to add RIC to the samples based on their concentration and not activity. This would probably give even more consistent results, since 500 cpm can give quite varying amounts of RIC because of its varying specific activities. Especially if the specific activity varies significantly from the range used in this project (500-1000 Bq/ $\mu$ g), the amount of RIC added to each sample should be adjusted. If not, the binding curve might be displaced compared to the curves seen in these experiments. However, Lindmo showed that the method is quite insensitive to changes in the concentration of antigen or RIC.<sup>[17]</sup> This is due to the principle of measuring IRF at antigen excess.

It could be convenient to coat a larger amount of beads and store them at 4°C. This would decrease the workload and similar conditions would apply to the experiments performed with the same batch of coated beads. However, the shelf life of the coated beads stored at 4°C should first be tested. The beads cannot be frozen.<sup>[76]</sup>

Even though the cells did not show a high nonspecific binding, 1% BSA could with advantage be added to the cell solution to obtain an even lower nonspecific binding. If the nonspecific binding still is high after applying 1% BSA, as seen for the bead-based assays

with  $^{227}\text{Th-AC0303}$ , it might be a good solution to add even more BSA to the bead- or cell solutions.

Additional experiments could also be performed to examine the incubation time for the binding assays. The results from the Scatchard analysis and binding plots indicated that  $^{227}\text{Th-AC0303}$  has slower binding kinetics than  $^{227}\text{Th-AC0103}$ . Therefore,  $^{227}\text{Th-AC0303}$  might need longer incubation times for the binding reaction to reach equilibrium. However, it might also be that the incubation times used in this project are longer than necessary. Lindmo *et. al.* reported the same estimated IRF from parallel experiments incubating 30 minutes and 4 hours. Thus, the method might be quite insensitive regarding the incubation time - as long as the reaction has reached equilibrium. If an incubation time of 30 minutes is sufficient for the reaction to reach equilibrium, the duration of the immunoreactivity assays could be nearly halved. However, this have to be tested for every antigen-antibody system, as different systems might have different binding kinetics.

There are still uncertainties regarding the clear differences in RIC-binding between the cell- and bead-based assays. The main reason for these differences is assumed to be the homogeneity of the beads versus the heterogeneity for the cells. However, there might also be other influencing factors. For example, the cells might express other receptors and structures interfering with the binding of the RIC to its target-antigen. One possibility to investigate the differences between bead- and cell-binding of the RICs, could be to use a LigandTracer<sup>®</sup>.<sup>[89]</sup> This technology has the potential to detect protein-cell interactions in real-time, and has been adapted to measure interactions of radiolabeled proteins with cell-surface structures and receptors.

The methods developed in this project have shown to be suitable for estimating IRF of different RICs. However, these assays cannot be used to measure the IRF of the naked MoAbs - thus, they cannot indicate if the conjugation of chelator to antibody or the radiolabeling has affected the IRF. Additional methods are required to test this. One potential method for detecting alterations of IRF is enzyme-linked immunosorbent assay (ELISA). ELISA is not dependent on radioactivity to measure binding, and might therefore be used to compare the binding fractions of the naked MoAb, MoAb conjugated to chelator and RIC in the same experiment. Any decrease of IRF from the naked MoAb, and the reason for the decrease can thus be detected. This method could therefore be performed in addition to a immunoreactivity assay. A procedure for this is already developed, and will be tested with the antibody-antigen systems used in this project.





## 6 Conclusion

---

In this project, a new, bead-based immunoreactivity assay was developed. This was done based on initial immunoreactivity experiments with cells. The immunoreactivity measurements included several experiments of the widely used Lindmo method and its simplified method, the one-point assay. The antigen binding capacity of the two RICs  $^{227}\text{Th-AC0103}$  and  $^{227}\text{Th-AC0303}$  was investigated using these methods.  $^{227}\text{Th-AC0103}$  was used to develop and assess the different methods, while  $^{227}\text{Th-AC0303}$  was used as a second RIC with different binding properties to examine the applicability of the bead-based method.

An additional binding assay, the Scatchard analysis, was performed to determine the association constants for the two RICs to their target antigens, and to estimate the antigen expression on the cells and beads. The Scatchard analysis indicated that  $^{227}\text{Th-AC0103}$  had a ten times higher affinity for Ag(01) than  $^{227}\text{Th-AC0303}$  had for Ag(03). The same analysis demonstrated that the Ag(01)-expressing cells had a ten times higher antigen expression than the Ag(03)-expressing cells.

The cell-based immunoreactivity measurements for  $^{227}\text{Th-AC0103}$  indicated relatively large variations between the experiments and relatively high uncertainties in the estimated immunoreactivities. The binding plots showed inconsistency between different experiments, and values deviating from the expected curve were found in nearly all the binding plots. These results demonstrated that there is a need for a new method that is less time consuming, more consistent and provides more reliable immunoreactivity measurements.

The antigens Ag(01) and Ag(03) were biotinylated and successfully coated to beads prior to the bead-based experiments. The coated beads were then used in several immunoreactivity measurements for the two different RICs. The conclusion from these experiments is that antigen-coated beads with advantage can be used as a substitute for cells. The bead-based assays provided more consistent and reliable measurements than the cell-based assays and demonstrated a high degree of reproducibility. The bead-based methods are both easier to perform and timesaving compared to the same methods using cells.

The immunoreactivity measurements for  $^{227}\text{Th-AC0103}$  indicated relatively high IRF values, giving average IRF values for the cell- and bead-based assays of 83% and 93%, respectively. The same experiments with  $^{227}\text{Th-AC0303}$  showed that the bead-based method easily can be used for different antibody-antigen systems, with different binding properties. This RIC demonstrated an average immunoreactivity of 63% from the bead-based

measurements. It is likely that a variety of different antibody-antigen systems can be used with the beads, the only requisition being that the antigen or the epitope of the antigen can be isolated. Therefore, beads provide a good way to compare different binding systems with similar conditions.

The one-point measurements in this project gave IRF\* measurements within 10% of IRF, and is thus a good approximation for the immunoreactivity (IRF). However, as this method only measures binding in one point, a higher uncertainty is accompanying this method. The conclusion from the one-point analysis can only be that  $IRF \geq IRF^*$ . The Lindmo assay, using several experimental data to estimate IRF at conditions corresponding to antigen excess, gives a more correct measurement of immunoreactivity. Therefore, a full Lindmo assay should be performed whenever a new system is being implemented, or whenever high accuracy is needed. However, the one-point analysis is a timesaving method that can be used as a routine quality check.

# List of references

---

1. Jemal, A., Bray, F., Center, M. M., Ferlay, J., Ward, E., & Forman, D. 2011. Global cancer statistics. *CA: A Cancer Journal for Clinicians*, 61(2): 69-90.
2. Papac, R. J. 2001. Origins of cancer therapy. *The Yale Journal of Biology and Medicine*, 74(6): 391-398.
3. Schrama, D., Reisfeld, R. A., & Becker, J. C. 2006. Antibody targeted drugs as cancer therapeutics. *Nature Reviews Drug Discovery*, 5(2): 147-159.
4. Himmelweit, F. 1960. *The Collected Papers of Paul Ehrlich. Vol. II. Immunology and Cancer Research*. Pergamon Press.
5. Koehler, G. & Milstein, C. 1975. Continuous cultures of fused cells secreting antibody of predefined specificity. *Nature (London, United Kingdom)*, 256(5517): 495-497.
6. Grillo-Lopez, A. J., Hedrick, E., Rashford, M., & Benyunes, M. 2002. Rituximab: Ongoing and future clinical development. *Seminars in Oncology*, 29: 105-112.
7. Senter, P. D. 2010. Recent advancements in the use of antibody drug conjugates for cancer therapy. *Biotechnology: Pharmaceutical Aspects*, 11(Current Trends in Monoclonal Antibody Development and Manufacturing): 309-322.
8. Press release from Algeta ASA 24.09.2011: Alpharadin Significantly Improves Overall Survival for Patients with Castration-Resistant Prostate Cancer and Symptomatic Bone Metastases. Available: [http://www.algeta.com/xml\\_press\\_underside.asp?xml=http://cws.huginonline.com/A/134655/PR/201109/1549445.xml&m=34572&s=34686&ss=&d=2011-09-24](http://www.algeta.com/xml_press_underside.asp?xml=http://cws.huginonline.com/A/134655/PR/201109/1549445.xml&m=34572&s=34686&ss=&d=2011-09-24). Last accessed 23.11.2011.
9. Presented at the 102nd Annual Meeting of the American Association for Cancer Research 05.04.2011: Alpharadin inhibits osteoclast differentiation *in vitro* and progression of established breast cancer bone metastases *in vivo*. Available: [http://www.pharmatest.com/pdf/Poster\\_AACR2011\\_Pharmatest-Bayer.pdf](http://www.pharmatest.com/pdf/Poster_AACR2011_Pharmatest-Bayer.pdf). Last accessed 23.11.2011.
10. The wall street journal - Health 23.08.2011: Bayer Prostate Drug Gets a Boost. Available: <http://online.wsj.com/article/SB10001424053111903327904576525672028018038.html>. Last accessed 29.11.2011.
11. Reilly, Raymond M. Biopharmaceutical as targeting vehicles for in situ radiotherapy of malignancies. *Mod.Biopharm.* 2, 497-535. 2005. Wiley-VCH Verlag GmbH & Co. KGaA.
12. Algeta ASA, Products, TTC. Available: <http://algeta.com/dynside.asp?m=34568&s=34660>. Last accessed: 20.12.2011.

13. Reilly, R. 2004. The immunoreactivity of radiolabeled antibodies - its impact on tumor targeting and strategies for preservation. *Cancer Biother.Radiopharm.*, 19(6): 669-672.
14. Reilly, R. M. & Editor. 2010. *Monoclonal Antibody and Peptide-Targeted Radiotherapy of Cancer*. John Wiley & Sons, Inc.
15. Konishi, S., Hamacher, K., Vallabhajosula, S., Kothari, P., Bastidas, D., Bander, N., & Goldsmith, S. 2004. Determination of immunoreactive fraction of radiolabeled monoclonal antibodies: What is an appropriate method? *Cancer Biotherapy & Radiopharmaceuticals*, 19(6): 706-715.
16. Pimm, M. V. & Baldwin, R. W. 1987. Comparative tumor localization properties of radiolabelled monoclonal antibody preparations of defined immunoreactivities. *European Journal of Nuclear Medicine*, 13(7): 348-352.
17. Lindmo, T., Boven, E., Cuttitta, F., Fedorko, J., & Bunn, P. A., Jr. 1984. Determination of the immunoreactive fraction of radiolabeled monoclonal antibodies by linear extrapolation to binding at infinite antigen excess. *Journal of Immunological Methods*, 72(1): 77-89.
18. Scatchard, G. 1949. The attraction of proteins for small molecules and ions. *Annals of the New York Academy of Sciences*, 51: 660-672.
19. Magill, J. & Galy, J. 2004. *Radioactivity-Radionuclides-Radiation*. Springer-Verlag.
20. Turner, J. E. 2007. *Atoms, radiation, and radiation protection*. Wiley-VCH.
21. Picture source: wikipedia.org; Alfa beta gamma radiation penetration. Available: [http://en.wikipedia.org/wiki/File:Alfa\\_beta\\_gamma\\_radiation\\_penetration.svg](http://en.wikipedia.org/wiki/File:Alfa_beta_gamma_radiation_penetration.svg). Last accessed: 20.12.2011.
22. Waggoner, W. H. 1975. Berzelius and the discovery of thorium. *Journal of Chemical Education*, 52(1): 53.
23. Ikezoe, H., Ikuta, T., Hamada, S., Nagame, Y., Nishinaka, I., Tsukada, K., Oura, Y., & Ohtsuki, T. 1996.  $\alpha$ -decay of a new isotope  $^{209}\text{Th}$ . *Physical Review C*, 54(4): 2043-2046.
24. Isotopes Project Home Page, Lawrence Berkeley National Laboratory. "Isotopes of Thorium (Z=90)". Available: [http://ie.lbl.gov/education/parent/Th\\_iso.htm](http://ie.lbl.gov/education/parent/Th_iso.htm). Last accessed: 18.12.2011.
25. World Nuclear Association. "Thorium". Available: <http://www.world-nuclear.org/info/inf62.html>. Last accessed: 18.12.2011.
26. Dahle, J. & Larsen, R. H. 2008. Targeted alpha-particle therapy with  $^{227}\text{Th}$ -labeled antibodies. *Current Radiopharmaceuticals*, 1(3).

27. McNaught, A. D. & Wilkinson, A. IUPAC. Compendium of Chemical Terminology, 2nd ed. Compiled by Blackwell Scientific Publications, Oxford (1997). Available: <http://goldbook.iupac.org/>. Last accessed: 19.12.2010.
28. Bureau International des Poids et Mesures. SI brochure (8th edition), 2006. Available: [http://www.bipm.org/utis/common/pdf/si\\_brochure\\_8\\_en.pdf](http://www.bipm.org/utis/common/pdf/si_brochure_8_en.pdf). Last accessed 19.12.2011.
29. Michigan State University, Environmental Health & Safety (EHS), Radiation Safety Manual. Available: [http://www.orcbs.msu.edu/radiation/programs\\_guidelines/radmanual/13rm\\_radiounits.htm](http://www.orcbs.msu.edu/radiation/programs_guidelines/radmanual/13rm_radiounits.htm). Last accessed 19.12.2011.
30. Knoll, G. F. 2010. *Radiation Detection and Measurement*. John Wiley & Sons.
31. Wallbrink, P. J., Walling, D. E., and He, Q. Radionuclide measurement using HPGe gamma spectrometry. Handb.Assess.Soil Erosion Sediment.Using Environ. Radionuclides, 67-96. 2002. Kluwer Academic Publishers.
32. Kaihola, L. Wallac Oy (Perkin Elmer), Turku, Finland. 1997. The gamma counting handbook. Available: [http://www.groco.is/groco/upload/files/nemi/fraedigreinar/\(perkin-elmer\)\\_gamma\\_counting\\_handbook.pdf](http://www.groco.is/groco/upload/files/nemi/fraedigreinar/(perkin-elmer)_gamma_counting_handbook.pdf). Last accessed: 19.12.2011.
33. Ortec, USA. GEM Series Coaxial HPGe Detector Product Configuration Guide. Available: [www.ortec-online.com/download/GEM.pdf](http://www.ortec-online.com/download/GEM.pdf). Last accessed 19.12.2011.
34. Ruddon, R. W. 2007. Chapter 1: Characteristics of cancer. *Cancer biology*. (1): 3-5. Oxford University Press.
35. Lea, T. 2006. Immunologi og immunologiske teknikker. Fagbokforlaget Vigmostad & Bjørke AS.
36. Ritchie, R. F. & Ledue, T. B. 2005. The Immunoassay Handbook, 3rd Ed. Edited by David Wild, ed. Elsevier Inc.
37. Slamon, D. J., Clark, G. M., Wong, S. G., Levin, W. J., Ullrich, A., & McGuire, W. L. 1987. Human breast cancer: correlation of relapse and survival with amplification of the HER-2/neu oncogene. *Science (Washington, DC, United States)*, 235(4785): 177-182.
38. Gancberg, D., Di, L. A., Cardoso, F., Rouas, G., Pedrocchi, M., Paesmans, M., Verhest, A., Bernard-Marty, C., Piccart, M. J., & Larsimont, D. 2002. Comparison of HER-2 status between primary breast cancer and corresponding distant metastatic sites. *Annals of Oncology : Official Journal of the European Society for Medical Oncology / ESMO*, 13(7): 1036-1043.
39. Harries, M. & Smith, I. 2002. The development and clinical use of trastuzumab (Herceptin). *Endocrine-Related Cancer*, 9(2): 75-85.

40. Valabrega, G., Montemurro, F., & Aglietta, M. 2007. Trastuzumab: mechanism of action, resistance and future perspectives in HER2-overexpressing breast cancer. *Annals of Oncology : Official Journal of the European Society for Medical Oncology / ESMO*, 18(6): 977-984.
41. Genentech, Inc. Herceptin in Breast Cancer Fact Sheet. Available: <http://www.gene.com/gene/products/information/oncology/herceptin/factsheet.html>. Last accessed: 20.12.2011.
42. Bale, W. F., Spar, I. L., & Goodland, R. L. 1960. Experimental radiation therapy of tumors using I131-carrying antibodies to fibrin. *United States Atomic Energy Commission*, UR-567: 25.
43. Pressman, D. 1980. The development and use of radiolabeled antitumor antibodies. *Cancer Research*, 40(8, Pt.2): 2960-2964.
44. Hiramoto, R., Yagi, Y., & Pressman, D. 1958. In vivo fixation of antibodies in the adrenal. *Proceedings of the Society for Experimental Biology and Medicine*, 98: 870-874.
45. Sharkey, R. M. & Goldenberg, D. M. 2005. Perspectives on cancer therapy with radiolabeled monoclonal antibodies. *Journal of Nuclear Medicine*, 46(Suppl. 1): 115S-127S.
46. Imam, S. K. 2001. Advancements in cancer therapy with alpha-emitters: a review. *International Journal of Radiation Oncology, Biology, Physics*, 51(1): 271-278.
47. Iagaru, A., Mitra, E. S., Ganjoo, K., Knox, S. J., & Goris, M. L. 2010. 131I-Tositumomab (Bexxar) vs. 90Y-Ibritumomab (Zevalin) therapy of low-grade refractory/relapsed non-Hodgkin lymphoma. *Molecular Imaging and Biology : MIB : the Official Publication of the Academy of Molecular Imaging*, 12(2): 198-203.
48. Dahle, J., Abbas, N., Bruland, O. S., & Larsen, R. H. 2011. Toxicity and relative biological effectiveness of alpha emitting radioimmunoconjugates. *Current Radiopharmaceuticals*, 4(4).
49. Jurcic, J. G., Larson, S. M., Sgouros, G., McDevitt, M. R., Finn, R. D., Divgi, C. R., Ballangrud, A. M., Hamacher, K. A., Ma, D., Humm, J. L., Brechbiel, M. W., Molinet, R., & Scheinberg, D. A. 2002. Targeted  $\alpha$ -particle immunotherapy for myeloid leukemia. *Blood*, 100(4): 1233-1239.
50. Zalutsky, M. R., Reardon, D. A., Akabani, G., Coleman, R. E., Friedman, A. H., Friedman, H. S., McLendon, R. E., Wong, T. Z., & Bigner, D. D. 2008. Clinical experience with  $\alpha$ -particle-emitting 211At: treatment of recurrent brain tumor patients with 211At-labeled chimeric antitenascin monoclonal antibody 81C6. *Journal of Nuclear Medicine*, 49(1): 30-38.

51. Andersson, H., Cederkrantz, E., Baeck, T., Divgi, C., Elgqvist, J., Himmelman, J., Horvath, G., Jacobsson, L., Jensen, H., Lindegren, S., Palm, S., & Hultborn, R. 2009. Intraperitoneal  $\alpha$ -particle radioimmunotherapy of ovarian cancer patients: pharmacokinetics and dosimetry of  $^{211}\text{At}$ -MX35 F(ab')<sub>2</sub>-A phase I study. *Journal of Nuclear Medicine*, 50(7): 1153-1160.
52. Rosenblat, T. L., McDevitt, M. R., Pandit-Taskar, N., Carrasquillo, J. A., Chanel, S., Frattini, M. G., Larson, S. M., Scheinberg, D. A., & Jurcic, J. G. 2007. Phase I trial of the targeted alpha-particle nano-generator Actinium-225 - HuM195 (Anti-CD33) in Acute Myeloid Leukemia (AML). *Blood*. 110.
53. Dahle, J., Borrebæk, J., Melhus, K. B., Bruland, O. S., Salberg, G., Olsen, D. R., & Larsen, R. H. 2006. Initial evaluation of ( $^{227}\text{Th}$ -p-benzyl-DOTA-rituximab for low-dose rate alpha-particle radioimmunotherapy. *Nucl.Med Biol.*, 33(2): 271-279.
54. Dahle, J., Jonasdottir, T. J., Heyerdahl, H., Nesland, J. M., Borrebæk, J., Hjelmerud, A. K., & Larsen, R. H. 2010. Assessment of long-term radiotoxicity after treatment with the low-dose-rate alpha-particle-emitting radioimmunoconjugate ( $^{227}\text{Th}$ -rituximab. *Eur.J Nucl.Med Mol.Imaging*, 37(1): 93-102.
55. Dahle, J., Bruland, O. S., & Larsen, R. H. 2008. Relative biologic effects of low-dose-rate alpha-emitting  $^{227}\text{Th}$ -rituximab and beta-emitting  $^{90}\text{Y}$ -tiuxetan-ibritumomab versus external beam X-radiation. *Int.J Radiat.Oncol.Biol.Phys.*, 72(1): 186-192.
56. Heyerdahl, H., Krogh, C., Borrebæk, J., Larsen, Å., & Dahle, J. 2011. Treatment of HER2-Expressing Breast Cancer and Ovarian Cancer Cells With Alpha Particle-Emitting  $^{227}\text{Th}$ -Trastuzumab. *International Journal of Radiation Oncology\*Biological\*Physics*, 79(2): 563-570.
57. Press release from Algeta ASA 17.06.2009: New research highlights potential of novel alpha-pharmaceutical in targeting and killing breast cancer cells. Available: [http://algeta.com/xml\\_press\\_underside.asp?xml=http://cws.huginonline.com/A/134655/PR/200906/1323280.xml&m=34572&s=&ss=&d=2009-06-17](http://algeta.com/xml_press_underside.asp?xml=http://cws.huginonline.com/A/134655/PR/200906/1323280.xml&m=34572&s=&ss=&d=2009-06-17). Last accessed 29.11.2011.
58. Press release from Algeta ASA 04.04.2011: Algeta enters research collaboration to evaluate thorium conjugated with a novel tumor-targeting antibody from Genzyme. Available: [http://algeta.com/xml\\_press\\_underside.asp?xml=http://cws.huginonline.com/A/134655/PR/201104/1502810.xml&m=34572&s=&ss=&d=2011-04-04](http://algeta.com/xml_press_underside.asp?xml=http://cws.huginonline.com/A/134655/PR/201104/1502810.xml&m=34572&s=&ss=&d=2011-04-04). Last accessed 29.11.2011.
59. Press release from Algeta ASA 05.05.2011: Algeta Signs Exclusive Worldwide License with Affibody for Two Proprietary Molecules for use in New Tumor-targeted Alpha-pharmaceuticals based on Thorium. Available: [http://algeta.com/xml\\_press\\_underside.asp?xml=http://cws.huginonline.com/A/134655/PR/201105/1512592.xml&m=34572&s=&ss=&d=2011-05-05](http://algeta.com/xml_press_underside.asp?xml=http://cws.huginonline.com/A/134655/PR/201105/1512592.xml&m=34572&s=&ss=&d=2011-05-05). Last accessed 29.11.2011.

60. Dux, R., Kindler-Roehrborn, A., Lennartz, K., & Rajewsky, M. F. 1991. Determination of immunoreactive fraction and kinetic parameters of a radiolabeled monoclonal antibody in the absence of antigen excess. *Journal of Immunological Methods*, 144(2): 175-183.
61. Lindmo, T. & Bunn, P. A. J. 1986. Determination of the true immunoreactive fraction of monoclonal antibodies after radiolabeling. *Methods in Enzymology*, 121: 678-691.
62. Mendenhall, W., Beaver, R. J., & Beaver, B. M. 2009. *Introduction to probability and statistics*. Brooks/Cole, Cengage Learning, (12):518.
63. Ugelstad, J. & Hansen, F. K. 1976. Kinetics and mechanism of emulsion polymerization. *Rubber Chemistry and Technology*, 49(3): 536-609.
64. Neurauter, A. A., Bonyhadi, M., Lien, E., Noekleby, L., Ruud, E., Camacho, S., & Aarvak, T. 2007. Cell isolation and expansion using Dynabeads. *Advances in Biochemical Engineering/Biotechnology*, 106(Cell Separation): 41-73.
65. Chen, Y.C., Lou, X., Ingram, P. & Yoon, E. 2011. Single Cell Migration Chip using hydrodynamic Cell Positioning. *15th International Conference on Miniaturized Systems for Chemistry and Life Sciences*. Seattle, Washington, USA. 1409-1411.
66. McMahon, R. J. & Editor. 2008. *Avidin-Biotin Interactions: Methods and Applications*. *Methods Mol. Biol. (Totowa, NJ, U. S.)*, 2008; 418. Humana Press Inc.
67. Green, N. M. 1963. Avidin. III. The nature of the biotin-binding site. *Biochemical Journal*, 89(3): 599-609.
68. Medscape. A Formalin-fixed, Paraffin processed Cell-line Standard, Results. Available: <http://img.medscape.com/fullsize/migrated/422/883/ajcp422883.fig3a.jpg>. Last accessed 08.01.2012.
69. Invitrogen Dynal, Dynabeads<sup>®</sup> Products and Technology. Available: [http://www.invitrogen.com/site/us/en/home/brands/Product-Brand/Dynal/dynabeads\\_technology.html](http://www.invitrogen.com/site/us/en/home/brands/Product-Brand/Dynal/dynabeads_technology.html). Last accessed: 21.12.2011.
70. Hnatowich, D. J., Virzi, F., & Rusckowski, M. 1987. Investigations of avidin and biotin for imaging applications. *Journal of Nuclear Medicine*, 28(8): 1294-1302.
71. Thermo Fisher Scientific Inc., EZ-Link Sulfo-NHS-LC-Biotin and Biotinylation Kits. Available: <http://www.piercenet.com/browse.cfm?fldID=01030901>. Last accessed 30.11.2011.
72. Vetter, S., Bayer, E. A., & Wilchek, M. 1994. Avidin Can be Forced to Adopt Catalytic Activity. *Journal of the American Chemical Society*, 116(20): 9369-9370.
73. Thermo Scientific, Pierce HABA calculator. Available: <http://www.piercenet.com/haba/habacalc.cfm>. Last accessed 25.12.2011.
74. The Norwegian Radiation Protection Authority (Statens strålevern). Available: <http://www.nrpa.no/>. Last accessed 30.11.2011.



75. Thermo Scientific, Instructions HABA 4'-hydroxyazobenzene-2-carboxylic acid. Available: <http://www.piercenet.com/instructions/2160212.pdf>. Last accessed 25.12.2011.
76. Invitrogen Dynal, Manuals and Protocols, Dynabeads® M-270 Streptavidin. Available: [http://tools.invitrogen.com/content/sfs/manuals/653%2005\\_06%20Dynabeads%20M-270%20Streptavidin\(rev007\).pdf](http://tools.invitrogen.com/content/sfs/manuals/653%2005_06%20Dynabeads%20M-270%20Streptavidin(rev007).pdf). Last accessed: 22.01.2012.
77. Pandit-Taskar, N., O'Donoghue, J. A., Morris, M. J., Wills, E. A., Schwartz, L. H., Gonen, M., Scher, H. I., Larson, S. M., & Divgi, C. R. 2008. Antibody mass escalation study in patients with castration-resistant prostate cancer using 111In-J591: lesion detectability and dosimetric projections for 90Y radioimmunotherapy. *Journal of Nuclear Medicine : Official Publication, Society of Nuclear Medicine*, 49(7): 1066-1074.
78. Tang, Y., Lou, J., Alpaugh, R. K., Robinson, M. K., Marks, J. D., & Weiner, L. M. 2007. Regulation of Antibody-Dependent Cellular Cytotoxicity by IgG Intrinsic and Apparent Affinity for Target Antigen. *Journal of Immunology*, 179(5): 2815-2823.
79. Chan, C., Scollard, D. A., McLarty, K., Smith, S., & Reilly, R. M. 2011. A comparison of 111In- or 64Cu-DOTA-trastuzumab Fab fragments for imaging subcutaneous HER2-positive tumor xenografts in athymic mice using microSPECT/CT or microPET/CT. *EJNMMI Research*, 1(1): 15-1-15/11.
80. Holland, J. P., Caldas-Lopes, E., Divilov, V., Longo, V. A., Taldone, T., Zatorska, D., Chiosis, G., & Lewis, J. S. 2010. Measuring the pharmacodynamic effects of a novel Hsp90 inhibitor on HER2/neu expression in mice using Zr-DFO-trastuzumab. *PLoS One*, 5(1): e8859.
81. Lub-de, H., Kosterink, J. G. W., Perik, P. J., Nijhuis, H., Tran, L., Bart, J., Suurmeijer, A. J. H., de, J., Jager, P. L., & de, V. 2004. Preclinical characterisation of 111In-DTPA-trastuzumab. *British Journal of Pharmacology*, 143(1): 99-106.
82. Life Technologies, Invitrogen, Frequently Asked Questions - Streptavidin-Coupled Dynabeads®. Available: [http://www.invitrogen.com/site/us/en/home/brands/ProductBrand/Dynal/Streptavidin-Coupled-Dynabeads/dynabeads\\_streptavidin.html](http://www.invitrogen.com/site/us/en/home/brands/ProductBrand/Dynal/Streptavidin-Coupled-Dynabeads/dynabeads_streptavidin.html). Last accessed: 19.01.2012.
83. Adams, G. P., Shaller, C. C., Dadachova, E., Simmons, H. H., Horak, E. M., Tesfaye, A., Klein-Szanto, A. J. P., Marks, J. D., Brechbiel, M. W., & Weiner, L. M. 2004. A Single Treatment of Yttrium-90-labeled CHX-A"-C6.5 Diabody Inhibits the Growth of Established Human Tumor Xenografts in Immunodeficient Mice. *Cancer Research*, 64(17): 6200-6206.
84. Engfeldt, T., Orlova, A., Tran, T., Bruskin, A., Widstrom, C., Karlstrom, A. E., & Tolmachev, V. 2007. Imaging of HER2-expressing tumors using a synthetic Affibody molecule containing the 99mTc-chelating mercaptoacetyl-glycyl-glycyl-glycyl (MAG3) sequence. *Eur J Nucl Med Mol Imaging*, 34(5): 722-733.

85. Ahlgren, S., Orlova, A., Waallberg, H., Hansson, M., Sandstroem, M., Lewsley, R., Wennborg, A., Abrahmsen, L., Tolmachev, V., & Feldwisch, J. 2010. Targeting of HER2-expressing tumors using <sup>111</sup>In-ABY-025, a second-generation affibody molecule with a fundamentally reengineered scaffold. *Journal of Nuclear Medicine*, 51(7): 1131-1138.
86. ISI Web of Knowledge - All databases - Search. Available: [apps.isiknowledge.com/](http://apps.isiknowledge.com/). Last accessed: 21.12.2011.
87. Mattes, M. J. 1995. Limitations of the Lindmo method in determining antibody immunoreactivity. *International Journal of Cancer*, 61(2): 286-288.
88. Glatting, G. & Reske, S. N. 2006. Determination of the Immunoreactivity of Radiolabeled Monoclonal Antibodies: a Theoretical Analysis. *Cancer Biother.Radiopharm.*, 21(1): 15-21.
89. Products from Ridgeview Instruments AB, LigandTracer<sup>®</sup>. Available: <http://www.ligandtracer.com/>. Last accessed: 22.01.2012.



# Appendix A

## NAP-5 Purification

Figure A.1 shows the volumes of buffer used in the purification of radiolabeled antibodies from free radionuclides, at different sample volumes.

### Quick Reference Protocol Card

Illustra™ NAP™-5 Columns

**Protocol for purification of oligonucleotides and small DNA fragments, desalting and buffer exchange.**

- Ensure suitable **Buffer 1** is available

⊕ : Add

17-0853-01 (20 purifications)  
17-0853-02 (50 purifications)

- 1. Column preparation**

  - Remove top and bottom caps
  - Allow excess liquid to drain by gravity flow

- 2. Column equilibration**


  - ⊕ 10 ml Buffer 1
  - Allow to completely enter gel bed by gravity flow

- 3. Sample application**

  - ⊕ 0.1–0.5 ml sample
  - Allow to completely enter gel bed by gravity flow
  - ⊕ Additional Buffer 1 as appropriate (see table below)
  - Allow to completely enter gel bed by gravity flow


- 4. Elution**

  - Place an appropriate collection tube under column
  - ⊕ Appropriate volume of Buffer 1
  - Collect eluate by gravity flow
  - Store purified sample at -20°C



Column Type	Sample volume (ml)	Volume of Buffer 1 for Column Equilibration step (ml)	Volume of Buffer 1 for Elution step (ml)
NAP-5	0.1	0.4	0.5
	0.25	0.25	0.7
	0.5 (max vol)	0	1.0

GE, Imagination at work and GE monogram are trademarks of General Electric Company.  
Illustra and NAP are trademarks of GE Healthcare Companies.  
© 2007 General Electric Company. All rights reserved. First published 2006.  
All goods and services are sold subject to the terms and conditions of sale of the company within GE Healthcare which supplies them. A copy of these terms and conditions is available upon request.  
Contact your GE Healthcare representative for the most current information.  
<http://www.gehealthcare.com/lifesciences>  
GE Healthcare UK Limited,  
Amersham Place, Little Chalfont,  
Buckinghamshire, HP7 9NA UK



Imagination at work

17-0853-01 PC Rev-B 06/2007

**Figure A.1:** The volumes used in the purification of radiolabeled antibody conjugates from free radionuclide, (Ref.: GE Healthcare).



# Appendix B

## Yield and Specific Activity

---

AC0103 was labeled with  $^{227}\text{Th}$  a total of 12 times for this project, while AC0303 was labeled two times. After purification of the radiolabeled immunoconjugate on a NAP-5 column, the product was found in the HMW fraction. Free  $^{227}\text{Th}$  was retained on the column as LMW fraction. The radioimmunoconjugate was always purified right after the radiolabeling, day 0, and the yield represents the fraction  $^{227}\text{Th}$  bound by chelator. A second purification was performed if the radiolabeled conjugate was used the day after radiolabeling, day 1. This gives a measurement for how stable the radiolabeling is. Each radiolabeling got its own number, and the letters a and b represents day 0 and 1, respectively. Table B.1 shows the yields and specific activities of  $^{227}\text{Th}$ -AC0103 after the first purification, and Table B.2 after the second purification. Table B.3 and B.4 show the yields and specific activities of  $^{227}\text{Th}$ -AC0303 after the first and second purification, respectively.

**Table B.1:** Yield and specific activity of  $^{227}\text{Th}$ -AC0103 after first purification, day 0. Here, V is the Void-fraction, HMW is the product-fraction and LMW is free  $^{227}\text{Th}$  on the column.

Radiolabeling number	Activity (A) [MBq]			Yield	Specific activity [Bq/ $\mu\text{g}$ ]
	V	HMW	LMW		
1a	$8.8 \cdot 10^{-5}$	$6.6 \cdot 10^{-1}$	$2.2 \cdot 10^{-2}$	97 %	680
2a	$1.5 \cdot 10^{-5}$	$6.6 \cdot 10^{-1}$	$3.0 \cdot 10^{-2}$	96 %	691
3a	$9.9 \cdot 10^{-5}$	$7.7 \cdot 10^{-1}$	$3.1 \cdot 10^{-2}$	96 %	807
4a	$1.7 \cdot 10^{-4}$	$5.0 \cdot 10^{-1}$	$6.8 \cdot 10^{-2}$	88 %	566
5a	$1.7 \cdot 10^{-4}$	$7.1 \cdot 10^{-1}$	$3.4 \cdot 10^{-2}$	95 %	749
6a	$1.3 \cdot 10^{-4}$	$9.1 \cdot 10^{-1}$	$5.0 \cdot 10^{-2}$	95 %	962
7a	$1.3 \cdot 10^{-4}$	$1.0 \cdot 10^0$	$4.6 \cdot 10^{-2}$	96 %	1054
8a	$1.3 \cdot 10^{-4}$	$7.1 \cdot 10^{-1}$	$4.8 \cdot 10^{-2}$	94 %	759
9a	$1.1 \cdot 10^{-4}$	$9.2 \cdot 10^{-1}$	$5.2 \cdot 10^{-2}$	95 %	965
10a	$1.7 \cdot 10^{-4}$	$7.9 \cdot 10^{-1}$	$5.2 \cdot 10^{-2}$	94 %	845
11a	$1.6 \cdot 10^{-4}$	$5.3 \cdot 10^{-1}$	$4.5 \cdot 10^{-2}$	92 %	893
12a	$1.4 \cdot 10^{-4}$	$8.4 \cdot 10^{-1}$	$3.9 \cdot 10^{-2}$	96 %	873

**Table B.2:** Yield and specific activity of  $^{227}\text{Th-AC0103}$  after second purification, day 1. Here, V is the Void-fraction, HMW is the product-fraction and LMW is free  $^{227}\text{Th}$  on the column.

Radiolabeling number	Activity (A) [MBq]			Yield	Specific activity [Bq/ $\mu\text{g}$ ]
	V	HMW	LMW		
1b	$1.7 \cdot 10^{-4}$	$3.4 \cdot 10^{-1}$	$2.4 \cdot 10^{-2}$	93 %	526
2b	$9.4 \cdot 10^{-5}$	$3.9 \cdot 10^{-1}$	$7.1 \cdot 10^{-3}$	98 %	568
4b	$1.5 \cdot 10^{-5}$	$3.5 \cdot 10^{-1}$	$9.2 \cdot 10^{-3}$	97 %	523
5b	$1.5 \cdot 10^{-4}$	$4.5 \cdot 10^{-1}$	$1.2 \cdot 10^{-2}$	97 %	668
6b	$2.0 \cdot 10^{-4}$	$5.9 \cdot 10^{-1}$	$2.2 \cdot 10^{-2}$	96 %	877
7b	$1.1 \cdot 10^{-4}$	$6.4 \cdot 10^{-1}$	$1.5 \cdot 10^{-2}$	98 %	935
8b	$1.1 \cdot 10^{-4}$	$4.6 \cdot 10^{-1}$	$8.6 \cdot 10^{-3}$	98 %	670
10b	$1.6 \cdot 10^{-4}$	$5.3 \cdot 10^{-1}$	$4.5 \cdot 10^{-2}$	92 %	821
12b	$6.0 \cdot 10^{-4}$	$5.2 \cdot 10^{-1}$	$2.2 \cdot 10^{-2}$	96 %	771

**Table B.3:** Yield and specific activity of  $^{227}\text{Th-AC0303}$  after first purification, day 0. Here, V is the Void-fraction, HMW is the product-fraction and LMW is free  $^{227}\text{Th}$  on the column.

Radiolabeling number	Activity (A) [MBq]			Yield	Specific activity [Bq/ $\mu\text{g}$ ]
	V	HMW	LMW		
10a	$1.3 \cdot 10^{-4}$	$7.5 \cdot 10^{-1}$	$7.7 \cdot 10^{-2}$	91 %	829
11a	$1.7 \cdot 10^{-4}$	$3.9 \cdot 10^{-1}$	$5.3 \cdot 10^{-2}$	88 %	574

**Table B.4:** Yield and specific activity of  $^{227}\text{Th-AC0303}$  after second purification, day 1. Here, V is the Void-fraction, HMW is the product-fraction and LMW is free  $^{227}\text{Th}$  on the column.

Radiolabeling number	Activity (A) [MBq]			Yield	Specific activity [Bq/ $\mu\text{g}$ ]
	V	HMW	LMW		
10b	$1.7 \cdot 10^{-4}$	$3.9 \cdot 10^{-1}$	$5.3 \cdot 10^{-2}$	88 %	638
11b	$1.7 \cdot 10^{-4}$	$3.6 \cdot 10^{-1}$	$1.9 \cdot 10^{-2}$	95 %	535

The following equations give a calculation example for yield and specific activity. The values used in this example are for sample 1a:

$$\text{Yield}_{1a} = \frac{A_{\text{HMW}}}{A_{\text{HMW}} + A_{\text{V}} + A_{\text{LMW}}} \cdot 100\% = \frac{6.6 \cdot 10^{-1}}{6.6 \cdot 10^{-1} + 8.8 \cdot 10^{-4} + 2.2 \cdot 10^{-2}} \cdot 100\% = 97\%$$

$$\text{Specific activity}_{1a} = \frac{A_{\text{HMW}}}{\text{mass of AC0103} \cdot \text{Yield}} = \frac{6.6 \cdot 10^5 \text{ Bq}}{1000 \mu\text{g} \cdot 0.97} = 680 \text{ Bq}/\mu\text{g}$$

The average specific activity with standard deviation was calculated from all values in the four tables to be  $750 \pm 150 \text{ Bq}/\mu\text{g}$ . From this, the number of  $^{227}\text{Th}$  bound per antibody-chelator conjugate (AC) was calculated to be approximately one per 2000. The calculations are given below.

Average specific activity (A):	750 Bq/ $\mu\text{g}$
$t_{1/2}$ for $^{227}\text{Th}$ = 18.72 days = 1617408 s	
$\lambda = \ln 2 / t_{1/2} =$	4,29E-07
$N = A / \lambda =$	1,8E+09 $^{227}\text{Th}/\mu\text{g}$
$n (^{227}\text{Th}) = N / \text{Avogadro constant} =$	2,9E-15 mol $^{227}\text{Th}/\mu\text{g}$
$n (\text{AC}) = 1 \mu\text{g} / (147.5 \cdot 10^9 \mu\text{g}/\text{mol}) =$	6,8E-12 mol AC/ $\mu\text{g}$
This corresponds to $\sim 1 ^{227}\text{Th} : 2000 \text{ AC}$	

Here,  $t_{1/2}$  is the half time,  $\lambda$  is the proportionality constant,  $N$  is the number of nuclei and  $n$  is the number of moles. 147.5 kDa is the average molecular weight of AC0103 and AC0303, and is used to calculate number of moles AC-conjugate.





# Appendix C

## Biotinylation

---

The degree of biotinylation was determined by the following four calculations:

**Calculation #1:** mmol protein per mL in original sample  

$$= \text{protein concentration (mg/mL)} / M_w \text{ of protein (mg/mmol)}$$

**Calculation #2:**  $\Delta A (\lambda = 492 \text{ nm}) = A (\text{HABA/Avidin}) - A (\text{HABA/Avidin/Biotin})$

**Calculation #3:** mmol biotin/mL reaction mixture  $= \Delta A (495) / (\epsilon \cdot b) = \text{Calc \#2} / (34000 \cdot 0.5)$

Where: [b = the cell path length expressed in cm]  
 [ε = extinction coefficient at the wavelength λ]

**Calculation #4:** Conjugation ratio (mol biotin: mol protein)

$$= \text{mmol biotin in original sample} / \text{mmol protein in original sample}$$

$$= (\text{mmol biotin in reaction mixture} \cdot \text{dilution factor}) / \text{mmol protein in original sample}$$

$$= (\text{Calc \#3} \times 10) / \text{Calc \#1}$$

The degree of biotinylation for Ag(01) and Ag(03) was calculated as below. The red values are the measured absorbances.

### Ag(01):

$$\text{Calc \#1:} = 2 \text{ mg/mL} / 192\,000 \text{ mg/mmol} = 1.04 \cdot 10^{-5} \text{ mmol/mL}$$

$$\text{Calc \#2:} = \mathbf{0.824} - \mathbf{0.622} = 0.202$$

$$\text{Calc \#3:} = \text{Calc \#2} / (34000 \cdot 0.5) = 1.19 \cdot 10^{-5} \text{ mmol/mL}$$

$$\text{Calc \#4:} = \text{Calc \#3} \times 10 / \text{Calc \#1} = \underline{\underline{\mathbf{11.4} \text{ mol biotin : 1 mol protein}}}$$

### Ag(03):

$$\text{Calc \#1:} = 2 \text{ mg/mL} / 86\,510 \text{ mg/mmol} = 2.31 \cdot 10^{-5} \text{ mmol/mL}$$

$$\text{Calc \#2:} = \mathbf{0.817} - \mathbf{0.674} = 0.143$$

$$\text{Calc \#3:} = \text{Calc \#2} / (34000 \cdot 0.5) = 8.41 \cdot 10^{-6} \text{ mmol/mL}$$

$$\text{Calc \#4:} = \text{Calc \#3} \times 10 / \text{Calc \#1} = \underline{\underline{\mathbf{3.6} \text{ mol biotin : 1 mol protein}}}$$



# Appendix D

## Scatchard Analysis

---

Table D.1 – D.4 give the raw data from the activity measurements in the Scatchard analysis, together with calculated data for binding. In these tables, P represents the cell/bead pellet activity (=bound(B) antibody(Ab)), while S represents the activity of the supernatant (=free(F) Ab). BL represents the activity from the blocked sample (=nonspecific bound RIC). Table D.1 gives binding data for  $^{227}\text{Th}$ -AC0103 binding to Ag(01)-expressing cells, Table D.2 for  $^{227}\text{Th}$ -AC0303 binding to Ag(03)-expressing cells, Table D.3 for  $^{227}\text{Th}$ -AC0103 binding to Ag(01)-coated beads and Table D.4 for  $^{227}\text{Th}$ -AC0303 binding to Ag(03)-coated beads.

**Table D.1:** Experimental raw data and calculated values for binding measurement with  $^{227}\text{Th}$ -AC0103 binding to Ag(01)-expressing cells

Sample	Activity [cpm]		Bound RIC [%]	Specific bound RIC [%]	Free RIC [%]	B/F	n(RIC, tot) [mol]	n(RIC, B) [mol]
	P	S						
1	16408.6	8593.4	31	25	75	0.35	7E-12	1.7E-12
2	5821.5	451.7	86	80	20	4.02	2E-12	1.4E-12
3	1400.8	77.1	90	84	16	5.27	4E-13	3.5E-13
4	335.7	23.5	87	81	19	4.38	1E-13	8.6E-14
BL	197.3	176.7	6					

**Table D.2:** Experimental raw data and calculated values for binding measurement with  $^{227}\text{Th}$ -AC0303 binding to Ag(03)-expressing cells

Sample	Activity [cpm]		Bound RIC [%]	Specific bound RIC [%]	Free RIC [%]	B/F	n(RIC, tot) [mol]	n(RIC, B) [mol]
	P	S						
1	10785.6	3575.3	50	50	50	0.99	3E-12	2E-12
2	2957.1	543.0	69	69	31	2.18	9E-13	6E-13
3	705.5	122.4	70	70	30	2.33	2E-13	1E-13
4	166.4	33.9	66	66	34	1.91	5E-14	3E-14
BL	388.1	384.5	0.5					

**Table D.3:** Experimental raw data and calculated values for binding measurement with  $^{227}\text{Th}$ -AC0103 binding to Ag(01)-coated beads

Sample	Activity [cpm]		Bound RIC [%]	Specific bound RIC [%]	Free RIC [%]	B/F	n(RIC, tot) [mol]	n(RIC, B) [mol]
	P	S						
1	12278.7	5601.5	37	36	64	0.56	3E-12	1E-12
2	3828.9	370.8	82	81	19	4.24	9E-13	4E-13
3	934.4	46.8	90	89	11	8.11	2E-13	1E-13
4	227.6	19.0	85	83	17	4.94	5E-14	3E-14
BL	474.2	460.8	1					

**Table D.4:** Experimental raw data and calculated values for binding measurement with  $^{227}\text{Th}$ -AC0303 binding to Ag(03)-coated beads

Sample	Activity [cpm]		Bound RIC [%]	Specific bound RIC [%]	Free RIC [%]	B/F	n(RIC, tot) [mol]	n(RIC, B) [mol]
	P	S						
1	11650.4	4805.8	42	32	68	0.48	3E-12	1E-12
2	3052.9	856.8	56	47	53	0.89	8E-13	7E-13
3	794.2	154.8	67	58	42	1.39	2E-13	2E-13
4	225.5	41.6	69	60	40	1.48	5E-14	4E-14
BL	497.4	414	9					

Equation D.1 – D.4 are the equations for the fitted straight lines obtained by plotting the B/F values against the Bound Ab [mol] values from Table D.1 – D.4, respectively. Only values in the yellow-labeled values of the table were included in these plots. Some of the samples of lowest RIC concentrations did not fit into a straight line, and was therefore not included in the plot. The reason for this is uncertain, but might be due to the high uncertainty that might exist with so low concentrations.

Here,  $x = \text{Bound RIC [mol]}$  and  $y = \text{B/F}$ .

$$y = -9 \cdot 10^{12} x + 16.87; \quad R^2 = 1 \quad (n = 2) \quad (\text{D.1})$$

$$y = -9 \cdot 10^{11} x + 2.564; \quad R^2 = 0.971 \quad (n = 3) \quad (\text{D.2})$$

$$y = -7 \cdot 10^{12} x + 9.419; \quad R^2 = 0.998 \quad (n = 3) \quad (\text{D.3})$$

$$y = -9 \cdot 10^{11} x + 1.445; \quad R^2 = 0.928 \quad (n = 4) \quad (\text{D.4})$$

## Calculation example

---

Values from  $^{227}\text{Th}$ -AC0103 binding to Ag(01) on cells (sample 1 in Table D.1) are used in calculation examples 1 to 5. The calculations 7-9 are based on Equation D.1, which again represents sample 1 and 2 in Table D.1. Calculation 10 are based on the values for  $^{227}\text{Th}$ -AC0103 binding to Ag(01) on beads (Table D.3, Equation D.3).

1. Bound RIC =  $[(A_P - A_S)/(A_P + A_S)] \cdot 100\%$   
 $= [(16408.6 - 8593.4)/(16408.6 + 8593.4)] \cdot 100\% = 31\%$
2. Specific bound RIC = Bound RIC (Sample 1) – Bound RIC (BL sample)  
 $= 31\% - 6\% = 25\%$
3. Free RIC =  $100\% - \text{Specific bound RIC} = 100\% - 25\% = 75\%$
4. B/F = Specific bound RIC / Free RIC =  $25\% / 75\% = 0.35$
5.  $n(\text{RIC}, \text{B}) = n(\text{RIC}, \text{tot}) \cdot \text{Specific bound RIC}$   
 $= (7 \cdot 10^{-12} \text{ mol}) \cdot 25\% = 1.7 \cdot 10^{-12} \text{ mol}$
6.  $K_a = -\text{slope of line described by Equation D.1} = 9 \cdot 10^{12}$
7.  $n(\text{Ag}, \text{tot}) = \text{intercept of the extrapolated line described by Equation D.1 with x-axis}$   
 $= (16.87 / 9 \cdot 10^{12}) = 1.9 \cdot 10^{-12} \text{ mol}$
8.  $n(\text{Ag})/\text{cell} = n(\text{Ag}, \text{tot}) / \text{number of cells}$   
 $= 1.9 \cdot 10^{-12} \text{ mol} / 500\,000 \text{ cells} = 3.7 \cdot 10^{-18} \text{ mol/cell}$
9.  $N(\text{Ag})/\text{cell} = n(\text{Ag})/\text{cell} \cdot N_A$   
 $= 3.7 \cdot 10^{-18} \text{ mol/cell} \cdot 6.022 \cdot 10^{23} \text{ mol}^{-1} = 2.3 \cdot 10^6 \text{ Ag/cell}$
10.  $\mu\text{g antigen/mg beads} = n(\text{Ag}) / \text{bead} \cdot M_w \cdot \text{beads/mg}$   
 $= 1.3 \cdot 10^{-19} \text{ mol/bead Ag(01)} \cdot 96\,000 \text{ g/mol} \cdot 10^6 \mu\text{g/g} \cdot 6.5 \cdot 10^7 \text{ beads/mg}$   
 $= 8.40 \mu\text{g/mg}$

Here, n = moles, N = number of atoms,  $N_A$  = the Avogadro constant, B = bound and F = free.



# Appendix E

## Initial development of the immunoreactivity assays

The raw data, binding data and binding plots from the initial experiments with cells and beads are given in this appendix. These results were used to develop the cell- and bead-based immunoreactivity assays for this project. The first section gives the results from the cell-based assays, and the second section gives the results from the bead-based assays. The experiments were numbered after the radiolabeled AC-conjugate used in the respective experiment (see Appendix B). A calculation example for the calculated values  $(B/T)^*$ ,  $B/T_{BL}$  and  $B/T$  can be found in Appendix F.

### E.1 Initial development of cell-based immunoreactivity assays

Figure E.1 shows the results from the two first experiments with cells and  $^{227}\text{Th}$ -AC0103. The purpose of these experiments was to find the suitable number of cells for the one-point- and Lindmo analysis.

**1b - initial experiment**

# Cells [mill]	Activity [cpm]		$(B/T)^*$	B/T
	P	S		
1	446.1	40.1	0.84	0.78
5	466.2	44.1	0.83	0.77
10	474.8	37.2	0.85	0.79
20	460.4	46.2	0.82	0.76
50	455.3	26.8	0.89	0.83
BL	257.8	228.7	0.06	

**2a - initial experiment**

# Cells [mill]	Activity [cpm]		$(B/T)^*$	B/T
	P	S		
0.10	426.3	57.1	0.76	0.73
0.25	451.2	36.9	0.85	0.82
0.50	457.2	34.3	0.86	0.83
0.60	452.0	38.3	0.84	0.81
0.75	458.3	27.8	0.89	0.85
1	446.2	24.0	0.90	0.86
10	471.7	33.5	0.87	0.83
BL	259.8	243.0	0.03	

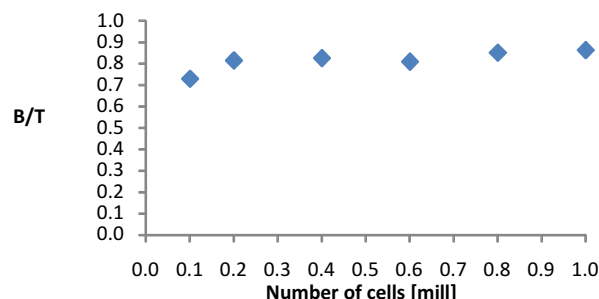
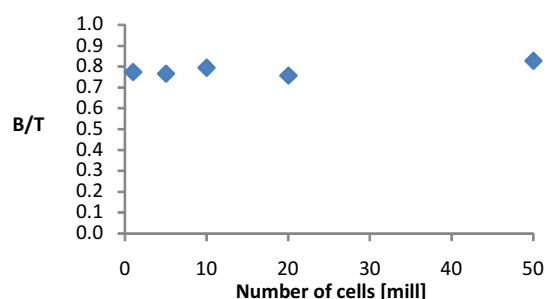


**Figure E.1:** Raw data from activity measurements, calculated binding fractions and binding plots for experiment 1b and 2a.  $^{227}\text{Th}$ -AC0103 was tested for binding to Ag(01)-expressing cells. These were initial experiments made to develop the method.



The results in Figure E.1 show that the cell numbers in these two experiments were too high to obtain a characteristic binding plot. Therefore, a third experiment was made using samples of lower cell numbers. The result is given in Figure E.2.

**2b**

# Cells [mill]	Activity [cpm]		(B/T)*	B/T
	P	S		
0.010	245.6	206.1	0.09	0.07
0.025	324.6	152.7	0.36	0.34
0.050	370.4	101.2	0.57	0.56
0.075	375.5	98.7	0.58	0.57
0.1	407.2	70.9	0.70	0.69
0.5	386.6	22.8	0.89	0.87
1	464.1	15.3	0.94	0.92
BL	239.5	232.1	0.02	

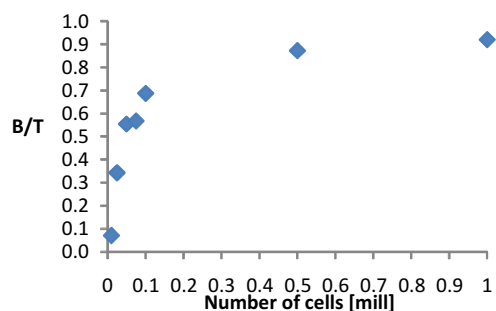


**Figure E.2:** Raw data from activity measurements, calculated binding fractions and binding plot for experiment 2b. This plot was used to determine the suitable cell-numbers for the one-point and Lindmo analysis. <sup>227</sup>Th-AC0103 was tested for binding to Ag(01)-expressing cells.

From the results presented in Figure E.1 and E.2, it was concluded that 1 million cells were sufficient for the one-point analysis and cell numbers in the range from 25 000 to 5 million were suitable for the Lindmo-analysis.

## E.2 Initial development of bead-based immunoreactivity assays

Figure E.3 shows the results from the three first experiments with  $^{227}\text{Th}$ -AC0103 and Ag(01)-coated beads. The purpose of these experiments was to find the suitable number of beads for the one-point- and Lindmo analysis. The beads were coated with 40  $\mu\text{g}$  biotinylated Ag(01) per mg beads (=40  $\mu\text{g}/\text{mg}$ ).

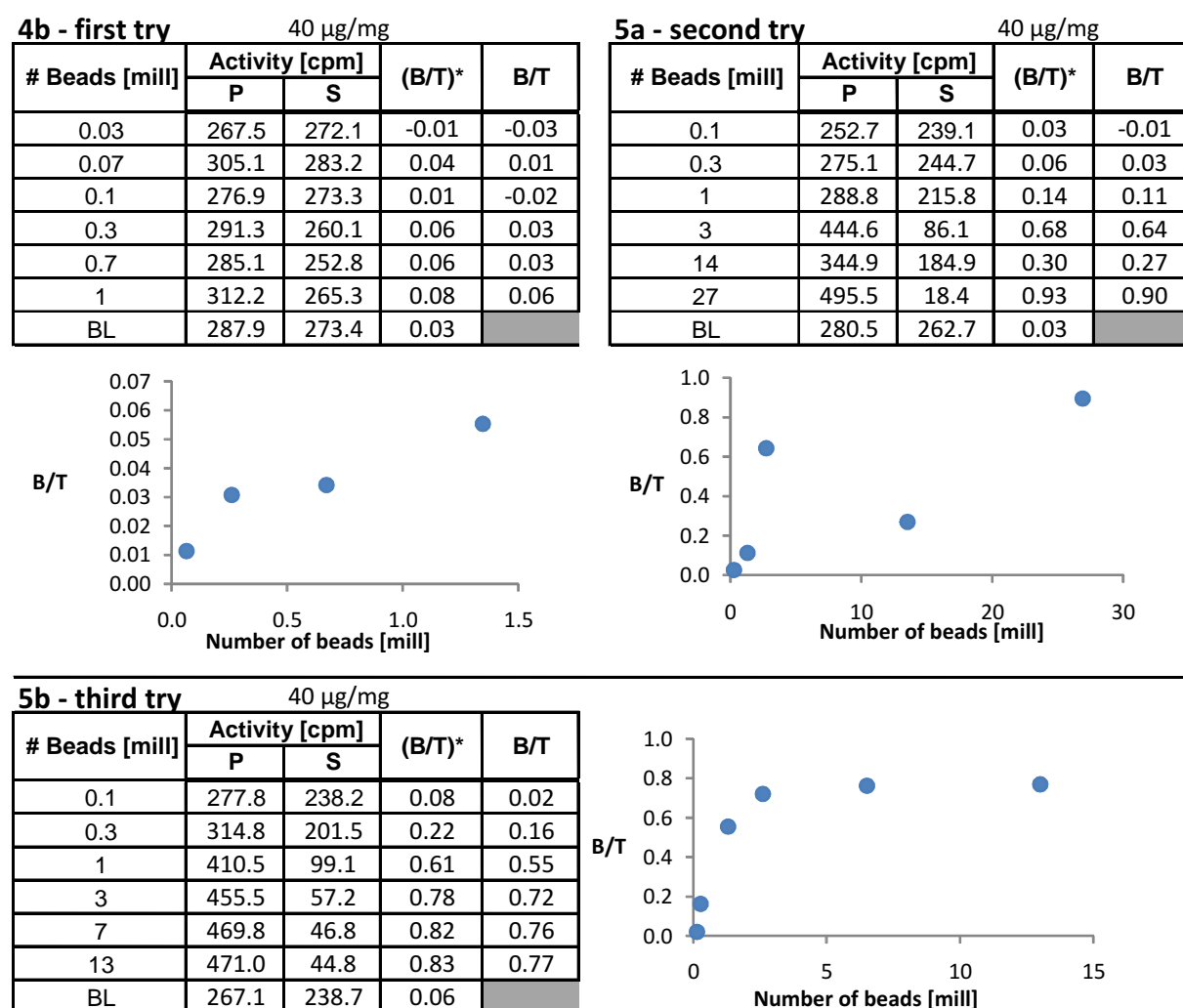


**Figure E.3:** The three first experiments with  $^{227}\text{Th}$ -AC0103 and Ag(01)-coated beads. The purpose of these experiments were to find the appropriate number of beads for the bead-based assays. The beads were coated with 40  $\mu\text{g}$  biotinylated Ag(01) per mg beads.

Figure E.3 shows that bead numbers from 100 000 to 10 million might be appropriate for the Lindmo analysis. Later, it was decided to test the binding capacity of the beads because it was thought that the assumed capacity of 40  $\mu\text{g}/\text{mg}$  might be too high. If this was true, not all of the added antigen would have bound to the beads, but would have gone to waste. To investigate if this was the case, one experiment with 40  $\mu\text{g}/\text{mg}$  and one with 10

$\mu\text{g}/\text{mg}$  was performed. The experiment with  $10 \mu\text{g}/\text{mg}$  had four times more beads in each sample than the experiment with  $40 \mu\text{g}/\text{mg}$ . If the binding capacity was  $40 \mu\text{g}/\text{mg}$ , the samples would then contain the same amount of antigen. And in this case, the two experiments should give the same result. The results from the two experiments are given in Figure E.4.

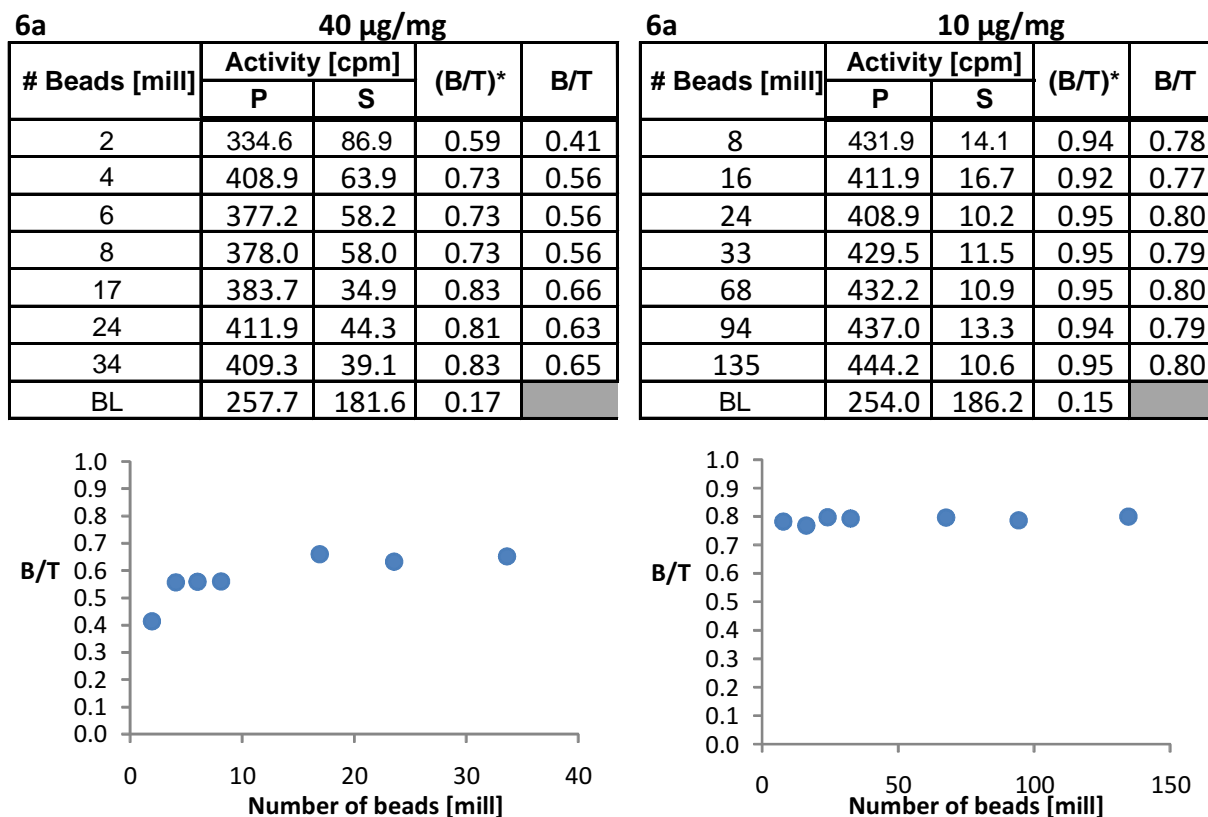


**Figure E.4:** Experiments with  $^{227}\text{Th}$ -AC0103 and Ag(01)-coated beads performed to investigate the binding capacity of the beads. The result presented to the left had  $40 \mu\text{g}$  biotinylated antigen per mg beads ( $=40 \mu\text{g}/\text{mg}$ ). The result to the right had  $10 \mu\text{g}/\text{mg}$ .

Figure E.4 shows that the samples in the experiment with  $10 \mu\text{g}/\text{mg}$  contained more antigen than the samples with  $40 \mu\text{g}/\text{mg}$ . This means that much of the antigens in the  $40 \mu\text{g}/\text{mg}$  coating had not bound to the beads, but gone to waste.

Due to these results,  $10 \mu\text{g}/\text{mg}$  was used for coating the beads in the further experiments. The capacity could be higher, for example  $20 \mu\text{g}/\text{mg}$ , but it was concluded that  $10 \mu\text{g}/\text{mg}$  gave convenient amounts of beads to work with. (A low number of beads gives small volumes to work with, as the beads are quite small compared to cells ( $2.8 \mu\text{m}$  in diameter compared to  $14 \mu\text{m}$  for SKOV-3 cells)).

Based on the results in Figure E.3 and E.4 it was thought that bead numbers from 25 000 to 40 million could be appropriate for the Lindmo analysis. This was further investigated in experiment 6b. The result is given in Figure E.5. The conclusion from this was that 50 000 to 25 million beads would be sufficient. It was also concluded that 15 million beads were adequate for the one-point analysis.

**6b - Parallel 1 - Without BSA**

# Beads [mill]	Activity [cpm]		(B/T)*	B/T
	P	S		
0.25	309.3	240.9	0.12	-0.01
0.65	355.6	190.8	0.30	0.16
1.30	382.1	148.8	0.44	0.30
2.00	434.7	111.1	0.59	0.46
2.6	458.4	93.5	0.66	0.52
6.5	478.4	68.4	0.75	0.61
13.0	501.6	54.2	0.80	0.67
BL	332.0	251.6	0.14	

**6b - Parallel 2 - Without BSA**

# Beads [mill]	Activity [cpm]		(B/T)*	B/T
	P	S		
1.3	436.4	135.8	0.53	0.53
2.6	475.5	101.4	0.65	0.65
6.5	489.1	56.5	0.79	0.79
13.0	478.7	58.6	0.78	0.78
20.0	477.8	53.2	0.80	0.80
27.0	506.5	53.3	0.81	0.81
40.0	524.3	51.6	0.82	0.82
BL	317.8	241.1	0.14	

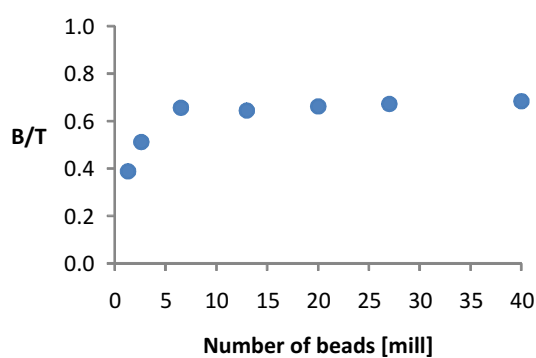
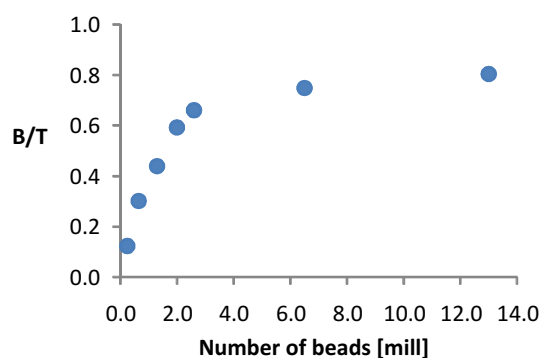


**Figure E.5:** Investigation of the appropriate number of beads for the bead-based Lindmo analysis. The binding of  $^{227}\text{Th-AC0103}$  to Ag(01)-coated beads was tested. The beads were coated with  $10\ \mu\text{g}$  Ag(01) per mg beads.



# Appendix F

## Cell-based Immunoreactivity Assays for $^{227}\text{Th-AC0103}$

---

In the next two sections, raw data and calculated values from the cell-based binding assays for  $^{227}\text{Th-AC0103}$  are presented. Data from the one-point analyses are presented first. Secondly, data and plots from the Lindmo analyses are given. Calculation examples are also included. The experiments were numbered after the radiolabeled AC-conjugate used in the respective experiment (see Appendix B).

---

### F.1 Cell-based one-point analyses for $^{227}\text{Th-AC0103}$

---

Raw data from the activity measurements from the cell-based one-point analyses for  $^{227}\text{Th-AC0103}$  are given in Table F.1. 1 million Ag(01)-expressing cells were used per sample in these experiments. Six of these measurements are the 1 million cell samples of the Lindmo analyses presented in the next section (2b, 4b, 5a, 5b, 6a and 7b).

The following calculations give an example of how nonspecific binding,  $B/T_{\text{BL}}$ , and immunoreactive fraction at limited antigen excess,  $\text{IRF}^*$ , were calculated.  $(B/T)^*$  is the fraction of bound RIC in one sample, with nonspecific binding included. Values from experiment 1b are used for these examples.

1.  $(B/T)^* = [(A_{\text{P}} - A_{\text{S}})/(A_{\text{P}} + A_{\text{S}})] \cdot 100\% = [(446.1 - 40.1)/(446.1 + 40.1)] \cdot 100\% = 84\%$
2. Nonspecific binding =  $B/T_{\text{BL}} = [(A_{\text{P, BL}} - A_{\text{S, BL}})/(A_{\text{P, BL}} + A_{\text{S, BL}})] \cdot 100\%$   
 $= [(257.8 - 228.7)/(257.8 + 228.7)] \cdot 100\% = 6\%$
3.  $\text{IRF}^* = B/T$  (in sample with excess of antigen) =  $(B/T)^* - B/T_{\text{BL}} = 84\% - 6\% = 78\%$

Averages and standard deviations (S.D.) were calculated in excel by the functions AVERAGE and STDEV, respectively.

**Table F.1:** Raw data from the activity measurements and calculated values from the one-point analyses of <sup>227</sup>Th-AC0103 using Ag(01)-expressing cells. UBL = unblocked analysis sample. BL = blocked control sample. P = sample containing cell pellet + 1/2 supernatant. S = sample containing 1/2 supernatant.

Experiment	Activity (UBL)		(B/T)*	Activity (BL)		B/T <sub>BL</sub>	IRF*
	P	S		P	S		
1b	446.1	40.1	<b>84%</b>	257.8	228.7	<b>6%</b>	<b>78%</b>
2a	426.3	57.1	<b>76%</b>	259.8	243.0	<b>3%</b>	<b>73%</b>
2b	464.1	15.3	<b>94%</b>	239.5	232.1	<b>2%</b>	<b>92%</b>
3a	469.3	35.6	<b>86%</b>	248.5	239.0	<b>2%</b>	<b>84%</b>
	475.1	39.3	<b>85%</b>	241.2	221.1	<b>4%</b>	<b>81%</b>
	474.4	29.0	<b>88%</b>	249.4	241.2	<b>2%</b>	<b>86%</b>
4b	553.3	43.8	<b>85%</b>	289.2	270.1	<b>3%</b>	<b>82%</b>
5a	501.3	42.6	<b>84%</b>	263.0	226.1	<b>8%</b>	<b>77%</b>
5b	483.5	36.8	<b>86%</b>	274.0	226.3	<b>10%</b>	<b>76%</b>
6a	414.5	33.9	<b>85%</b>	226.5	212.7	<b>3%</b>	<b>82%</b>
7a	504.3	35.2	<b>87%</b>	255.9	250.4	<b>1%</b>	<b>86%</b>
7b	468.7	52.6	<b>80%</b>	261.7	253.4	<b>2%</b>	<b>78%</b>

AVERAGE:	<b>4%</b>	<b>81%</b>
S.D.:	<b>3%</b>	<b>5%</b>

## F.2 Cell-based Lindmo analyses for $^{227}\text{Th-AC0103}$

There were performed six Lindmo analyses for  $^{227}\text{Th-AC0103}$  with Ag(01)-expressing cells. The resulting IRF-values from each experiments and average IRF with S.D. are given in Table F.2.

**Table F.2:** The calculated IRF values for each Lindmo analysis of  $^{227}\text{Th-AC0103}$  with Ag(01)-expressing cells. Average IRF with standard deviation is given below.

Experiment	IRF	R <sup>2</sup>
2b	97%	0.982
4b	83%	0.887
5a	74%	0.874
5b	81%	0.893
6a	77%	0.397
7b	83%	0.926
Average	<b>83%</b>	<b>0.83</b>
S.D.	<b>8%</b>	<b>0.21</b>

Raw data, calculated values, binding plots and Lindmo plots for the six experiments used to calculate the IRF values in Table F.2 are given in Figure F.1-F.3. IRF is determined from each Lindmo-plot as the intercept of the fitted straight line with the y-axis. The red labeled values in Figure F.1 and F.3 were omitted from the respective Lindmo-plot.

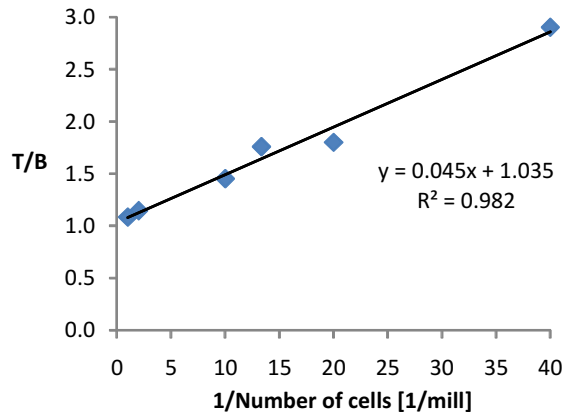
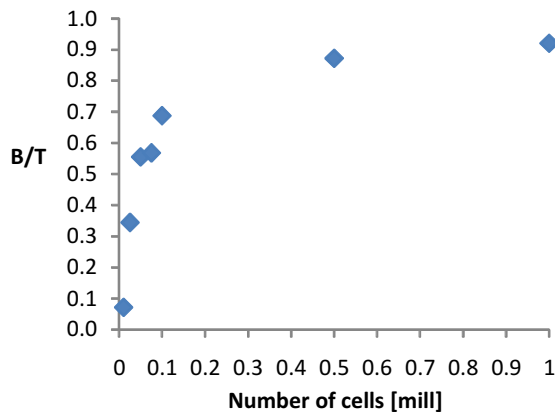
A calculation example for the calculated values is given below. For this example, values from the 1 million cell sample in experiment 2b are used. For calculation of the immunoreactive fraction at unlimited antigen excess, IRF, the Lindmo plot from the same experiment is used (see Figure F.1).

1.  $(B/T)^* = [(A_P - A_S)/(A_P + A_S)] \cdot 100\% = [(464.1 - 15.3)/(464.1 + 15.3)] \cdot 100\% = 94\%$
2.  $\text{Nonspecific binding} = B/T_{BL} = [(A_{P,BL} - A_{S,BL})/(A_{P,BL} + A_{S,BL})] \cdot 100\%$   
 $= [(239.5 - 232.1)/(239.5 + 232.1)] \cdot 100\% = 2\%$
3.  $B/T = (B/T)^* - B/T_{BL} = 94\% - 2\% = 92\%$
4.  $T/B = 1/(B/T) = 1/0.92 = 1.09$
5.  $\text{IRF} = x \text{ when } y \rightarrow 0 = 1.035/0.045 = 0.97 = 97\%$



**2b**

# Cells [mill]	Activity [cpm]		(B/T)*	B/T	1/# Cells [1/mill]	T/B
	P	S				
0.010	245.6	206.1	0.09	0.07	100	13.94
0.025	324.6	152.7	0.36	0.34	40	2.90
0.050	370.4	101.2	0.57	0.56	20	1.80
0.075	375.5	98.7	0.58	0.57	13	1.76
0.1	407.2	70.9	0.70	0.69	10	1.45
0.5	386.6	22.8	0.89	0.87	2	1.15
1	464.1	15.3	0.94	0.92	1	1.09
BL	239.5	232.1	0.02			IRF 97%



**4b**

# Cells [mill]	Activity [cpm]		(B/T)*	B/T	1/# Cells [1/mill]	T/B
	P	S				
0.025	399.4	122.2	0.53	0.50	40	2.01
0.05	443.8	124.7	0.56	0.53	20	1.90
0.1	505.2	72.3	0.75	0.72	10	1.40
0.2	544.0	54.8	0.82	0.78	5	1.28
0.5	514.1	35.9	0.87	0.84	2	1.20
1	553.3	43.8	0.85	0.82	1	1.22
BL	289.2	270.1	0.03			IRF 83%

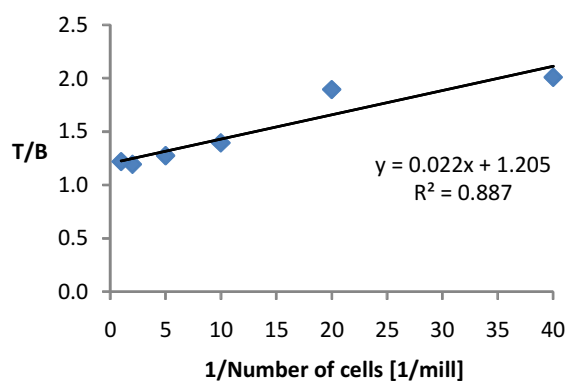
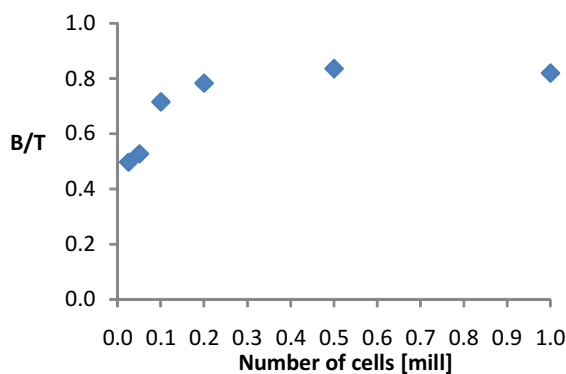
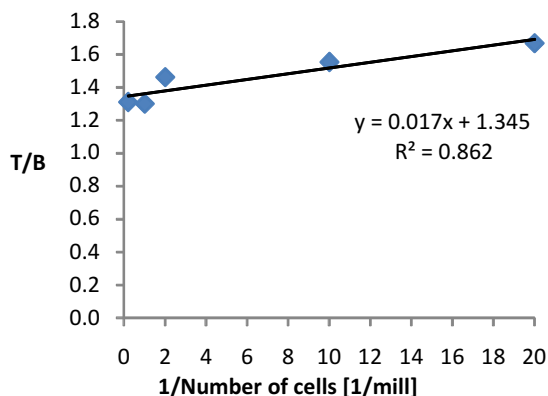
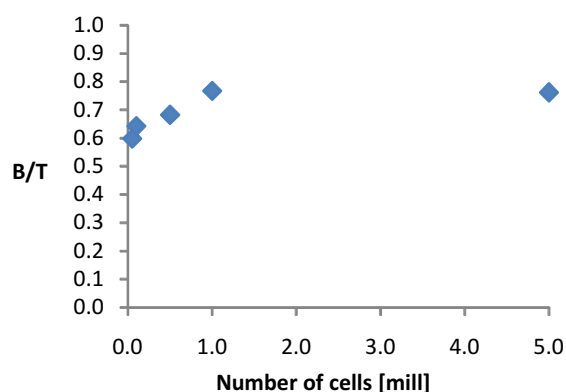


**Figure F.1:** Raw data from activity measurements, calculated binding fractions, binding plots and Lindmo plots for experiment 2b and 4b. <sup>227</sup>Th-AC0103 was tested for binding to Ag(01)-expressing cells. IRF was calculated from the equation of the fitted straight line.

### 5a

# Cells [mill]	Activity [cpm]		(B/T)*	B/T	1/# Cells [1/mill]	T/B	
	P	S					
0.050	432.6	84.2	0.67	0.60	20	1.67	
0.10	452.1	74.1	0.72	0.64	10	1.56	
0.5	437.5	60.0	0.76	0.68	2	1.46	
1.0	501.3	42.6	0.84	0.77	1	1.30	
5.0	478.8	42.4	0.84	0.76	0.2	1.31	
BL	263.0	226.1	0.08				IRF 74%



### 5b

# Cells [mill]	Activity [cpm]		(B/T)*	B/T	1/# Cells [1/mill]	T/B	
	P	S					
0.05	364.1	138.1	0.45	0.35	20	2.82	
0.10	433.1	67.5	0.73	0.63	10	1.57	
0.50	465.6	46.0	0.82	0.72	2	1.38	
1.0	483.5	36.8	0.86	0.76	1	1.31	
2.5	479.9	46.4	0.82	0.73	0.4	1.37	
5.0	451.0	39.3	0.84	0.74	0.2	1.34	
BL	274.0	226.3	0.10				IRF 81%

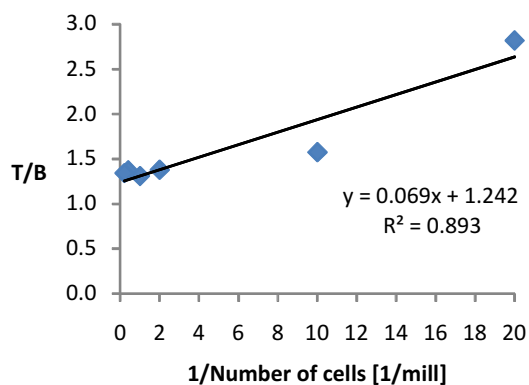
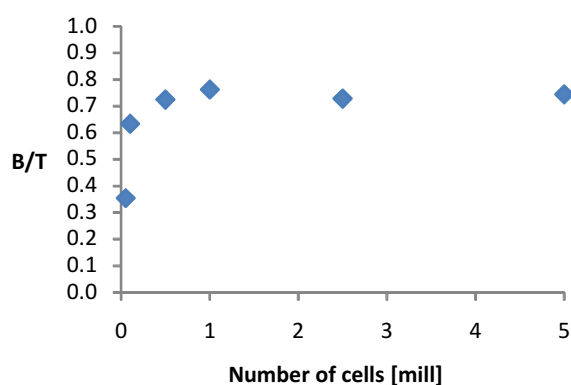
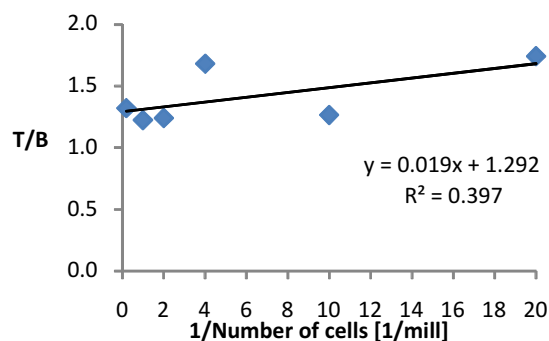
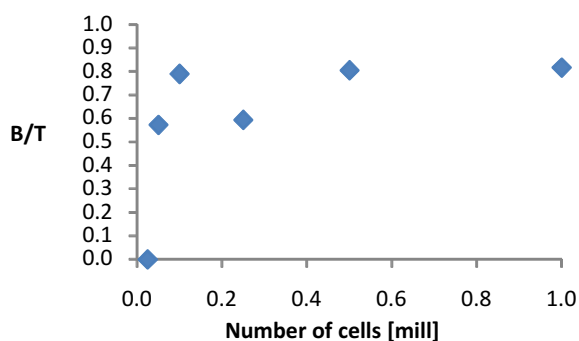


**Figure F.2:** Raw data from activity measurements, calculated binding fractions, binding plots and Lindmo plots for experiment 5a and 5b. <sup>227</sup>Th-AC0103 was tested for binding to Ag(01)-expressing cells. IRF was calculated from the equation of the fitted straight line.

### 6a

# Cells [mill]	Activity [cpm]		(B/T)*	B/T	1/# Cells [1/mill]	T/B
	P	S				
0.025	233.1	221.5	0.03	0.00	40	0.00
0.05	346.9	85.4	0.60	0.57	20	1.74
0.10	397.9	39.0	0.82	0.79	10	1.27
0.25	364.5	83.9	0.63	0.59	4	1.68
0.50	405.1	35.9	0.84	0.81	2	1.24
1	414.5	33.9	0.85	0.82	1	1.22
BL	226.5	212.7	0.03			IRF 77%



### 7b

# Cells [mill]	Activity [cpm]		(B/T)*	B/T	1/# Cells [1/mill]	T/B
	P	S				
0.05	386.1	120.3	0.52	0.51	20	1.97
0.10	470.0	76.5	0.72	0.70	10	1.42
0.25	456.5	60.1	0.77	0.75	4	1.33
0.50	484.1	47.6	0.82	0.80	2	1.24
0.75	471.5	59.7	0.78	0.76	1.3	1.32
1.0	468.7	52.6	0.80	0.78	1.0	1.28
BL	261.7	253.4	0.02			IRF 83%

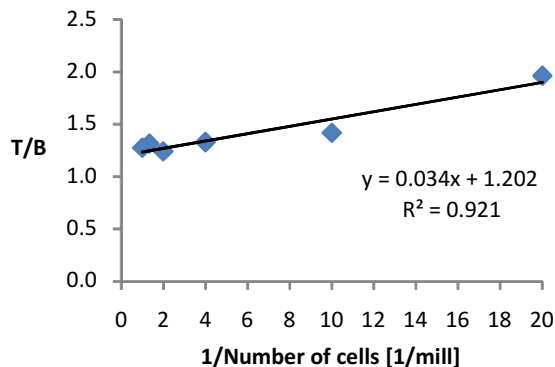
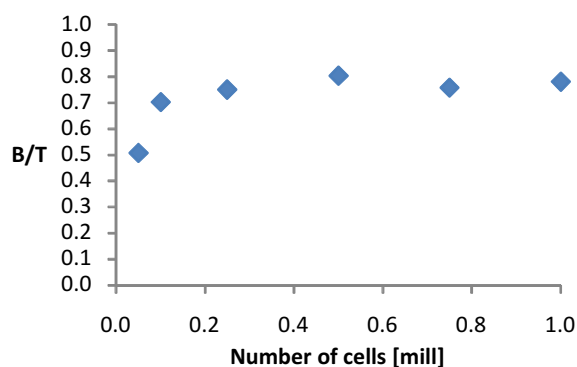


**Figure F.3:** Raw data from activity measurements, calculated binding fractions, binding plots and Lindmo plots for experiment 6a and 7b. <sup>227</sup>Th-AC0103 was tested for binding to Ag(01)-expressing cells. IRF was calculated from the equation of the fitted straight line.

# Appendix G

## Bead-based Immunoreactivity Assays for $^{227}\text{Th-AC0103}$

---

In the next two sections, raw data and calculated values from the bead-based binding assays for  $^{227}\text{Th-AC0103}$  are presented. Data from the one-point analyses are presented first. Secondly, data and plots from the Lindmo analyses are given. Calculations were the same as for the cell-based immunoreactivity assays for  $^{227}\text{Th-AC0103}$  (see example in Appendix F). The experiments were numbered after the radiolabeled AC-conjugate used in the respective experiment (see Appendix B).

---

### G.1 Bead-based one-point analyses for $^{227}\text{Th-AC0103}$

---

Raw data from the activity measurements from the bead-based one-point analyses for  $^{227}\text{Th-AC0103}$  are given in Table G.1. 15 million Ag(01)-coated beads were used per sample in these experiments.

**Table G.1:** Raw data from the activity measurements and calculated values from the one-point analyses of <sup>227</sup>Th-AC0103 using Ag(01)-coated beads. UBL = unblocked analysis sample. BL = blocked control sample. P = sample containing cell pellet + 1/2 supernatant. S = sample containing 1/2 supernatant.

Experiment	Activity (UBL)		(B/T)*	Activity (BL)		B/T <sub>BL</sub>	IRF*	Comments	
	P	S		P	S				
6b	501.6	54.2	<b>81%</b>	332.0	251.6	<b>14%</b>	<b>67%</b>	Without BSA	
	478.7	58.6	<b>78%</b>	317.8	241.1	<b>14%</b>	<b>64%</b>		
7a	506.8	23.3	<b>91%</b>	284.2	246.9	<b>7%</b>	<b>84%</b>		
	499.2	22.0	<b>92%</b>	290.8	229.3	<b>12%</b>	<b>80%</b>		
7b	505.2	29.1	<b>89%</b>	321.2	255.6	<b>11%</b>	<b>78%</b>		
	509.9	16.8	<b>94%</b>	288.6	244.6	<b>8%</b>	<b>85%</b>		
	532.7	28.5	<b>90%</b>	307.0	232.5	<b>14%</b>	<b>76%</b>		
8a	538.2	10.5	<b>96%</b>	290.1	226.7	<b>12%</b>	<b>84%</b>		Without BSA
	481.6	16.8	<b>93%</b>	282.5	219.4	<b>13%</b>	<b>81%</b>		
	499.8	13.3	<b>95%</b>	302.0	221.1	<b>15%</b>	<b>79%</b>		
	522.1	19.9	<b>93%</b>	278.1	236.8	<b>8%</b>	<b>85%</b>		
	483.2	26.6	<b>90%</b>	256.5	243.3	<b>3%</b>	<b>87%</b>	1% BSA	
	492.7	29.5	<b>89%</b>	245.4	254.9	<b>0%</b>	<b>89%</b>		
	481.3	35.6	<b>86%</b>	252.4	242.2	<b>2%</b>	<b>84%</b>		
	470.8	24.6	<b>90%</b>	268.4	254.4	<b>3%</b>	<b>87%</b>		
	497.8	37.3	<b>86%</b>	251.7	236.4	<b>3%</b>	<b>83%</b>	5% BSA	
	272.3	20.4	<b>86%</b>	276.1	248.3	<b>5%</b>	<b>81%</b>		
	488.0	36.8	<b>86%</b>	257.4	268.0	<b>0%</b>	<b>86%</b>		
491.3	38.5	<b>85%</b>	265.6	249.1	<b>3%</b>	<b>82%</b>			
8b	517.3	40.0	<b>86%</b>	276.4	241.4	<b>7%</b>	<b>79%</b>	1% BSA	
	518.8	51.7	<b>82%</b>	264.6	271.8	<b>0%</b>	<b>82%</b>		
9a	534.7	21.0	<b>92%</b>	255.5	241.9	<b>3%</b>	<b>89%</b>		
10a	522.1	24.2	<b>91%</b>	257.3	257.0	<b>0%</b>	<b>91%</b>		
10b	544.0	52.7	<b>82%</b>	304.2	284.1	<b>3%</b>	<b>79%</b>		

<b>Without BSA:</b>	AVERAGE:	<b>12%</b>	<b>78%</b>
n=11	SD:	<b>3%</b>	<b>7%</b>

<b>With BSA:</b>	AVERAGE:	<b>2%</b>	<b>85%</b>
n=13	SD:	<b>2%</b>	<b>4%</b>

## G.2 Bead-based Lindmo analyses for $^{227}\text{Th-AC0103}$

There were initially performed six Lindmo analyses for  $^{227}\text{Th-AC0103}$  with Ag(01)-coated beads. BSA was not added to the samples of these experiments. The resulting IRF-values from each experiments and average IRF with S.D. from these six experiments are given in Table F.3. Five more Lindmo analyses for  $^{227}\text{Th-AC0103}$  with Ag(01)-coated beads were performed with BSA added to the samples. The resulting IRF-values from each experiments and average IRF with S.D. from these five experiments are given in Table G.3.

**Table G.2:** The calculated IRF values for each Lindmo analysis of  $^{227}\text{Th-AC0103}$  with Ag(01)-coated beads. BSA was not added to the samples of these experiments. Calculated average IRF with standard deviation is given below.

Experiment	IRF
6b	86%
6b	71%
7a	90%
7a	86%
7b	87%
7b	79%
Average	<b>83%</b>
S.D.	<b>7%</b>

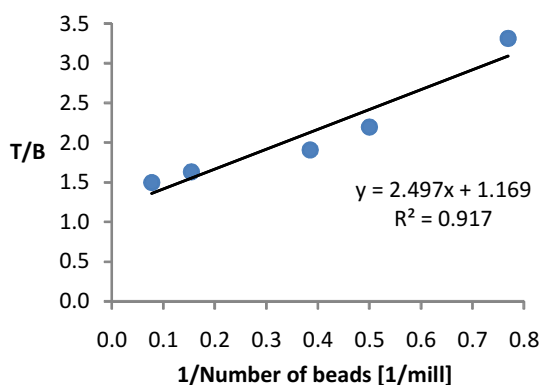
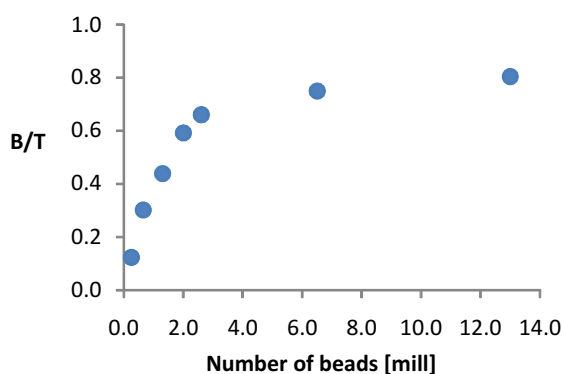
**Table G.3:** The calculated IRF values for each Lindmo analysis of  $^{227}\text{Th-AC0103}$  with Ag(01)-coated beads. BSA was added to the samples of these experiments. Calculated average IRF with standard deviation is given below.

Experiment	IRF
8b	89%
8b	89%
9a	98%
10a	99%
10b	88%
Average	<b>93%</b>
S.D.	<b>5%</b>

Raw data, calculated values, binding plots and Lindmo plots for the six experiments without BSA (see Table G.2) are given in Figure G.1-G.3. Raw data, calculated values, binding plots and Lindmo plots for the five experiments with BSA (see Table G.3) are given in Figure G.4-G.6. The red labeled values in Figure G.1-G.6 were omitted from the respective Lindmo-plot.

### 6b - Parallel 1 - Without BSA

# Beads [mill]	Activity [cpm]		(B/T)*	B/T	1/# Beads [1/mill]	T/B
	P	S				
0.25	309.3	240.9	0.12	-0.01	4.0	-74.37
0.65	355.6	190.8	0.30	0.16	1.5	6.10
1.30	382.1	148.8	0.44	0.30	0.8	3.31
2.00	434.7	111.1	0.59	0.46	0.5	2.20
2.6	458.4	93.5	0.66	0.52	0.4	1.91
6.5	478.4	68.4	0.75	0.61	0.2	1.63
13.0	501.6	54.2	0.80	0.67	0.1	1.50
BL	332.0	251.6	0.14			IRF 86%



### 6b - Parallel 2 - Without BSA

# Beads [mill]	Activity [cpm]		(B/T)*	B/T	1/# Beads [1/mill]	T/B
	P	S				
1.3	436.4	135.8	0.53	0.39	0.77	2.58
2.6	475.5	101.4	0.65	0.51	0.38	1.96
6.5	489.1	56.5	0.79	0.66	0.15	1.53
13.0	478.7	58.6	0.78	0.64	0.08	1.55
20.0	477.8	53.2	0.80	0.66	0.05	1.51
27.0	506.5	53.3	0.81	0.67	0.04	1.49
40.0	524.3	51.6	0.82	0.68	0.03	1.46
BL	317.8	241.1	0.14			IRF 71%

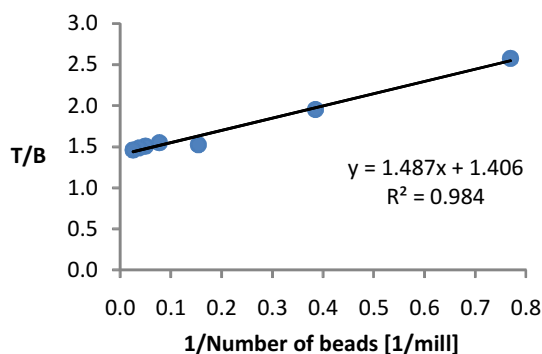
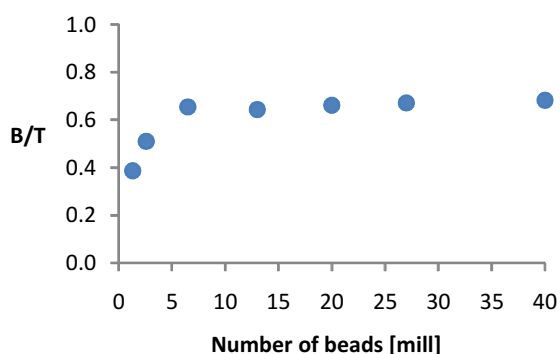
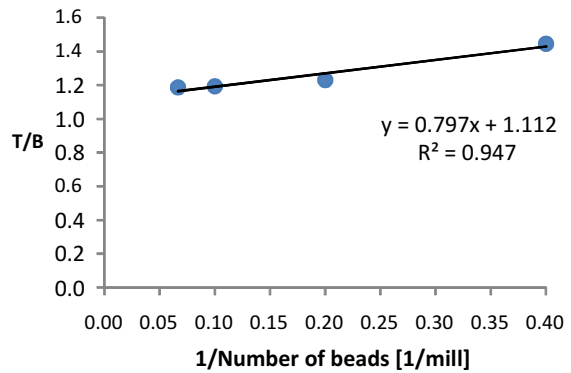
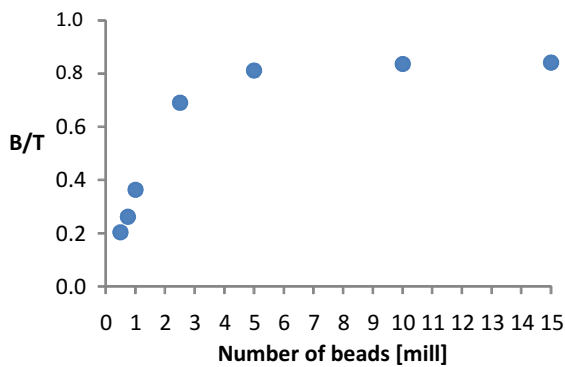


**Figure G.1:** Raw data from activity measurements, calculated binding fractions, binding plots and Lindmo plots for the two parallels of experiment 6b. <sup>227</sup>Th-AC0103 was tested for binding to Ag(01)-coated beads. IRF was calculated from the equation of the fitted straight line.

**7a - Parallel 1 - Without BSA**

# Beads [mill]	Activity [cpm]		(B/T)*	B/T	1/# Beads [1/mill]	T/B
	P	S				
0.50	340.4	194.0	0.27	0.20	2.00	4.91
0.75	337.0	168.8	0.33	0.26	1.33	3.81
1.0	366.9	144.8	0.43	0.36	1.00	2.75
2.5	451.2	61.2	0.76	0.69	0.40	1.45
5.0	517.6	32.4	0.88	0.81	0.20	1.23
10	474.6	23.1	0.91	0.84	0.10	1.19
15	506.8	23.3	0.91	0.84	0.07	1.19
BL	284.2	246.9	0.07			

**IRF 90%**



**7a - Parallel 2 - Without BSA**

# Beads [mill]	Activity [cpm]		(B/T)*	B/T	1/# Beads [1/mill]	T/B
	P	S				
0.50	307.6	186.6	0.24	0.13	2.00	7.90
0.75	337.7	164.7	0.34	0.23	1.33	4.42
1.0	382.1	158.7	0.41	0.29	1.00	3.39
2.5	428.5	75.2	0.70	0.58	0.40	1.71
5.0	471.7	37.4	0.85	0.73	0.20	1.36
10	484.5	36.6	0.86	0.74	0.10	1.35
15	499.2	22.0	0.92	0.80	0.07	1.25
BL	290.8	229.3	0.12			

**IRF 86%**

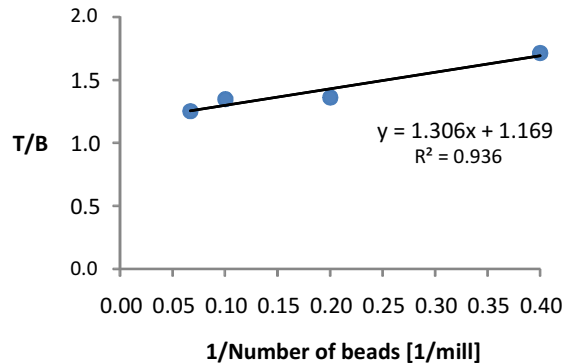


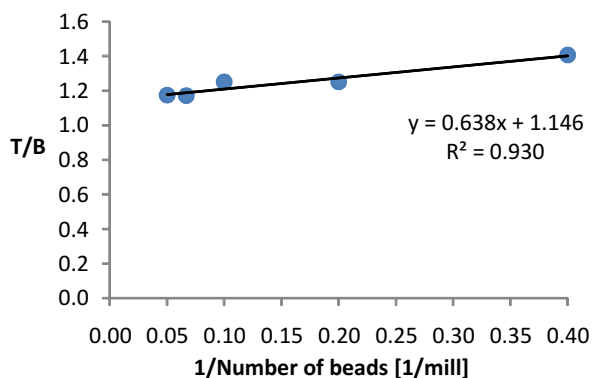
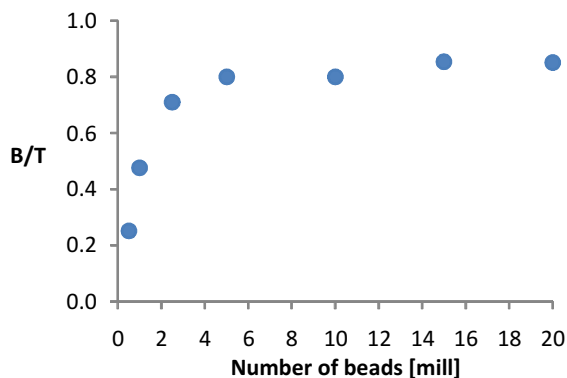
**Figure G.2:** Raw data from activity measurements, calculated binding fractions, binding plots and Lindmo plots for the two parallels of experiment 7a. <sup>227</sup>Th-AC0103 was tested for binding to Ag(01)-coated beads. IRF was calculated from the equation of the fitted straight line.



### 7b - Parallel 1 - Without BSA

# Beads [mill]	Activity [cpm]		(B/T)*	B/T	1/# Beads [1/mill]	T/B
	P	S				
0.50	358.7	179.2	0.33	0.25	2.00	3.98
1.0	414.1	117.2	0.56	0.48	1.00	2.10
2.5	491.5	56.8	0.79	0.71	0.40	1.41
5.0	526.6	33.0	0.88	0.80	0.20	1.25
10.0	519.5	32.6	0.88	0.80	0.10	1.25
15.0	509.9	16.8	0.94	0.85	0.07	1.17
20.0	542.3	18.7	0.93	0.85	0.05	1.18
BL	288.6	244.6	0.08			

**IRF 87%**



### 7b - Parallel 2 - Without BSA

# Beads [mill]	Activity [cpm]		(B/T)*	B/T	1/# Beads [1/mill]	T/B
	P	S				
0.50	366.1	174.1	0.36	0.22	2.00	4.60
1.0	404.8	132.4	0.51	0.37	1.00	2.71
2.5	475.3	50.0	0.81	0.67	0.40	1.49
5.0	534.9	34.4	0.88	0.74	0.20	1.35
10.0	527.3	24.3	0.91	0.77	0.10	1.29
15.0	532.7	28.5	0.90	0.76	0.07	1.32
20.0	536.0	28.5	0.90	0.76	0.05	1.31
BL	307.0	232.5	0.14			

**IRF 79%**

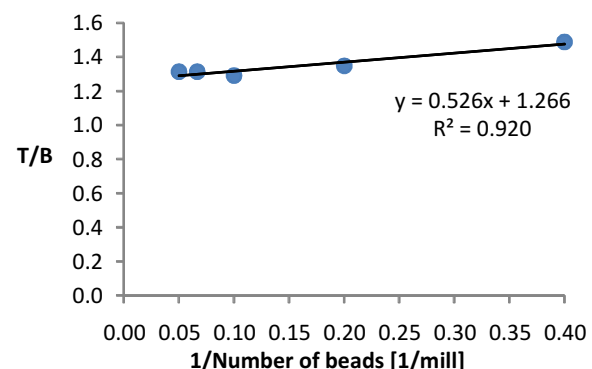
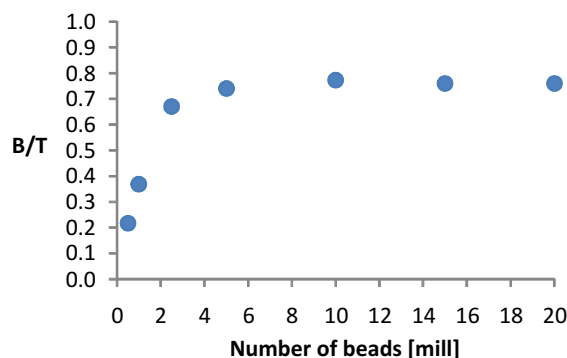
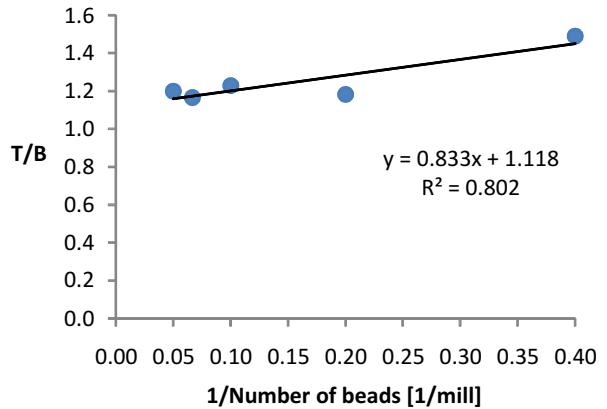
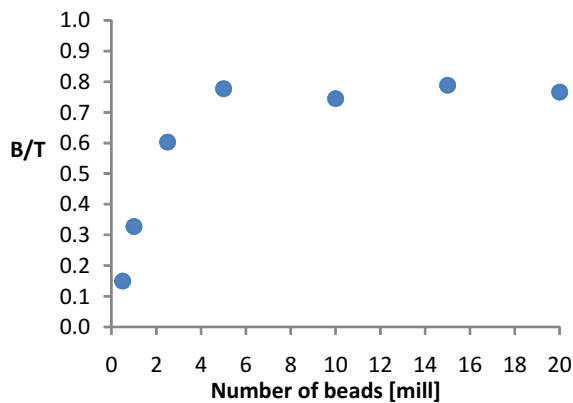


**Figure G.3:** Raw data from activity measurements, calculated binding fractions, binding plots and Lindmo plots for the two parallels of experiment 7b. <sup>227</sup>Th-AC0103 was tested for binding to Ag(01)-coated beads. IRF was calculated from the equation of the fitted straight line.

### 8b - Parallel 1 - 1% BSA

# Beads [mill]	Activity [cpm]		(B/T)*	B/T	1/# Beads [1/mill]	T/B
	P	S				
0.50	321.5	206.5	0.22	0.15	2.00	4.59
1.0	381.8	165.4	0.40	0.33	1.00	2.53
2.5	473.1	93.3	0.67	0.60	0.40	1.49
5.0	496.5	41.8	0.84	0.78	0.20	1.18
10.0	497.3	51.4	0.81	0.75	0.10	1.23
15.0	517.3	40.0	0.86	0.79	0.07	1.17
20.0	504.8	45.8	0.83	0.77	0.05	1.20
BL	276.4	241.4	0.07			IRF 89%



### 8b - Parallel 2 - 1% BSA

# Beads [mill]	Activity [cpm]		(B/T)*	B/T	1/# Beads [1/mill]	T/B
	P	S				
0.50	324.3	208.2	0.22	0.22	2.00	4.59
1.0	361.5	190.7	0.31	0.31	1.00	3.23
2.5	459.4	97.8	0.65	0.65	0.40	1.54
5.0	487.1	62.0	0.77	0.77	0.20	1.29
10.0	495.0	47.1	0.83	0.83	0.10	1.21
15.0	518.8	51.7	0.82	0.82	0.07	1.22
20.0	502.8	42.0	0.85	0.85	0.05	1.18
BL	264.6	271.8	-0.01			IRF 89%

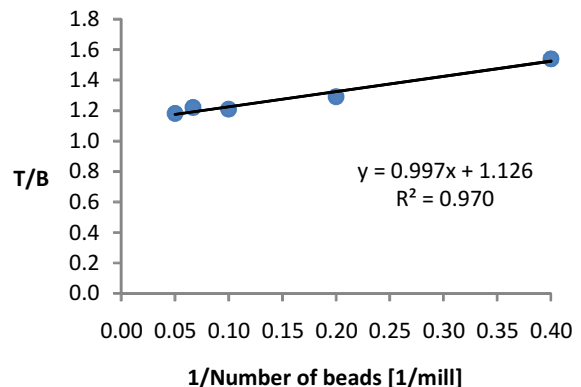
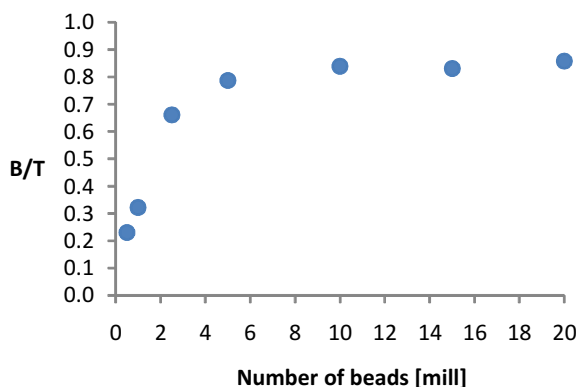
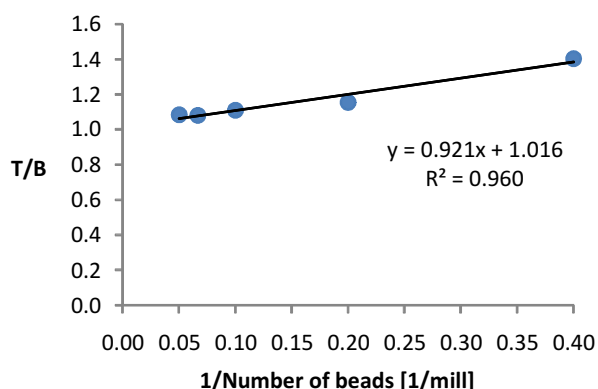
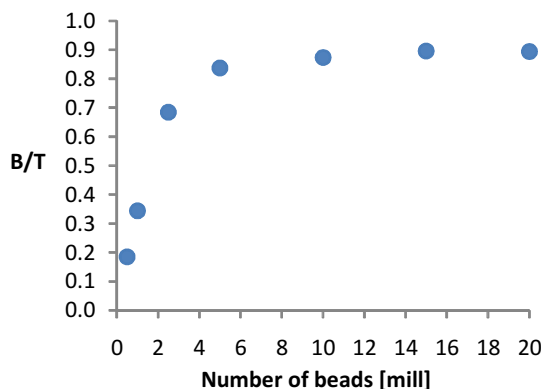


**Figure G.4:** Raw data from activity measurements, calculated binding fractions, binding plots and Lindmo plots for the two parallels of experiment 8b. <sup>227</sup>Th-AC0103 was tested for binding to Ag(01)-coated beads. IRF was calculated from the equation of the fitted straight line.

**9a - 1 % BSA**

# Beads [mill]	Activity [cpm]		(B/T)*	B/T	1/# Beads [1/mill]	T/B
	P	S				
0.50	319.0	207.2	0.21	0.19	2.00	4.71
1.0	384.6	176.1	0.37	0.34	1.00	2.69
2.5	460.3	77.4	0.71	0.68	0.40	1.40
5.0	500.0	36.1	0.87	0.84	0.20	1.16
10.0	517.6	26.8	0.90	0.87	0.10	1.11
15.0	534.7	21.0	0.92	0.90	0.07	1.08
20.0	518.9	21.0	0.92	0.89	0.05	1.08
BL	255.5	241.9	0.03			IRF 98%



**10a - 1% BSA**

# Beads [mill]	Activity [cpm]		(B/T)*	B/T	1/# Beads [1/mill]	T/B
	P	S				
1	393.4	186.6	0.36	0.36	1.00	2.81
2.5	480.2	96.8	0.66	0.66	0.40	1.50
5	514.6	50.2	0.82	0.82	0.20	1.22
10	535.0	36.1	0.87	0.87	0.10	1.14
15	522.1	24.2	0.91	0.91	0.07	1.10
BL	257.3	257.0	0.001			IRF 99%

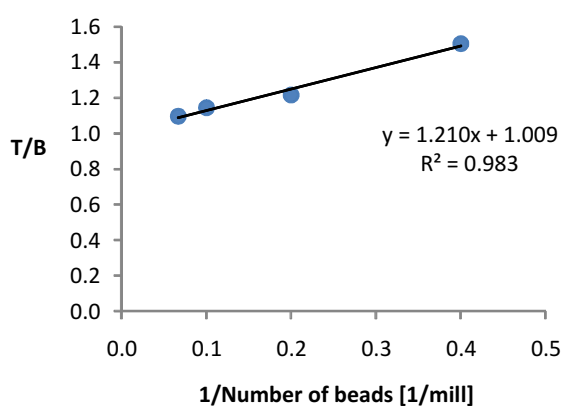
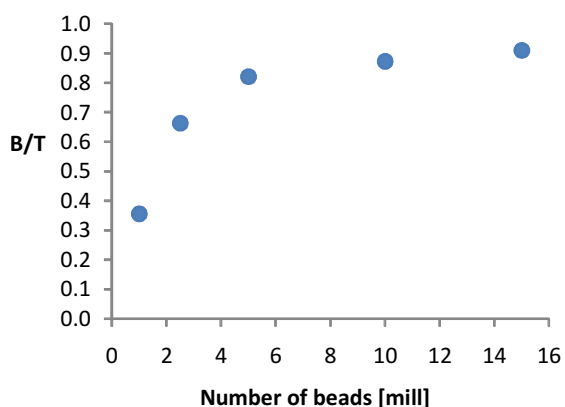


**Figure G.5:** Raw data from activity measurements, calculated binding fractions, binding plots and Lindmo plots for the two experiments 9a and 10a. <sup>227</sup>Th-AC0103 was tested for binding to Ag(01)-coated beads. IRF was calculated from the equation of the fitted straight line.

10b - 1% BSA

# Beads [mill]	Activity [cpm]		(B/T)*	B/T	1/# Beads [1/mill]	T/B
	P	S				
0.5	362.1	237.7	0.21	0.17	2.00	5.77
1	414.1	179.1	0.40	0.36	1.00	2.76
2.5	488.1	111.8	0.63	0.59	0.40	1.69
5	504.6	60.9	0.78	0.75	0.20	1.33
10	549.7	41.6	0.86	0.83	0.10	1.21
15	544.0	52.7	0.82	0.79	0.07	1.27
20	589.2	39.6	0.87	0.84	0.05	1.19
25	541.3	47.1	0.84	0.81	0.04	1.24
BL	304.2	284.1	0.03			IRF 88%

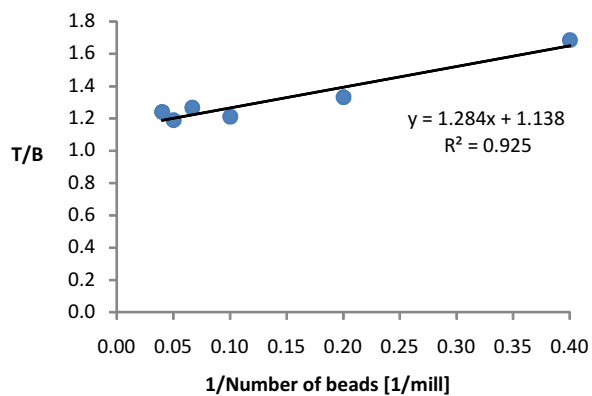
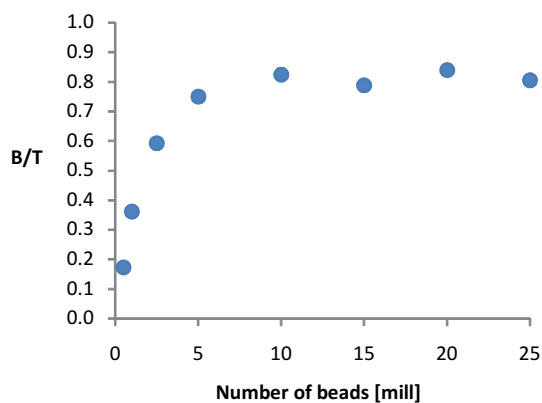


Figure G.6: Raw data from activity measurements, calculated binding fractions, binding plots and Lindmo plots for the experiments 10b. <sup>227</sup>Th-AC0103 was tested for binding to Ag(01)-coated beads. IRF was calculated from the equation of the fitted straight line.



# Appendix H

## Cell-based Immunoreactivity Assay for $^{227}\text{Th-AC0303}$

It was performed only one Lindmo analysis for  $^{227}\text{Th-AC0303}$  with Ag(03)-expressing cells. Figure H.1 shows raw data, calculated values, the binding plot and Lindmo plot from this experiment. IRF was determined from the Lindmo-plot as the intercept of the fitted straight line with the y-axis. Calculations were the same as for the cell-based immunoreactivity assays for  $^{227}\text{Th-AC0103}$  (see example in Appendix F). The experiment was numbered after the radiolabeled AC-conjugate used in the experiment (see Appendix B).

The 50 million cell sample was used as a one-point analysis. As seen in Figure H.1:  $\text{IRF}^* = \text{B/T (50 million sample)} = 71\%$ .

### 11b

# Cells [mill]	Activity [cpm]		(B/T)*	B/T	1/# Cells [1/mill]	T/B	
	P	S					
5	357.1	86.2	0.61	0.56	0.20	1.64	
10	371.7	77.7	0.65	0.60	0.10	1.53	
25	381.6	66.7	0.70	0.65	0.04	1.42	
50	404.1	55.0	0.76	0.71	0.02	1.32	
75	379.1	67.8	0.70	0.65	0.01	1.44	
BL	233.3	211.2	0.05				<b>IRF 73%</b>

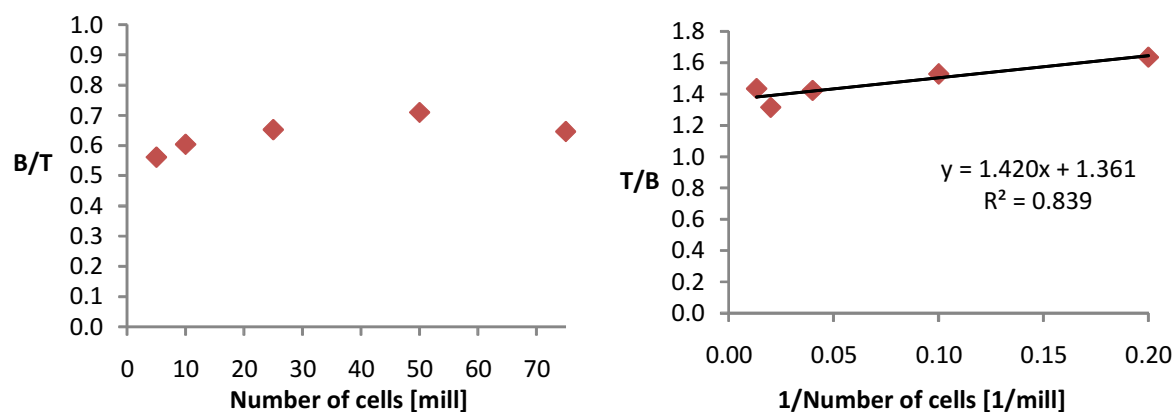


**Figure H.1:** Raw data from activity measurements, calculated binding fractions, binding plot and Lindmo plot for experiment 11b.  $^{227}\text{Th-AC0303}$  was tested for binding to Ag(03)-expressing cells. IRF was calculated from the equation of the fitted straight line.



# Appendix I

## Bead-based Immunoreactivity Assays for $^{227}\text{Th-AC0303}$

---

In the next two sections, raw data and calculated values from the bead-based binding assays for  $^{227}\text{Th-AC0303}$  are presented. Data from the one-point analyses are presented first. Secondly, data and plots from the Lindmo analyses are given. Calculations were the same as for the cell-based immunoreactivity assays for  $^{227}\text{Th-AC0103}$  (see example in Appendix F). The experiments were numbered after the radiolabeled AC-conjugate used in the respective experiment (see Appendix B).

---

### I.1 Bead-based one-point analyses for $^{227}\text{Th-AC0303}$

---

Raw data from the activity measurements from the bead-based one-point analyses for  $^{227}\text{Th-AC0303}$  are given in Table I.1. 15 million Ag(03)-coated beads were used per sample in these experiments.

**Table I.1:** Raw data from the activity measurements and calculated values from the one-point analyses of  $^{227}\text{Th-AC0303}$  using Ag(03)-coated beads. UBL = unblocked analysis sample. BL = blocked control sample. P = sample containing cell pellet + 1/2 supernatant. S = sample containing 1/2 supernatant.

Experiment	Activity (UBL)		(B/T)*	Activity (BL)		B/T <sub>BL</sub>	IRF*
	P	S		P	S		
10b	405.1	88.5	64%	277.4	234.1	8%	56%
	406.1	97.1	61%	275.4	243.5	6%	55%
11b	428.9	72.7	71%	236.6	208.7	6%	65%

AVERAGE:	7%	59%
S.D.:	1%	6%



---

## I.2 Bead-based Lindmo analyses for $^{227}\text{Th-AC0303}$

---

There were performed three Lindmo analyses for  $^{227}\text{Th-AC0303}$  with Ag(03)-coated beads. BSA was added to all samples of these experiments. The resulting IRF-values from each experiments and average IRF with S.D. from these three experiments are given in Table I.2.

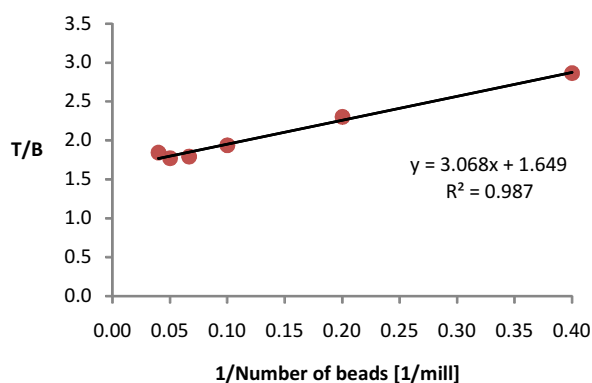
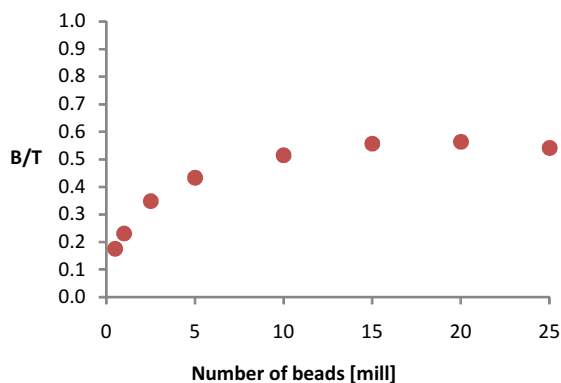
**Table I.2:** The calculated IRF values for each Lindmo analysis of  $^{227}\text{Th-AC0303}$  with Ag(03)-coated beads. Average IRF with standard deviation is given below.

<b>Experiment</b>	<b>IRF</b>
10b parallel 1	61%
10b parallel 2	57%
11b	72%
<hr/>	
Average	<b>63%</b>
S.D.	<b>6%</b>

Raw data, calculated values, binding plots and Lindmo plots for the three experiments are given in Figure I.1 and I.2. The red labeled values in the tables of these figures are omitted from the respective Lindmo-plot.

### 10b parallel 1

# Beads [mill]	Activity [cpm]		(B/T)*	B/T	1/# Beads [1/mill]	T/B
	P	S				
0.5	350.0	205.2	0.26	0.18	2.00	5.68
1	339.1	176.2	0.32	0.23	1.00	4.32
2.5	361.9	143.0	0.43	0.35	0.40	2.87
5	370.1	117.3	0.52	0.43	0.20	2.30
10	382.3	95.6	0.60	0.52	0.10	1.94
15	405.1	88.5	0.64	0.56	0.07	1.80
20	450.7	96.1	0.65	0.56	0.05	1.77
25	422.9	97.0	0.63	0.54	0.04	1.84
BL	277.4	234.1	0.08			IRF 61%



### 10b parallel 2

# Beads [mill]	Activity [cpm]		(B/T)*	B/T	1/# Beads [1/mill]	T/B
	P	S				
0.5	331.2	185.1	0.28	0.22	2.00	4.51
1	347.8	179.4	0.32	0.26	1.00	3.88
2.5	364.8	150.3	0.42	0.35	0.40	2.82
5	377.6	120.9	0.51	0.45	0.20	2.21
10	401.4	125.0	0.53	0.46	0.10	2.16
15	406.1	97.1	0.61	0.55	0.07	1.81
20	407.3	113.3	0.56	0.50	0.05	1.99
25	396.3	93.6	0.62	0.56	0.04	1.80
BL	275.4	243.5	0.06			IRF 57%

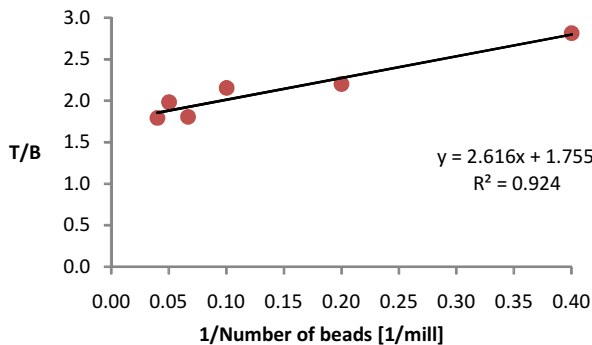
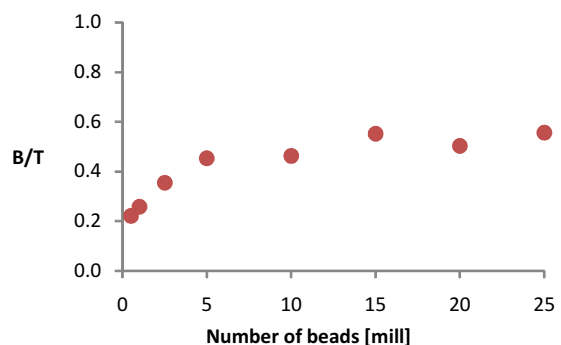


**Figure I.1:** Raw data from activity measurements, calculated binding fractions, binding plots and Lindmo plots for the two parallels of experiment 10b. <sup>227</sup>Th-AC0303 was tested for binding to Ag(03)-coated beads. IRF was calculated from the equation of the fitted straight line.

11b

# Beads [mill]	Activity [cpm]		(B/T)*	B/T	1/# Beads [1/mill]	T/B
	P	S				
0.5	293.3	160.7	0.29	0.23	2.00	4.36
1	333.3	153.2	0.37	0.31	1.00	3.25
2.5	339.1	112.8	0.50	0.44	0.40	2.28
5	356.0	93.3	0.58	0.52	0.20	1.92
10	377.2	68.6	0.69	0.63	0.10	1.59
15	428.9	72.7	0.71	0.65	0.07	1.54
20	418.5	62.3	0.74	0.68	0.05	1.47
BL	236.6	208.7	0.06			IRF 72%

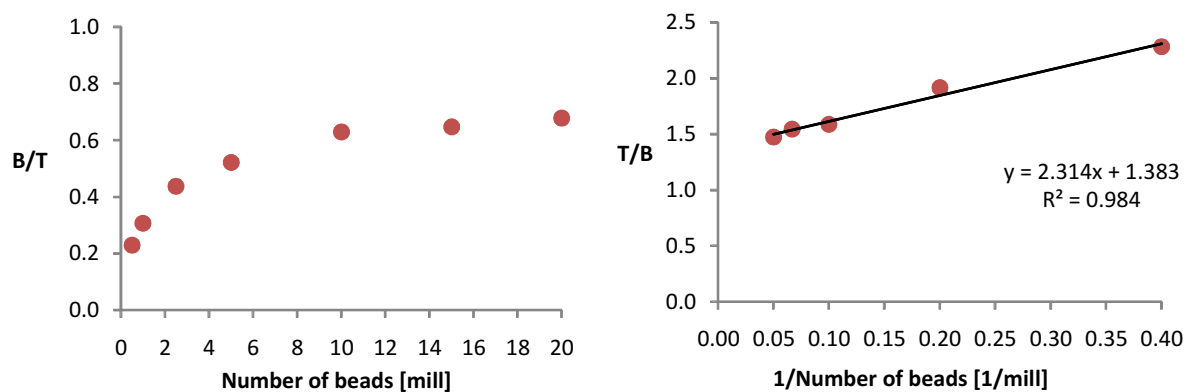


**Figure I.2:** Raw data from activity measurements, calculated binding fractions, binding plot and Lindmo plot for experiment 11b.  $^{227}\text{Th-AC0303}$  was tested for binding to Ag(03)-coated beads. IRF was calculated from the equation of the fitted straight line.